

TR 89-05

INVESTIGATION OF THE CAUSATIVE AGENTS OF THE 1982  
GAZANKULU POLIOMYELITIS OUTBREAK, USING FOUR BIOCHEMICAL  
TECHNIQUES

BY

KATHERINE MARGARET GIBSON

Submitted in fulfilment of the requirements for the degree of Master of Science in the Faculty of Science, Rhodes University, Grahamstown.

DECEMBER 1987

## CONTENTS

	PAGE
LIST OF FIGURES	vii
LIST OF TABLES	xi
<u>ACKNOWLEDGEMENTS</u>	xii
<u>ABSTRACT</u>	1
<u>CHAPTER ONE</u>	
<u>INTRODUCTION</u>	2
1.1. <u>Classification and General Characteristics of Poliovirus</u>	3
1.1.1. Physico-Chemical Characteristics	4
1.2. <u>Disease Aspects</u>	6
1.3. <u>Poliovirus Vaccines</u>	8
1.3.1. Inactivated Salk Vaccine	8
1.3.2. Live Attenuated Sabin Vaccine	9
1.4. <u>Epidemiology</u>	13
1.4.1. Identification of Vaccine Related Strains of Poliovirus	15
1.5. <u>Scope of This Study</u>	16
 <u>CHAPTER TWO</u>	
<u>MATERIALS AND METHODS</u>	19
2.1. <u>Propagation and Purification of Virus Strains</u>	19
2.1.1. Virus and Cell Stocks	19
2.1.2. Propagation of Virus	19
2.1.3. Extraction and Purification	20
2.1.3.1. Ammonium sulphate precipitation	20
2.1.3.2. Sucrose density gradient centrifugation	22

	PAGE
2.1.3.3. Fractionation of purified virus	23
2.2. <u>Phenol Extraction of RNA</u>	23
2.2.1 Extraction of Viral RNA	23
2.2.1.1. Calculation of viral RNA yield	25
2.2.2. Extraction of BHK RNA For Use as Carrier RNA	27
2.2.2.1. Calculation of BHK RNA concentration	28
2.2.3. Storage of RNA	30
2.3. <u>Extraction of Virus Protein From Phenol</u>	30
2.3.1. Extraction of Viral Protein	30
2.3.1.1. Calculation of protein concentration	30
2.4. <u>Polyacrylamide Gel Electrophoresis</u>	31
2.4.1. Polyacrylamide Gel Preparation	31
2.4.2. Sample Preparation	32
2.4.3. Electrophoresis	34
2.4.4. Staining and Storage of Gels	34
2.5. <u>Tryptic Peptide Mapping of Poliovirus Proteins</u>	35
2.5.1. Production of Radiolabelled Peptides	35
2.5.1.1. Preparation of gel slices	35
2.5.1.2. Iodination of proteins in gel slices	35
2.5.1.3. Trypsinization of proteins	36
2.5.2. Controls	37
2.5.3. Two-Dimensional Thin Layer Chromatography	38
2.5.3.1. Preparation of TLC plates	38
2.5.3.2. Electrophoresis	38
2.5.3.3. Ascending chromatography	39
2.5.3.4. Autoradiography	41

	PAGE
2.5.4. Reversed-Phase High-Performance Liquid-Chromatography	41
2.5.4.1. Apparatus	41
2.5.4.2. Solvents	43
2.5.4.3. RP-HPLC of trypsin-generated peptides	44
2.5.4.4. Column storage	45
2.6. <u>RNase T<sub>1</sub> Oligonucleotide Mapping</u>	46
2.6.1. 5'-End Labelling of RNA Oligonucleotides	46
2.6.1.1. Preparation of RNA	46
2.6.1.2. Digestion of viral RNA	46
2.6.1.3. Radiolabelling of oligonucleotides	46
2.6.2. Two-Dimensional Electrophoresis of Oligonucleotides	47
2.6.2.1. Apparatus	47
2.6.2.2. First-dimension gel electrophoresis	48
2.6.2.2.1. First-dimension polyacrylamide gel preparation	48
2.6.2.2.2. Sample preparation	52
2.6.2.2.3. Electrophoresis	53
2.6.2.3. Second-dimension gel electrophoresis	53
2.6.2.3.1. Preparation of the first dimension gel strip for second-dimension electrophoresis	53
2.6.2.3.2. Second-dimension polyacrylamide gel preparation	54
2.6.2.3.3. Electrophoresis	55
2.6.2.4. Autoradiography	56

### CHAPTER THREE

<u>COMPARISON OF POLIOVIRUS CAPSID PROTEINS USING DISCONTINUOUS SDS-POLYACRYLAMIDE GEL ELECTROPHORESIS</u>	58
--	----

	PAGE
3.1. <u>Introduction</u>	58
3.2. <u>Results</u>	60
3.2.1. Comparison of Capsid Proteins of Type 1 Polioviruses	60
3.2.2. Comparison of Capsid Proteins of Type 2 Polioviruses	64
3.2.3. Comparison of Capsid Proteins of Type 3 Polioviruses	65
3.3. <u>Discussion</u>	65
 <u>CHAPTER FOUR</u>	
<u>COMPARISON OF POLIOVIRUS CAPSID PROTEINS BY MAPPING TRYPTIC PEPTIDES USING THIN-LAYER CHROMATOGRAPHY (TLC) AND REVERSED-PHASE HIGH-PERFORMANCE LIQUID-CHROMATOGRAPHY (RP-HPLC)</u>	68
4.1. <u>Introduction</u>	68
4.2. <u>Comparison of Poliovirus Capsid Proteins by Two-Dimensional Thin-Layer Chromatography of Tryptic Peptides</u>	70
4.2.1. Results	73
4.2.1.1. Comparison of tryptic peptide maps of the capsid proteins from poliovirus type 1	73
4.2.1.2. Comparison of tryptic peptide maps of the capsid proteins of type 2 polioviruses	81
4.2.1.3. Comparison of tryptic peptide maps of the capsid proteins of type 3 polioviruses	88
4.2.2. Results of Control Experiments Carried Out to Determine Accuracy and Reproducibility of Two-Dimensional TLC of Tryptic Peptides	100
4.3. <u>Comparison of Poliovirus Capsid Proteins by Reversed-Phase High-Performance Liquid-Chromatography of Tryptic Peptides</u>	104
4.3.1. Results	108
4.3.1.1. Comparison of tryptic peptide maps of capsid proteins of type 1 polioviruses	108
4.3.1.2. Comparison of tryptic peptide maps of capsid proteins of type 2 polioviruses	112

	PAGE
4.3.1.3. Comparison of tryptic peptide maps of capsid proteins of type 3 polioviruses	117
4.3.2. Results of Control Experiments Carried Out to Determine Accuracy and Reproducibility of RP-HPLC of Tryptic Peptides	119
4.4. Discussion of Results Obtained After Mapping Tryptic Peptides of Poliovirus Capsid Proteins	129
 <u>CHAPTER FIVE</u>	
<u>COMPARISON OF POLIOVIRUS RNA BY RNase T<sub>1</sub> OLIGO-NUCLEOTIDE MAPPING</u>	138
5.1. <u>Introduction</u>	138
5.2. <u>Results</u>	142
5.2.1. Comparison of RNA oligonucleotide maps of type 1 poliovirus strains	144
5.2.2. Comparison of RNA oligonucleotide maps of type 2 poliovirus strains	147
5.2.3. Comparison of RNA oligonucleotide maps of type 3 poliovirus strains	150
5.3. Discussion	153
 <u>CHAPTER SIX</u>	
<u>COMMENTS ON TECHNIQUES USED IN THIS STUDY</u>	157
 <u>CHAPTER SEVEN</u>	
<u>GENERAL DISCUSSION</u>	168
 <u>CHAPTER EIGHT</u>	
<u>SUMMARY</u>	171
 <u>REFERENCES CITED</u>	 173

LIST OF FIGURES

	PAGE
FIGURE 1.1. Lateral view of the human brain stem and the mid-sagittal surface of the brain stem.....	7
FIGURE 2.1. Flow chart showing stages in the purification of poliovirus.....	21
FIGURE 2.2. Typical ISCO trace of absorbance at 254nm of poliovirus purified using SDGC.....	24
FIGURE 2.3. Trace of absorbance of a purified BHK RNA sample, scanned from 320 - 220nm.....	29
FIGURE 2.4. Cross-section of the thin-layer chromatography apparatus.....	40
FIGURE 2.5.a. Photograph of a TLC plate after completion of electrophoresis and chromatography.....	42
FIGURE 2.5.b. Diagramatic representation of a TLC plate, showing directions of electrophoresis and chromatography.....	42
FIGURE 2.6.a. First-dimension electrophoresis apparatus used for RNase T <sub>1</sub> oligonucleotide mapping of poliovirus RNA.....	49
FIGURE 2.6.b. Schematic drawing of electrophoresis apparatus...	49
FIGURE 2.7.a. Second-dimension electrophoresis apparatus used for RNase T <sub>1</sub> oligonucleotide mapping of poliovirus RNA....	50
FIGURE 2.7.b. Schematic drawing of electrophoresis apparatus....	50
FIGURE 2.8. Diagramatic representation of a second-dimension oligonucleotide mapping gel.....	57
FIGURE 3.1.a. Photograph of SDS-PAGE gel after electrophoresis of type 1 and 2 polioviruses.....	61
FIGURE 3.1.b. Standard curve obtained by plotting log. molecular weight of marker proteins against distance migrated.....	61
FIGURE 3.2.a. Photograph of SDS-PAGE gel after electrophoresis of type 3 polioviruses.....	62
FIGURE 3.2.b. Standard curve obtained by plotting log. molecular weight of marker proteins against distance migrated.....	62

FIGURE 4.1.	Incorporation of $^{125}\text{I}$ into tyrosine residues.....	72
FIGURE 4.2.a.	Maps produced after TLC of peptides from VP1 of poliovirus type 1 strains.....	74
FIGURE 4.2.b.	Diagrammatic representation of the peptide maps of VP1 from 5061, LS-c and LS-a.....	75
FIGURE 4.3.a.	Maps produced after TLC of peptides from VP2 of poliovirus type 1 strains.....	77
FIGURE 4.3.b.	Diagrammatic representation of the peptide maps of VP2 from 5061, LS-c and LS-a.....	78
FIGURE 4.4.a.	Maps produced after TLC of peptides from VP3 of poliovirus type 1 strains.....	79
FIGURE 4.4.b.	Diagrammatic representation of the peptide maps of VP3 from 5061, LS-c and LS-a.....	80
FIGURE 4.5.a.	Maps produced after TLC of peptides from VP1 of poliovirus type 2 strains.....	83
FIGURE 4.5.b.	Diagrammatic representation of the peptide maps of VP1 from 5068, P712 and Lansing.....	84
FIGURE 4.6.a.	Maps produced after TLC of peptides from VP2 of poliovirus type 2 strains.....	86
FIGURE 4.6.b.	Diagrammatic representation of the peptide maps of VP2 from 5068, P712 and Lansing.....	87
FIGURE 4.7.a.	Maps produced after TLC of peptides from VP3 of poliovirus type 2 strains.....	89
FIGURE 4.7.b.	Diagrammatic representation of the peptide maps of VP3 from 5068, P712 and Lansing.....	90
FIGURE 4.8.a.	Maps produced after TLC of peptides from VP1 of poliovirus type 3 strains.....	92
FIGURE 4.8.b.	Diagrammatic representation of the peptide maps of VP1 from Leon 3 and Leon III.....	93
FIGURE 4.9.a.	Maps produced after TLC of peptides from VP2 of poliovirus type 3 strains.....	95
FIGURE 4.9.b.	Diagrammatic representation of the peptide maps of VP2 from Leon 3 and Leon III.....	96
FIGURE 4.10.a.	Maps produced after TLC of peptides from VP3 of poliovirus type 3.....	97



FIGURE 4.10.b. Diagrammatic representation of the peptide maps of VP3 from Leon 3 and Leon III.....	98
FIGURE 4.11. Photograph showing autoradiograph of TLC map of gel slice containing no protein.....	101
FIGURE 4.12. Maps produced after TLC of peptides from 2 samples of ovalbumin.....	102
FIGURE 4.13.a. Map produced after a sample of trypsin was radiolabelled and digested with trypsin.....	103
FIGURE 4.13.b. Diagrammatic representation of intense spots on peptide map of trypsin.....	103
FIGURE 4.14. Structure of silica-organic phase used for RP-HPLC.....	106
FIGURE 4.15. Radioactivity traces obtained after RP-HPLC of tryptic peptides of radiolabelled VP1 from poliovirus type 1 strains.....	109
FIGURE 4.16. Radioactivity traces obtained after RP-HPLC of tryptic peptides of radiolabelled VP2 from poliovirus type 1 strains.....	111
FIGURE 4.17. Radioactivity traces obtained after RP-HPLC of tryptic peptides of radiolabelled VP3 from poliovirus type 1 strains.....	113
FIGURE 4.18. Radioactivity traces obtained after RP-HPLC of tryptic peptides of radiolabelled VP1 from poliovirus type 2 strains.....	115
FIGURE 4.19. Radioactivity traces obtained after RP-HPLC of tryptic peptides of radiolabelled VP2 from poliovirus type 2 strains.....	116
FIGURE 4.20. Radioactivity traces obtained after RP-HPLC of tryptic peptides of radiolabelled VP3 from poliovirus type 2 strains.....	118
FIGURE 4.21. Radioactivity traces obtained after RP-HPLC of tryptic peptides of radiolabelled VP1 from poliovirus type 3 strains.....	120
FIGURE 4.22. Radioactivity traces obtained after RP-HPLC of tryptic peptides of radiolabelled VP2 from poliovirus type 3 strains.....	121
FIGURE 4.23. Radioactivity traces obtained after RP-HPLC of tryptic peptides of radiolabelled VP3 from poliovirus type 3 strains.....	123

FIGURE 4.24.	Radioactivity trace obtained after radio-labelling, trypsin treatment and RP-HPLC mapping of a gel slice containing no protein.....	124
FIGURE 4.25.	Radioactivity traces obtained after RP-HPLC of individual samples of BSA labelled with <sup>125</sup> I and trypsin digested.....	126
FIGURE 4.26.a.	Radioactivity trace obtained after RP-HPLC of a radiolabelled tryptic digest of trypsin.....	127
FIGURE 4.26.b.	Trace of absorbance at 220nm of peptide sample used in figure 4.26.a.....	127
FIGURE 4.27.	RP-HPLC map of autodigestion products of trypsin showing trace of absorbance at 220nm.....	130
FIGURE 4.28.	Amino-acid sequence for capsid proteins of all three Sabin vaccine strains of poliovirus.....	131
FIGURE 5.1.	Structure of $\gamma^{32}\text{P-ATP}$ .....	141
FIGURE 5.2.	Theoretical patterns of oligonucleotide distribution after two-dimensional electrophoresis.....	143
FIGURE 5.3.a.	Oligonucleotide maps of RNA from poliovirus type 1 strains.....	145
FIGURE 5.3.b.	Diagrammatic representation of oligonucleotide maps of RNA from poliovirus type 1 strains.....	146
FIGURE 5.4.a.	Oligonucleotide maps of RNA from poliovirus type 2 strains.....	148
FIGURE 5.4.b.	Diagrammatic representation of oligonucleotide maps of RNA from poliovirus type 2 strains.....	149
FIGURE 5.5.a.	Oligonucleotide maps of RNA from poliovirus type 3 strains.....	152
FIGURE 5.5.b.	Diagrammatic representation of oligonucleotide maps of RNA from poliovirus type 3 strains.....	152
FIGURE 6.1.a.	Theoretical oligonucleotide map for poliovirus type 2 strain P712.....	163
FIGURE 6.1.b.	Photograph of oligonucleotide map of P712 obtained under experimental conditions.....	164
FIGURE 6.1.c.	Diagrammatic representation of the experimental oligonucleotide map of P712.....	164

LIST OF TABLES

	PAGE
TABLE 1.1. Physico-chemical characteristics of polioviruses...	5
TABLE 2.1. Molecular weights of Sigma marker proteins used in SDS-PAGE.....	33
TABLE 2.2. Stock solutions for the first-dimension gel system.....	51
TABLE 2.3. Stock solutions for the second-dimension gel system.....	55
TABLE 3.1. Molecular weight of poliovirus capsid proteins calculated after SDS-PAGE. ....	63
TABLE 4.1. Comparison of tryptic peptide maps of capsid proteins 1,2 and 3 of poliovirus type 1 Gazankulu outbreak strain 5061 with similar maps of vaccine strain LS-c and wild-type LS-a.....	82
TABLE 4.2. Comparison of tryptic peptide maps of capsid proteins 1,2 and 3 of poliovirus type 2 Gazankulu outbreak strain 5068 with similar maps of vaccine strain P712 and wild-type Lansing. ....	91
TABLE 4.3. Comparison of tryptic peptide maps of capsid proteins 1,2 and 3 of poliovirus type 3 vaccine strain Leon 3 with similar maps of wild-type 3 strain Leon III.....	99
TABLE 4.4. Radiolabelled peptides expected for each radio- labelled virus capsid protein after trypsin digestion, determined using sequence data.....	133
TABLE 4.5. Number of peptides found to be shared by capsid proteins of poliovirus strains within poliovirus types 1 and 2.....	135
TABLE 5.1. Number of oligonucleotides found to be shared between RNA of poliovirus strains within poliovirus types 1 and 2.....	155

## ACKNOWLEDGEMENTS

I would like to thank my supervisor, Professor John Newman, for the guidance and support that I received, even during his absence from Rhodes. It was, no doubt, not an easy task.

My thanks also to Mrs. Val Hodgson for her help in supplying HeLa and Vero cell monolayers, and to Professor Don Hendry who frequently gave me his time and assistance. I would also like to thank Gail Hagemann for the hours that she spent proof reading this manuscript.

To my co-workers in the laboratory, Dee Blackhurst and Michelle Martin, thanks for the hours of amusement and discussion. Thanks to Jenny Wright for technical advice and assistance, and to Regina Nelo, Mike Nqweniso and Victor Ntsendwana - their job was not the easiest.

I owe much to my family - without their support, both financially and otherwise, I would never have been able to finish this thesis. My thanks also to William for his support and encouragement.

I acknowledge financial support from the South African Medical Research Council and from Rhodes University, without which I would have been unable to further my studies.

## ABSTRACT

Comparison of poliovirus strains was carried out to determine the origin of the virus in two isolates obtained during the 1982 outbreak of poliomyelitis in Gazankulu. Comparisons of the outbreak isolates with vaccine and wild-type strains of the same poliovirus type were carried out using four biochemical techniques. SDS-polyacrylamide gel electrophoresis (SDS-PAGE), two-dimensional thin-layer chromatography (TLC) and reversed-phase high-performance liquid-chromatography (RP-HPLC) were used for comparing viral capsid proteins. Comparison of poliovirus strains at a genetic level was carried out using two-dimensional oligonucleotide mapping of viral RNA. Results showed the type 1 poliovirus isolate, 5061, to be a novel wild-type poliovirus. The type 2 isolate, 5068, was closely related to the poliovirus type 2 Sabin vaccine strain, P712. It was concluded that the intrinsic variability of poliovirus strains was responsible for the appearance of isolate 5068.

## CHAPTER ONE

### INTRODUCTION

Between May and September 1982 an epidemic of poliomyelitis occurred in Gazankulu, a self-governing National State in north-eastern South Africa. Paralytic poliomyelitis occurred in 260 cases. A case fatality rate of 13.8% was recorded, and 92% of patients were 0 - 5 years old. Vaccination rates appeared to have been low: 69% of the patients said that they had not been vaccinated while 15% were unsure <sup>95</sup>.

The aetiological agent responsible for the outbreak was found to be poliovirus type 1 (determined initially by serology and later by virus isolation, primarily from stool specimens). No type 2 or 3 isolates were made during May and June, the first two months of the epidemic. During July poliovirus type 2 was isolated from four samples while one isolate each of type 2 and type 3 poliovirus was made in August <sup>95</sup>.

Type 2 and 3 virus was only isolated after initiation of an extensive immunization programme using the Sabin trivalent oral poliovaccine (TOPV) <sup>48</sup>. Consequently, vaccine stocks were recalled from the field in order to be tested for potency. Of the recalled vaccine samples, 8 out of 17 were found to be below the minimal required potency of 300 000 TCID<sub>50</sub>/dose (tissue culture infective dose required for destruction of 50% of the cell monolayer), ranging from 240 000 TCID<sub>50</sub> down to 4 823 TCID<sub>50</sub>/dose <sup>48</sup>.

The loss of potency had occurred in the field, presumably due to breaks in the cold chain. This was proved by testing TOPV produced by the National Institute of Virology on 13 seronegative children aged between 1 and 5 years old. All developed antibodies to type 2 poliovirus after one dose of TOPV and 30% became seropositive to all three serotypes <sup>48</sup>, indicating that the vaccine was effective.

Because of the temporal association between administration of the vaccine and isolation of type 2 and 3 poliovirus strains, it was suspected that the type 2 and type 3 isolates were vaccine related. Experimental work using polyacrylamide gel electrophoresis and two-dimensional mapping of tryptic peptides carried out by Martin (1984) and Eve (1985) indicated that the poliovirus type 2 strain isolated was vaccine related. The type 1 outbreak strain did not appear to be vaccine related. Type 3 poliovirus from the outbreak was not available for comparison with the wild and vaccine type 3 strains.

This study was carried out in order to investigate the origin of the isolates obtained from the Gazankulu poliomyelitis outbreak of 1982. It was hoped that the results would give a clear indication of the relationship between the Gazankulu outbreak poliovirus strains and the attenuated vaccine strains.

### **1.1. Classification and General Characteristics of Poliovirus**

Poliovirus is a member of the Picornaviridae, a family of small, ether resistant, polyhedral RNA-containing viruses which infect man and animals <sup>66</sup>. The name Picornaviridae refers to the size

(pico meaning small) and nucleic acid component (nucleic acid is RNA) of the members of this virus family <sup>62</sup>.

#### 1.1.1. Physico-Chemical Characteristics

The physical and chemical properties of polioviruses are shown in table 1.1. The capsid consists of 32 capsomeres <sup>33,93</sup> and contains four structural proteins comprising 70% by mass of the virion <sup>91</sup>. Myristic acid is present, bound covalently to the N-terminus of the VP4 capsid protein <sup>17</sup>. It is generally accepted that the proteins are not glycosylated <sup>88</sup>. The single strand of linear RNA is of a positive polarity and contains all the genetic information. A poly-adenylic acid (poly-A) region of variable length is present at the 3' end. Conflicting evidence exists as to the necessity of the poly-A region for infectivity <sup>33,88,97,99</sup>.

The 5' end of the RNA terminates in pUp instead of  $m^7G^5'ppp^5'Np$ . A small, virus encoded protein, designated VPg (virus protein genome-linked), is covalently linked to this. VPg is necessary for initiation of RNA replication <sup>22,33,88,97</sup>, and antibodies to VPg prevent de novo synthesis of poliovirus RNA in an in vitro system <sup>77</sup>.

A single polyprotein, NCVPOO (Molecular weight 247 000), is translated off the RNA and accounts for 95% of the virus genome. Post-translational cleavage into structural and non-structural proteins occurs. To date 26 cleavage products have been detected <sup>83</sup>. In addition to the 60 molecules each of structural



Table 1.1: Physico-Chemical Characteristics of Polioviruses <sup>4</sup>

Diameter of virion	27-30nm
Diameter of internal core	16nm
Diameter of capsomere	6nm
Molecular weight of RNA	$2.5 \times 10^6$ (7.7 Kb)
Base composition (C+G)	46 moles % *
Molecular weight of virion proteins**	
VP1	$35 \times 10^3$
VP2	$28 \times 10^3$
VP3	$24 \times 10^3$
VP4	$6 \times 10^3$
VPg	$\sim 7 \times 10^3$
Sedimentation coefficient of virion	157-160 S 20
Particle mass of virion	$1,1 \times 10^{-17}g$
Molecular weight of virion	$8-9 \times 10^6$

\* composition is closely similar for all three types

\*\* virion proteins 1 - 4 are present in equal molar amounts

proteins VP1, VP2, VP3 and VP4 found in the capsid, there may be two molecules of VP0, the precursor to VP2 and VP4 <sup>93</sup>.

## 1.2. Disease Aspects

Poliovirus is primarily an enterovirus, infecting the gastrointestinal tract and generally causing a mild or sub-clinical illness. In approximately 1-2% of cases the virus infects the central nervous system, where the release of virus particles causes cell lysis <sup>62</sup>. Subsequent lesions in the brain tissue (figure 1.1) result in the characteristic paralytic disease associated with poliovirus infections.

Three distinct immunologic types of poliovirus exist, each of which causes paralytic poliomyelitis. The three serotypes, referred to as types 1,2 and 3, may be recognised by neutralization, complement fixation (CF) or gel-diffusion precipitation reactions with type-specific sera <sup>33</sup>. Cross-hybridisation experiments between virion RNA and replicative forms of RNA from infected cells show that base compositions of the three serotypes are very similar: 36% to 52% of the nucleotide sequences are shared <sup>33</sup>.

Polioviruses have a limited host range, and man is the only known natural host. Infection of other primates, generally by direct inoculation of the brain or spinal cord, is possible <sup>66</sup>. In the case of chimpanzees and cynomolgus monkeys infection by the oral route is also effective <sup>33</sup>. The disease is generally subclinical in chimpanzees, and the animals become intestinal carriers. Most polio virus strains can be grown in primary or

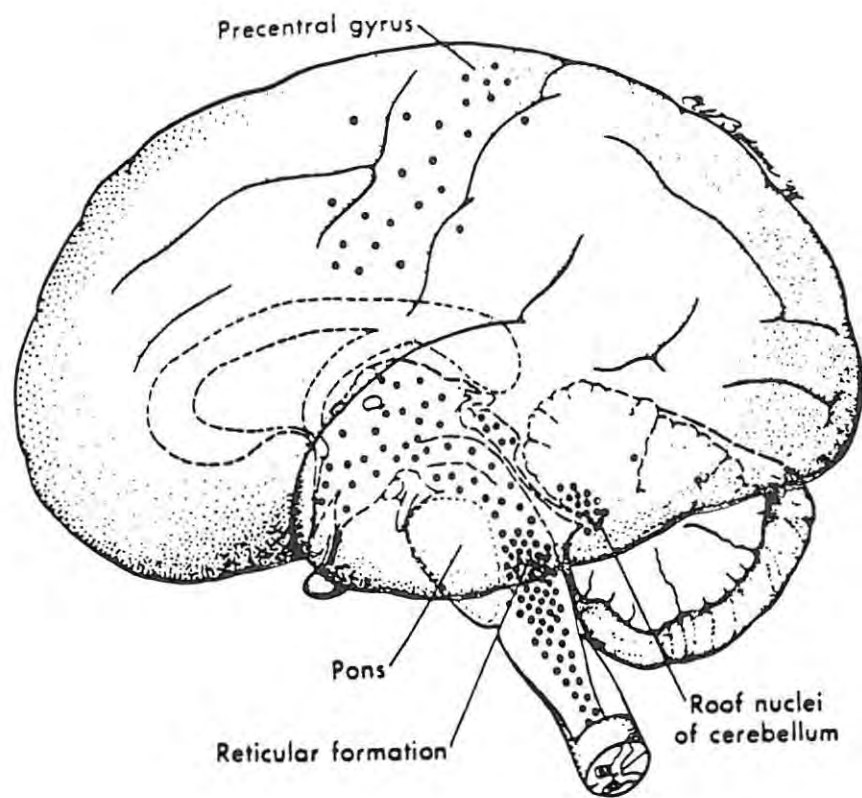


FIGURE 1.1. Lateral view of the human brain stem and the mid-sagittal surface of the brain stem. Black dots = usual distribution of lesions. (Bodian, D. in Ginsberg, 1980).

continuous cell lines derived from a variety of human tissues or from monkey kidney, testis or muscle <sup>66</sup>.

Currently two poliovirus vaccines exist - the Salk and the Sabin vaccines, introduced in 1954 and 1959 respectively. Use of these vaccines has resulted in a radical decrease in the number of cases of poliomyelitis. Over 12 years the incidence of poliomyelitis in the USSR, 23 other European countries, the United States, Australia, Canada and New Zealand decreased by 99% - from over 76 000 cases in 1955 to 1 013 cases in 1967 <sup>66</sup>. Currently, fewer than ten cases of paralytic poliomyelitis occur annually in most developed countries.

### 1.3. Poliovirus Vaccines

#### 1.3.1. Inactivated Salk Vaccine

The first vaccine to be used against poliovirus was developed by Jonas Salk and was first used on a wide scale in 1954. Poliovirus was incubated for about 1 week at 37°C with 1:4 000 formalin, pH7, after which the virus was inactivated but still antigenic. There were some serious initial problems with this vaccine, largely because the inactivation curve of crude virus tails off rapidly. The procedure has since been modified by carrying out inactivation at 50°C in the presence of 1M magnesium chloride. This also inactivates any adventitious viruses (such as SV 40) that may be present in monkey cell cultures. The resultant vaccine is safe and effective, with an immunization rate of 70% - 90% <sup>33</sup>.

The Salk injected poliovirus vaccine (IPV) contains all three poliovirus serotypes. Three subcutaneous (SC) injections are administered over 3 to 6 months. Antibody levels fall to about 20% within two years then decline slowly, and booster injections every five years are recommended. Infection of the oropharyngeal mucosa and tonsils is prevented, blocking transmission by oropharyngeal secretions <sup>33</sup>. Despite vaccination, reinfection of the alimentary tract may occur. This may result in a vaccinated individual acting as a "carrier" of the disease <sup>66</sup>. Administration of the Salk vaccine requires trained medical personnel. This increases the costs and difficulty of ensuring an effective vaccination programme. The IPV may however be incorporated into other injected vaccines such as the DPT (diphtheria, pertussis, tetanus) vaccine for ease of administration <sup>57</sup>. Rare side effects such as anaphylaxis or neurological illness such as Guillain-Barré syndrome <sup>57</sup> may occur as a result of use of the Salk IPV.

#### 1.3.2. Live Attenuated Sabin Vaccine

Three different sets of live attenuated poliovirus were independently selected by Cox, Koprowski and Sabin by multiple passage in a foreign host (usually tissue culture). The attenuated poliovirus strains developed in 1956 by Albert Sabin were chosen by the US Public Health Service for commercial production of vaccines.

Neurovirulent type 1 strain Mahoney virus was isolated from three healthy children in 1941. Attenuation was achieved by 50

in vitro and 24 in vivo passages of the virus. Initially 14 in vivo passages and 2 in vitro monkey tissue culture passages were carried out. These were followed by 31 in vitro passages (through both the CNS of white mice and monkey cell cultures) and 10 in vivo passages through cynomolgus or rhesus monkey skin alternating with 10 in vitro tissue culture passages. Further in vitro passages were carried out, resulting in the attenuated poliovirus strain LSc 2ab/KP<sub>2</sub>. This was used for the production of vaccine stocks against poliovirus type 1<sup>96</sup>.

P712 was a naturally occurring type 2 poliovirus strain found to have a low virulence for cynomolgus and rhesus monkeys. After four in vitro passages in cynomolgus monkey kidney cells and three plaque passages a single in vivo passage in chimpanzees was carried out. This was followed by six in vitro passages. The resultant virus was used for the attenuated Sabin type 2 poliovirus vaccine, P712 Ch2ab/KP<sub>3</sub><sup>96</sup>.

Type 3 strain P3/Leon/37 was isolated from the brain and spinal cord of a fatal case of paralytic poliomyelitis. This was the neurovirulent progenitor of attenuated vaccine strain Leon 12 a<sub>1</sub>b/KP<sub>3</sub>. Attenuation was achieved by passaging the virus through unnatural hosts, 53 times in vitro interspersed with 21 in vivo passages intracerebrally through rhesus monkeys<sup>96</sup>.

Initially the three Sabin virus types were administered monovalently. Interference with one another upon simultaneous administration of the three vaccine types was not, however, found to occur. The three types are now administered together

as the trivalent oral polio vaccine (TOPV). Interference is minimized by having type 1 present in the greatest concentration and type 2 in the lowest <sup>33</sup>. Usually interference may be overcome by giving three doses of the vaccine at 6-week intervals <sup>57</sup>.

Because the Sabin vaccine is live it can be given orally, following the route of infection by wild-type virus. As a result, trained medical personnel are not required for the administration of the vaccine. This is an advantage in underdeveloped countries suffering from a lack of medical personnel in rural areas <sup>66</sup>. Because the vaccine is given orally, on a sugar cube, it may be more acceptable to the public than the injected Salk vaccine <sup>6</sup>. This could lead to a higher rate of voluntary vaccination.

In addition to triggering the production of humoral antibodies the Sabin vaccine induces the production of IgA, which is secreted into the gut. This results in resistance of the intestinal tract to infection by wild-type poliovirus. Spread of the virus through the population is thus blocked.

A higher than expected degree of vaccination has been observed in populations vaccinated with the Sabin TOPV. It is thought that the live vaccine may spread within the population in much the same way as the wild-type virus. This results in "passive" vaccination and herd immunity <sup>6,58,66</sup>. Consequently, it is not necessary to have such a high vaccine acceptance rate within the population as with the Salk vaccine <sup>66</sup>.

Despite the greater safety of the Salk vaccine, it has generally been replaced by the Sabin TOPV, which is cheaper to produce, easier to administer and results in induction of gut immunity and herd immunity <sup>35</sup>. The Salk inactivated vaccine is still popular in several countries, and some notable success has been achieved in the prevention of poliomyelitis. Exclusive use of the Salk IPV in Holland, Finland and Sweden has apparently eliminated paralytic poliomyelitis <sup>66</sup>. However, these countries have an excellent public health service and a vaccine acceptance rate of at least 90% <sup>57,58</sup>.

In certain conditions use of the Sabin vaccine is contraindicated, and the Salk vaccine is used. In immunosuppressed individuals <sup>6,66</sup>, and in some tropical areas with a high incidence of enteric viruses, the Sabin vaccine fails to induce a satisfactorily high level of antibodies <sup>66</sup>. General use of the Salk IPV is, however, unlikely because of its production costs and administration requirements.

Vaccines containing one strain of each serotype of poliovirus have proved highly effective in controlling poliomyelitis. This implies that immunization with one serotype induces immunity to all viruses of the same serotype, and that polio viruses are unable to avoid host immunity by antigenic drift, as is seen with influenza virus <sup>71</sup>. There was, however, a small outbreak of poliomyelitis (with nine cases of paralysis) in Finland between August 1984 and January 1985. This involved a type 3 polio virus having an unusual antigenic nature <sup>63</sup>. It therefore appears that occasionally antigenic drift may occur in vivo.



Certainly, antigenic drift has been detected in vitro <sup>22</sup>.

#### 1.4. Epidemiology

Three major epidemiological phases of poliomyelitis exist - endemic, epidemic and postvaccination. In areas where the standard of living is low and sanitation poor, the disease appears to be endemic. It is still primarily a disease of infants (hence "infantile paralysis"), and virtually all children over the age of four years are immune. Antibody levels to the virus are generally high throughout the population, resulting in protection of infants by maternal antibodies. Additionally, infants and young children are most likely to have an inapparent infection, rendering them immune to poliovirus. Consequently paralytic poliomyelitis tends to be rare <sup>66</sup>.

Since the 1900's, living conditions and sanitation have improved greatly. In the 75 years preceding widespread vaccination programmes in the 1960's, poliomyelitis changed from being endemic to epidemic. Concurrently the age distribution of the disease and its severity increased as it appeared in young adults <sup>33</sup>.

Increased levels of hygiene appear to be responsible for the increase in poliomyelitis epidemics. Improved sanitation prevented individuals from being infected while still protected by the maternal antibodies. Increasing numbers of individuals encountered the virus for the first time in later childhood or in adult life, when the disease is more likely to take on the

paralytic form. The delay in exposure to the virus resulted in the build-up of susceptibles in the population. Once a critical number sufficient to support wide and rapid circulation of the virus existed, an epidemic was more likely <sup>66</sup>.

At present, in well vaccinated parts of the world, the post-vaccine epidemiological patterns of poliomyelitis are emerging. These patterns are highly variable. Isolations of poliovirus are rare, with wild-type virus generally being imported from other countries <sup>66</sup>. In most developed countries with a good vaccination programme, the majority of poliomyelitis cases are those occurring within vaccinees and their contacts <sup>6,98</sup>. These cases are the result of reversion to neurovirulence by the attenuated Sabin vaccine.

Little is yet known about the nature and extent of the changes involved in virus attenuation but it probably occurs by a series of mutational steps <sup>52</sup>. Reversion to neurovirulence probably results from a similar series of steps. Under immune pressure in vitro the poliomyelitis vaccine appears to be highly mutable <sup>70,72</sup>, although Yoneyama et al (1981) found low in vitro mutability of the Sabin type 2 vaccine. The capacity for back-mutation by the live vaccine has been used by Dr J. Salk and others in arguing against use of the Sabin vaccine.

Fortunately in vivo reversion appears to occur only at a very low rate, suggesting that the vaccine is stable in vivo. Figures available support this - in the United States approximately one case of paralytic poliomyelitis occurs per

11.5 million vaccinees and one case per 3.9 million vaccinee contacts <sup>66</sup>.

Most cases of poliomyelitis temporally associated with administration of the TOPV involve polio viruses of type 2 and 3 <sup>98</sup>. The attenuated type 3 virus, in particular, may attain a high level of neurovirulence very early in the course of infection and requires only a single nucleotide change at a specific position to attain increased neurovirulence <sup>26</sup>. Despite the possibility of reversion, the World Health Organization (WHO) considers the TOPV to be one of the safest vaccines currently available <sup>112</sup>.

#### 1.4.1. Identification of Vaccine Related Strains of Poliovirus

Several tests have been developed in order to monitor the characteristics of polio viruses recovered from individuals suspected of having vaccine-related poliovirus infections. One problem has been positive identification of vaccine-related poliovirus strains.

In 1981, the World Health Organization organized a collaborative study to compare various markers of poliovirus, both antigenic and phenotypic. Antigenic marker tests with cross-adsorbed immune sera were the most dependable for differentiating between wild-type strains and those of vaccine origin <sup>112</sup>. Aluminium hydroxide (Al(OH)<sub>3</sub>) gel elution marker tests were useful for characterising type 1 and 3 isolates. The rct/40 marker test, which tests for the presence of a genotypic marker controlling the ability to replicate at elevated temperature (40°C), gave

highly variable results <sup>112</sup>.

Biochemical methods have also been widely used for differentiating between wild-type and vaccine-related cases of poliomyelitis. Such tests include the use of monoclonal antibodies (MoAb) <sup>71</sup>, mapping of trypsin-generated peptides in two dimensions <sup>52</sup>, polyacrylamide gel electrophoresis (PAGE) <sup>52</sup>, high performance liquid chromatography (HPLC) <sup>43,44</sup>, hybridization experiments using DNA complementary to the virus RNA <sup>115</sup>, and two-dimensional mapping of RNase T<sub>1</sub> resistant oligonucleotides <sup>13,51,63,80</sup>. Of these methods, RNase T<sub>1</sub> oligonucleotide mapping is probably the most widely used.

#### 1.5. Scope of This Study

In this study four biochemical techniques were used for comparing the Gazankulu outbreak strains, vaccine strains and wild-type strains of poliovirus. Comparison of the capsid proteins of poliovirus strains should show which capsid proteins are the most subject to alteration and the degree of relatedness between virus capsid proteins. Studies of the RNAs of different poliovirus strains should indicate the extent of genetic differences between strains. The biochemical techniques used were compared in order to find which was the most rapid, easy to perform and cost-effective. Viral capsid proteins were compared using SDS-polyacrylamide gel electrophoresis (SDS-PAGE) and mapping of trypsin-generated peptides by two-dimensional thin-layer chromatography (TLC) and reversed-phase high-performance liquid-chromatography (RP-HPLC). The fourth technique, two-dimensional

mapping of oligo-nucleotides produced by digestion of viral RNA with Aspergillus RNase T<sub>1</sub>, indicated the degree of relatedness between poliovirus strains at a genetic level.

Discontinuous polyacrylamide gel electrophoresis in sodium dodecyl sulphate-containing gels (SDS-PAGE) is a powerful tool for the separation of polypeptide chains in biological systems. The high resolving power of discontinuous gel electrophoresis is combined with the capability of the anionic detergent, SDS, to break proteins into individual polypeptide chains <sup>54,78</sup>.

Radiolabelling of proteins, followed by digestion with an enzyme such as trypsin, and mapping of the subsequent peptides by TLC or RP-HPLC, allows for a comparison of proteins at the amino acid level. Such mapping can also give a more accurate indication of relatedness than can SDS-PAGE, with proteins differing by as little as one amino acid giving different maps <sup>59</sup>.

Mapping the oligonucleotides obtained by the digestion of viral RNA allows comparison of the entire genome of the virus, and not merely the proteins that it codes for. "Fingerprint" mapping of oligonucleotides produced by specific nuclease cleavage of RNA is carried out by electrophoresis in two dimensions.

Oligonucleotide mapping is most frequently applied as an analytical technique for comparing genomes of RNA viruses <sup>3,12,15,51</sup>. Because the enzymatic cleavage is selective, a specific collection of RNA fragments are formed. Comparisons are based on the principle that large, structurally unique oligonucleotides

separate into patterns, or "fingerprints", which are highly characteristic of the original RNA sequence. The genetic relationships of different virus strains may thus be compared <sup>51</sup>.

Since the characteristic oligonucleotides originate from all regions of the RNA, the distribution of similarities and differences is surveyed over the entire RNA. This allows comparison of the whole genome. Although oligonucleotide fingerprinting does not allow for the sequence of oligonucleotides to be determined, the technique is simple and permits fairly rapid comparison of RNAs <sup>51</sup>.

It was hoped that comparison of the Gazankulu outbreak strains of poliovirus with the Sabin vaccine strains and wild-type strains using SDS-PAGE, TLC, RP-HPLC and oligonucleotide mapping would lead to:

1. Confirmation of the causative agents of the Gazankulu poliomyelitis outbreak of 1982.
2. Determination of the relatedness of Gazankulu outbreak, vaccine and wild-type poliovirus strains at protein and nucleic acid levels.
3. Development of a rapid, inexpensive and relatively easy to perform technique for the comparative identification of poliovirus strains.

## CHAPTER TWO

### MATERIALS AND METHODS

#### 2.1. Propagation and Purification of Virus Strains

##### 2.1.1. Virus and Cell Stocks

Wild-type polioviruses type 1 LS-a, type 2 Lansing and type 3 Leon III were all obtained from the American Type Culture Collection, Rockville, Maryland USA. Sabin live-attenuated virus type 1 LS-c TL13, type 2 P712 TL13 and type 3 Leon 3 were all kindly donated by Professor B. Schoub, Director of the National Institute of Virology (NIV; Johannesburg, South Africa) while Gazankulu outbreak isolates type 1 (strain 5061) and type 2 (strain 5068) were kindly donated by Professor J. Moodie, Virology Department, University of Cape Town, South Africa. No outbreak type 3 was received.

With the exception of poliovirus type 1 strain LS-c, all virus strains were grown in HeLa S<sub>3</sub> cells. Because the virus yield is very poor when poliovirus strain LS-c is used to infect HeLa S<sub>3</sub> cells, this strain was grown in vero cells, derived from the African Green Monkey (Cercopithecus aethiops). Both cell lines were kindly donated by Professor B. Schoub, NIV.

##### 2.1.2. Propagation of Virus

Cells were grown to monolayer in 75cm<sup>2</sup> Falcon flasks containing Eagle's Minimal Essential Medium (MEM)<sup>23</sup>. (Sigma Chemical Company, St. Louis, USA) supplemented with 10% foetal calf serum (FCS; State Vaccine Institute Cape Town), with penicillin (0.1

mg/ml) and streptomycin (0.2 mg/ml).

Once cells had formed a confluent monolayer the culture medium was poured off. This was replaced with 5ml of serum-free medium containing penicillin, streptomycin, fungizone and 0.22% sodium bicarbonate. Sodium bicarbonate is a requirement for Sabin vaccine strain virus growth. Freshly harvested high-titre virus stock (0.2ml) was added to each of 150 to 200 flasks, representing an infectivity of approximately  $10^4$  pfu (plaque forming units) per cell. One flask was left uninfected as a control. High-titre virus stocks were prepared by infecting 10 75cm<sup>2</sup> Falcon flasks with a high multiplicity of infection (0.5ml virus stock per flask). This high-titre stock virus was never more than 5 passages from the original stock.

Infected cells were incubated at 37°C in a Gallenkamp orbital incubator for 16 - 24 hours. Cells were visually examined using a Zeiss inverted light microscope. Once gross cytopathic effects (cpe), involving rounding-up and granulation of the infected cells prior to cell lysis, had been noted and the cells had lifted off the surface of the flask, the contents of the flasks were pooled and stored at 4°C until thorough cooling had occurred. This ensured lysis of infected cells and consequent release of virus.

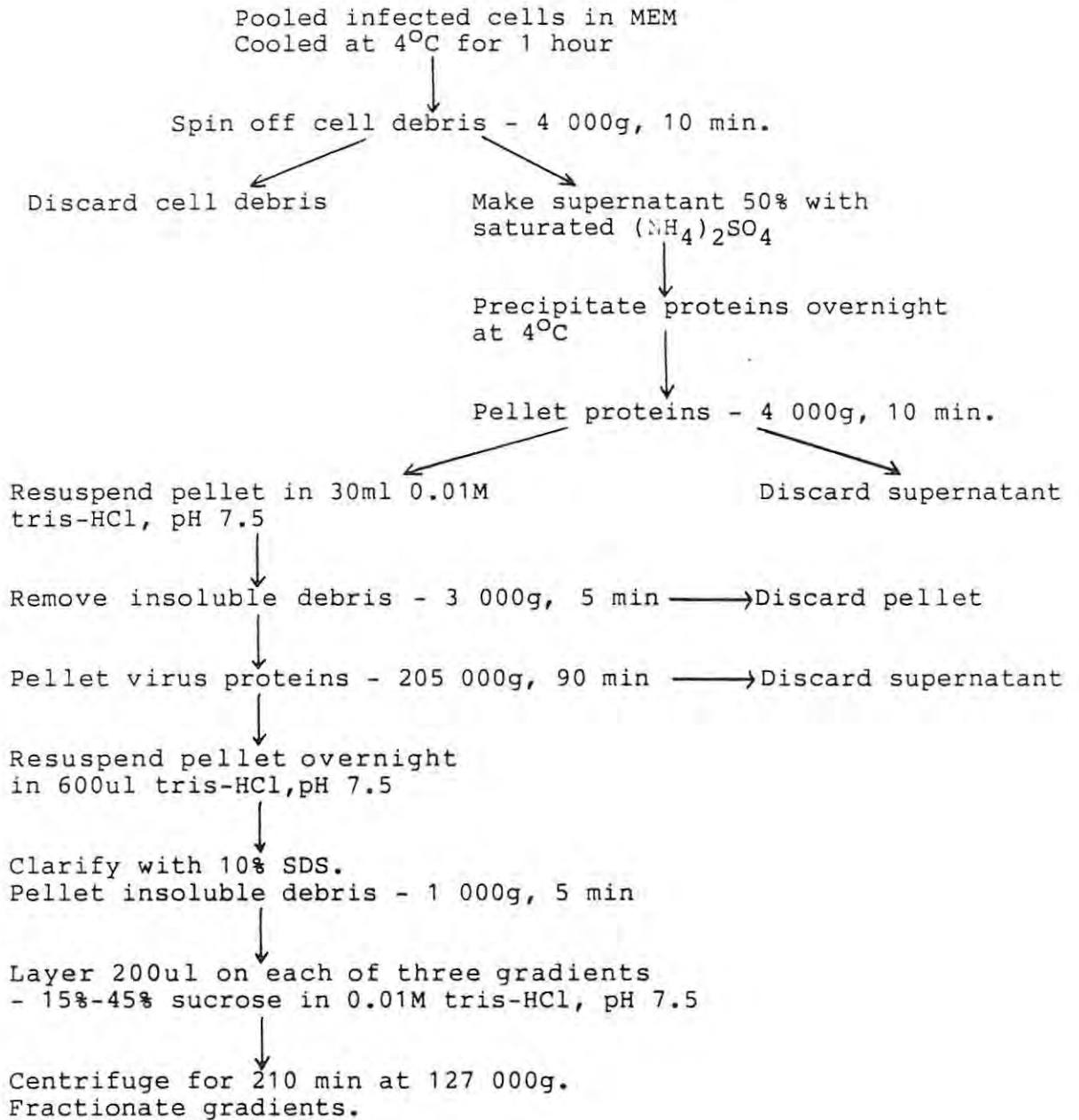
### 2.1.3. Extraction and Purification (see fig.2.1)

#### 2.1.3.1. Ammonium sulphate precipitation

After storage at 4°C for approximately one hour, the pooled MEM



Figure 2.1. Flow chart showing stages in the purification of poliovirus.



containing poliovirus was centrifuged in a Sorvall RC-5 Super Speed refrigerated centrifuge at 4 000g for 10 minutes. This pelleted the cellular debris present in the medium. The pelleted debris was then discarded. Delaying the removal of cellular debris for longer than one hour resulted in reduced virus yields due to the adsorption of virus particles onto cellular membranes.

The supernatant from the 4 000g spin was made 50% with ammonium sulphate (saturated at room temperature) and stored overnight at 4°C. This precipitated the soluble proteins which were then pelleted by centrifuging for 10 minutes at 4 000g in the Sorvall centrifuge. The supernatant was discarded and the pellet resuspended in 30ml of 0.01M tris-HCl buffer, pH 7.5. After centrifugation at 3 000g for 5 minutes, to remove any insoluble contaminants, the clarified supernatant was spun at 205 000g for 90 minutes. The pellet was macerated in 600ul of 0.01M tris-HCl buffer pH 7.5 and left to resuspend overnight at 4°C, after which sucrose density gradient centrifugation was carried out.

#### 2.1.3.2. Sucrose density gradient centrifugation

Purification by sucrose density gradient centrifugation (SDGC) was carried out within 24 hours of pelleting the virus. This minimized viral loss through adsorption to the walls of the centrifuge tube. Solutions of 15 and 45% (w/v) sucrose were made up in 0.01M tris-HCl pH 7.5, and made 0.5M with sodium chloride. The addition of 0.5M NaCl to the sucrose enhanced virus yield by preventing virus aggregation, ensuring uniform sedimentation of virus through the gradient.

Prior to sucrose density gradient centrifugation, 10% sodium dodecyl sulphate (SDS) was added to the resuspended virus pellet to a final concentration of 1%. This separated the virus from cell debris that might be present. Once clarification had taken place the resuspended pellet was centrifuged for 5 minutes at 1 000g to pellet insoluble debris. Three gradients containing 11ml of 15 - 45% sucrose in buffer were prepared in polyallomer tubes and 200ul of the resuspended virus was carefully layered onto each of the gradients before being centrifuged for 210 minutes at 127 000g.

#### 2.1.3.3. Fractionation of purified virus

After centrifugation, the sucrose gradient was fractionated using an ISCO Model 640 Density Gradient Fractionator set at a flow rate of 3ml min<sup>-1</sup> and a trace of absorbance at 254nm obtained using an ISCO UA-5 Absorbance/Fluorescence monitor set at a sensitivity of 0.5 A. Fractions 0.6ml in volume were collected in sterile, silanized glass tubes of 6ml volume and those containing the virus peak were pooled in a sterile, silanized McCartney bottle. Figure 2.2 illustrates a typical trace of poliovirus purified by SDGC. Virus was generally recovered in fractions 11 and 12.

## 2.2. Phenol Extraction of RNA

### 2.2.1 Extraction of Viral RNA

A modified version of the method of Palmiter (1974) was used for the extraction of poliovirus RNA. Pooled SDG fractions containing virus were diluted with 2 volumes of 0.1M sodium acetate

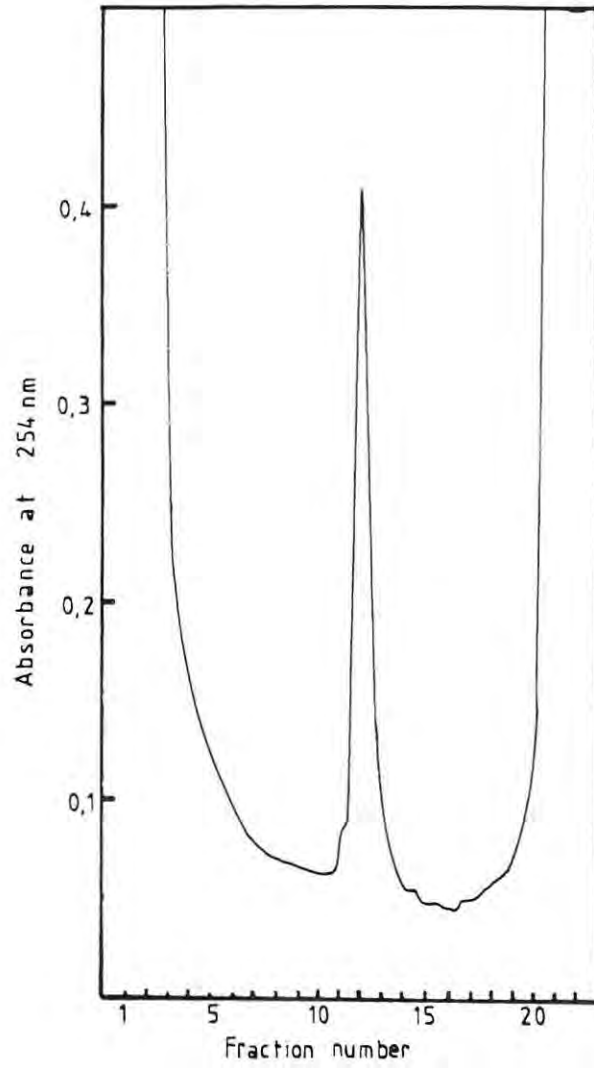


FIGURE 2.2. Typical ISCO trace of absorbance at 254nm of poliovirus purified using SDGC. Trace obtained from poliovirus type 2, Lansing.

buffer pH 5.0, and made 1% with SDS. An equal volume of 0.1M, pH 5.0 sodium acetate buffer-saturated phenol, containing 0.1% 8-hydroxyquinoline was added. After mixing on a Sorvall whirli-mixer for 2 minutes the sample was centrifuged at 3 000g for 5 minutes to separate the phases.

It was important to extract the RNA from the purified virus as soon as possible after fractionation in order to prevent sample loss due to viral adsorption to the walls of the glass tubes/McCartney bottle.

The lower (phenol) phase was removed and retained for protein extraction, along with insoluble proteinaceous material which collected at the phenol interface. The aqueous phase was extracted once more with an equal volume each of buffer-saturated phenol and chloroform. The second phenol phase, and any material at the organic/aqueous interface, was discarded.

#### 2.2.1.1. Calculation of viral RNA yield

Initially the amount of RNA present after phenol extraction was calculated by UV spectrophotometry using a Pye-Unicam SP8-400 UV/VIS spectrophotometer and carrying out a scan of UV absorbance from 320 to 220 nm.

The aqueous phase, containing viral RNA, was washed twice with ether (rapid agitation for 2 minutes, after which the sample was left to stand for one minute so that separation of ether and aqueous phases could take place) in order to remove trace amounts of phenol dissolved in the buffer. A volume corresponding to 1/100 of the aqueous phase i.e. approximately 50ul, was

removed, diluted up to 1ml with distilled water and an absorbance scan carried out.

From the absorbance at 260nm and knowing that 40ug/ml of RNA has an absorbance of 1.0 at 260nm it was possible to calculate the amount of viral RNA present, and thus the concentration of the RNA in the aqueous phase.

Yields of RNA were found to be lower than expected, presumably due to sample loss during the ether washes. For this reason these washes were not carried out in later extractions. The presence of residual phenol rendered spectrophotometry of the extracted RNA impossible. Consequently, approximate yields of RNA had to be calculated from the ISCO absorbance traces obtained after SDGC purification.

At 254nm, the wavelength at which the ISCO monitor was set, RNA absorbance is almost the same as that at 260nm. Protein absorbance is minimal. Consequently the UV absorbance trace obtained is primarily an absorbance trace of RNA.

Assuming the absorbance peak plotted by the ISCO chart recorder to be symmetrical and essentially linear, the area under the curve may be calculated as follows:

$$\text{height} \times \text{base} \times 0.5 \text{ (to compensate for the slope of the peak)}$$

with "height" being the maximum absorbance at 254nm and "base" being the volume of the fractions containing the virus peak. To calculate the concentration of the RNA present the absorbance

value is multiplied by 40, for an absorbance value of 1.0 at 260nm indicates an RNA concentration of 40ug ml<sup>-1</sup>. The answer obtained from the above calculation gives the approximate concentration of the RNA obtained in ug ml<sup>-1</sup>.

This calculation does not, unfortunately, take into account any loss of RNA that may occur during the extraction procedure. However all precautions were taken to minimize the risk of RNase contamination and thus limit RNA loss during all stages of extraction. Gloves were worn and all glassware and buffer solutions (where possible) were autoclaved. The efficiency of such precautions was shown by the fact that RNA samples stored in 95% ethanol at -20°C could still be used several months after initial preparation with no degradation apparent.

#### 2.2.2. Extraction of BHK RNA For Use as Carrier RNA

Baby hamster kidney cells used for the production of carrier RNA (cRNA) were obtained from the State Vaccine Institute, Cape Town. Cells were grown in Glasgow's modification of Eagle's medium supplemented with 10% FCS and antibiotics. Ten 75ml Falcon flasks containing BHK-21 cell monolayers were drained and 5ml of phenol saturated with 0.1M sodium acetate buffer, pH 5.0, and containing 8-hydroxyquinoline, was added to the first flask. The cell monolayer was disrupted using a rubber policeman and the contents poured into the next flask. This procedure was followed for all ten flasks.

The extract was poured into a sterile, silanized McCartney bottle and 5ml of 0.1M sodium acetate buffer, pH 5.0, added.

After mixing for 5 minutes using a vortex mixer the mixture was centrifuged at 3 000g for 5 minutes. The aqueous phase was removed, made 1% with SDS and re-extracted twice with phenol, centrifuging at 3 000g each time in order to separate the phases.

Following the removal of the phenol phase, the aqueous phase was washed three times with an equal volume of ether. As SDS may inhibit separation of the phases <sup>84</sup>, centrifugation at 3 000g for 5 minutes was carried out. The ether was discarded and RNA precipitated by the addition of 2.5 volumes of chilled 95% ethanol followed by storage for at least 24 hours at -20°C.

It should be noted that the SDS was added after the first phenol extraction to prevent DNA contamination of the RNA <sup>84</sup>.

#### 2.2.2.1. Calculation of BHK RNA concentration

After precipitation at -20°C, the RNA was spun at 27 000g for 30 minutes to pellet it. The supernatant was discarded and the pellet carefully drained before vacuum drying. Once dry, the pellet was resuspended in 500ul of 0.1M acetate buffer, pH 5.0, and 50ul removed in order to carry out UV spectrophotometry. The remaining buffer and RNA was transferred to a 1.5ml sterile, silanized Eppendorf tube, mixed with 2.5 volumes of 95% ethanol and precipitated by overnight storage at -20°C.

The 50ul of RNA solution was diluted up to 1ml with distilled water and a scan of UV absorbance from 320-220nm (fig.2.3.) carried out using a Pye-Unicam SP8-400 UV/VIS spectrophotometer. The RNA concentration could then be calculated as mentioned in



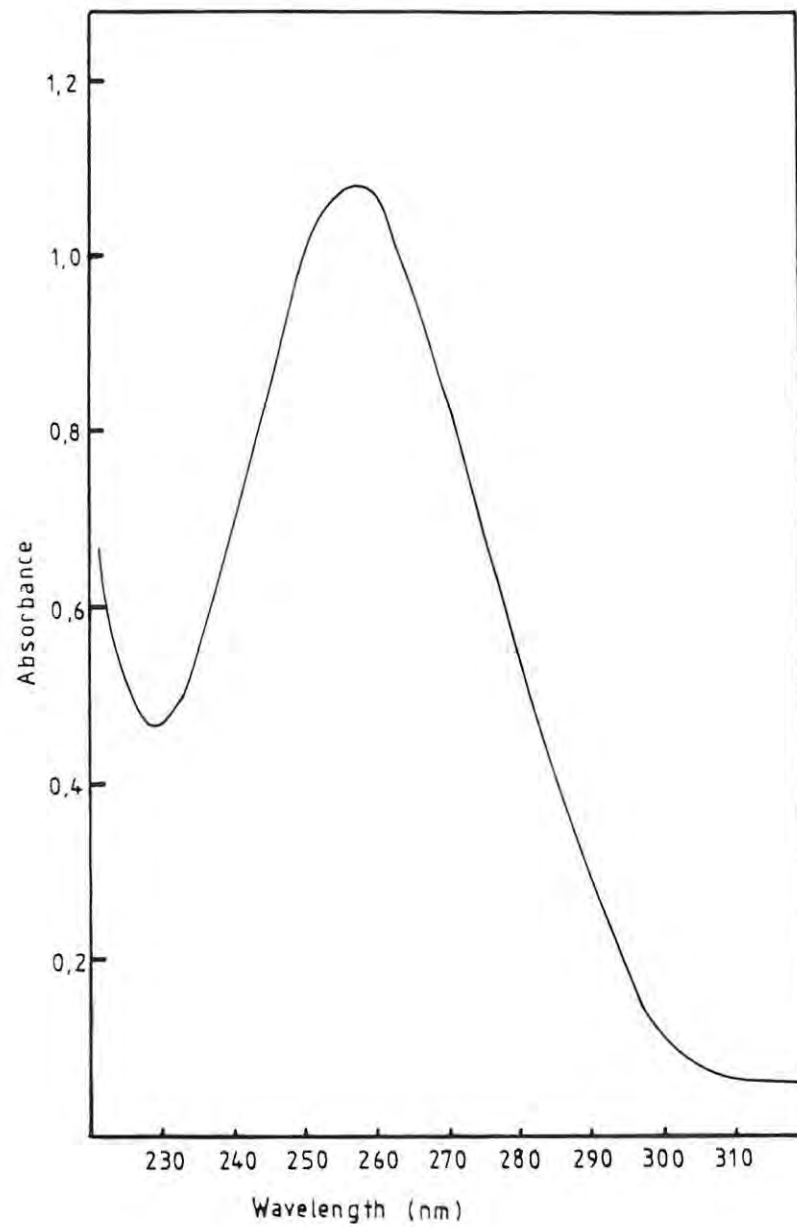


FIGURE 2.3. Trace of absorbance of a purified BHK RNA sample, scanned from 320 - 220 nm.

section 2.2.1.1. Additionally, the steepness of the peak slope indicated the purity of the RNA and whether it had been degraded or not.

### 2.2.3. Storage of RNA

Ethanol precipitated RNA was pelleted at 27 000g for 30 minutes and the pellet carefully drained and vacuum dried. The RNA was resuspended in 0.5ml of 0.1M sodium phosphate buffer, pH 5.0, and 2.5 volumes of 95% ethanol added.

As the concentration of the viral RNA was known, having been calculated from the ISCO trace at 254nm, the RNA solution was divided up into aliquots each containing approximately 5ug of RNA. These were stored at -20°C in sterile, silanized 0.5ml Eppendorf tubes. This eliminated the necessity of constantly re-opening a single stock of viral RNA and risking RNase contamination of the entire stock.

## 2.3. Extraction of Virus Protein From Phenol

### 2.3.1. Extraction of Viral Protein

The first phenol phase from the RNA extraction was made 0.1M with ammonium acetate (NH<sub>4</sub>OAc) and 1% β-mercaptoethanol (β-Me). After thorough mixing, 6 volumes of chilled 95% ethanol were added and the sample stored at -20°C in a silanized McCartney bottle. Storage for at least 12 hours at -20°C was required for protein precipitation.

#### 2.3.1.1. Calculation of protein concentration

The concentration of the virus protein obtained by SDGC was

calculated from the ISCO trace using the formula  $E_{260}^{1\%} = 77.93$ . Alternatively, once the RNA concentration had been calculated the virus protein yield could be calculated on the basis that the ratio of RNA to protein, in poliovirus, is 30 : 70.

## 2.4. Polyacrylamide Gel Electrophoresis

### 2.4.1. Polyacrylamide Gel Preparation

Gels containing 10% (resolving gel) or 4% (stacking gel) acrylamide were prepared according to the method of Laemmli (1970), from a stock solution of 30% (w/v) acrylamide and 0.8% (w/v) N,N'-bis-methylene acrylamide. The resolving gel was made 0.375M with respect to tris-HCl, pH 8.8, and SDS was added to a concentration of 0.1%. Polymerization was carried out chemically by adding 0.025% (v/v) tetramethylethylenediamine (TEMED) and 0.075% ammonium persulphate. TEMED accelerates the polymerization reaction catalysed by ammonium persulphate.

Concentrations in the stacking gel were 0.125M tris-HCl (pH 6.8), 5.33% (v/v) glycerol and 0.1% SDS. Chemical polymerization was carried out by adding 0.13% (v/v) TEMED and 0.07% ammonium persulphate. Care was taken when handling acrylamide because of its neurotoxicity. Even fully polymerized gels may have up to 15% monomeric reactants <sup>36</sup>.

Once the 27ml stacking gel had polymerized, the surface was rinsed with distilled water in order to remove any unpolymerized acrylamide. The gel surface was then carefully dried and overlaid with 7ml of stacking gel and a slot-forming comb inserted

to form 10 wells each of 50ul capacity.

After complete polymerization of the stacking gel the comb was carefully removed and the wells and upper and lower reservoirs of the electrophoresis apparatus filled with electrophoresis buffer (0.303% Tris (w/v), 1.44% glycine (w/v) and 0.1% SDS (w/v)). Protein samples were layered onto the bottom of the wells using a 50ul Hamilton microsyringe. The wells at either end of the gel were loaded with 50ul of dissociation buffer (10% SDS (w/v), 10%  $\beta$ -Me (v/v), 15% glycerol (v/v), 0.01% bromophenol blue (w/v) in 1M tris-HCl pH 6.8) in order to ensure a constant ionic strength across the gel and prevent distortion ("smiling") of protein bands.

#### 2.4.2. Sample Preparation

Phenol-extracted virus protein, stored in 95% ethanol at -20°C, was pelleted by centrifugation at 27 000g for 30 minutes. The pellet was carefully drained and vacuum dried, before being resuspended in 50ul of dissociation buffer. This was heated at 100°C for 5 minutes in order to dissociate the virus prior to protein separation on polyacrylamide gels containing sodium dodecyl sulphate (SDS-PAGE).

Sufficient viral protein (concentration calculated as described in section 2.3.1.1) was applied to the gel for there to be approximately 10ug of each of the viral capsid proteins.

Virus proteins were co-electrophoresed with molecular weight marker proteins (table 2.1). Markers were prepared according to

TABLE 2.1. Molecular weights of Sigma marker proteins used in SDS-PAGE.

PROTEIN	MOLECULAR WEIGHT
Bovine serum albumin (BSA)	66 000
Ovalbumin (Ov)	45 000
Glyceraldehyde-3-phosphate dehydrogenase (GPD)	36 000
Carbonic anhydrase (CA)	29 000
Trypsinogen (T)	24 000
Trypsin inhibitor, soybean (TI)	20 100
$\alpha$ -Lactalbumin (L)	14 200

manufacturer's instructions (Sigma Chemical Co., St.Louis, USA) and stored at  $-20^{\circ}\text{C}$  in 40ul fractions.

#### 2.4.3. Electrophoresis

Proteins were resolved by electrophoresis in a Bio-Rad Model 220 dual vertical slab gel electrophoresis cell (Hoeffer Scientific Instruments). Electrophoresis was carried out at 100V using a Gelman Instrument Company powerpack for 4.5 to 5 hours. When the ionization front had migrated off the bottom of the gel and the bromophenol blue band was 2mm from the end of the gel electrophoresis was ended. During electrophoresis the temperature of the gels was controlled by circulating water through the apparatus.

#### 2.4.4. Staining and Storage of Gels

Following electrophoresis gels were removed from the apparatus and protein bands were fixed and stained with Coomassie blue (0.2% coomassie brilliant blue R250 (w/v), 10% acetic acid (v/v), 45% methanol (v/v)) for 1.5 hours at  $37^{\circ}\text{C}$  in a Gallenkamp orbital incubator. For effective staining of gels 10 gel-volumes of stain or more were used to eliminate competition for stain between SDS in the gel and protein <sup>106</sup>.

Destaining was carried out at  $37^{\circ}\text{C}$  using several changes of destain (45% methanol (v/v), 7% acetic acid (v/v)) until the protein bands could be clearly visualised and the background was almost colourless. Gels were vacuum dried onto Whatman no. 1 paper at  $89^{\circ}\text{C}$  for 1.5 hours using a Model SE 540 Slab Gel Dryer

(Hoeffer Scientific Instruments) attached to a vacuum pump. They could then be stored indefinitely.

## 2.5. Tryptic Peptide Mapping of Poliovirus Proteins

### 2.5.1. Production of Radiolabelled Peptides

#### 2.5.1.1. Preparation of gel slices

Virus proteins were resolved using SDS-PAGE, and individual protein bands were cut out of the gel using a sterile scalpel and placed in separate beakers. One gel slice per protein was used, and each slice contained approximately 10ug of protein. Gel slices were washed extensively to remove SDS and other contaminants which might interfere with the labelling and digestion processes. The initial wash was in 1l 25% iso-propanol and the second in 1l 10% methanol. In each case the gel slice was washed for at least one hour, with constant stirring. After washing, the gel slices were dried in sterile iodination tubes, either overnight at 37°C or for 2 hours under vacuum.

#### 2.5.1.2. Iodination of proteins in gel slices.

Proteins to be used for either two-dimensional thin-layer chromatography (TLC) or reversed-phase high-performance liquid-chromatography (RP-HPLC) were iodinated with  $^{125}\text{I}$  (Amersham International plc, England). Iodination was carried out with the proteins still in the gel slice using the chloramine-T method as used by Greenwood et al (1963) and modified by Elder et al (1977).

The chloramine-T reaction has a pH optimum of about 7.5, and  $^{125}\text{I}$  from Amersham is supplied in NaOH, pH 8-10. The pH of the

$^{125}\text{I}$  was adjusted to 7.5 with 180ul 0.5M sodium phosphate buffer. Addition of the sodium phosphate buffer also diluted the  $^{125}\text{I}$  from 100uCi/ul to its working concentration of 10uCi/ul.

To each dried gel slice, 20ul of 0.5M sodium phosphate buffer, pH 7.5, followed by 100uCi of  $^{125}\text{I}$  and 5ul of freshly prepared chloramine-T (1mg/ml)(May and Baker Ltd., Dagenham, England) was added. Gel slices were allowed to absorb the reagents for 1 hour at room temperature. The reaction was terminated by the addition of 1ml of fresh sodium metabisulphite (1mg/ml)(BDH Chemicals Ltd., Poole, England). After 15 minutes the sodium metabisulphite was poured off and the gel slices washed (separately) overnight in three 1l changes of 10% methanol, with continuous stirring. The washing served to elute unreacted  $^{125}\text{I}$  from the gel slices, and the radioactivity of the methanol after the final wash was less than 1% that of the original wash.

After washing the gel slices were put individually into sterile 1.5ml Eppendorf tubes and dried for 2-3 hours under vacuum.

#### 2.5.1.3. Trypsinization of proteins

Immediately prior to tryptic digestion of the radiolabelled proteins, 60ul of 0.1M sodium iodide was added to the gel slices in order to oxidise any remaining free  $^{125}\text{I}$  <sup>10</sup>. Trypsinization was carried out by the addition of 50ug of 1mg/ml DPCC (diphenyl carbamyl chloride) treated trypsin (Sigma Chemical Co.) in 0.5ml of 0.1M ammonium hydrogen carbonate, pH 8.0, followed by incubation for 24hr at 37°C. In order to prevent bacterial



contamination 20ul of toluene was added. After 24 hours, a further 20ug of trypsin was added and digestion allowed to continue for 2 hours, at 37°C, to ensure complete digestion. The supernatant was carefully withdrawn and dried under a gentle stream of sterile air in sterile 0.5ml glass tubes.

During all stages of radiolabelling and trypsinization care was taken to ensure that there was no contact with the gels which could result in the labelling of contaminating proteins. Additionally, the introduction of proteolytic enzymes could cause non-specific proteolytic cleavage of the proteins.

#### 2.5.2. Controls

Similar controls were run for both thin layer chromatography (TLC) and reversed-phase high-performance liquid-chromatography (RP-HPLC). In the first control a "blank" slice of polyacrylamide gel was excised from an area which contained no proteins and was distant from tracks which did contain proteins. This was treated in the same manner as those slices which contained proteins, and mapped by TLC and RP-HPLC. In the second control trypsin was electrophoresed using SDS-PAGE. A gel slice containing 10ug of trypsin excised then radiolabelled and digested before being mapped.

As an additional control, reproducibility of the results obtained by mapping radiolabelled peptides was determined. Two samples of ovalbumin, resolved using SDS-PAGE, were labelled and digested before being subjected to TLC. Two samples of bovine

serum albumin (BSA) were treated in the same manner and their peptides mapped using RP-HPLC.

### 2.5.3. Two-Dimensional Thin Layer Chromatography (TLC)

#### 2.5.3.1. Preparation of TLC plates

TLC analysis of  $^{125}\text{I}$  labelled tryptic peptides was carried out on cellulose TLC plates, 20cm x 20cm with a 100um layer of cellulose (Merck, Darmstadt, Germany). Two marks were made on the underside of the plate 3cm from opposite sides of the plate and 2.5cm from the shared edge. Over one of the marks 1ul of marker dye (2% orange G (w/v) and 1% acid fuchsin (w/v) in a 1:1 ratio) <sup>24</sup> was applied. Radiolabelled peptides, resuspended in 10ul of deionized, "polished" water, were applied over the opposite mark.

In order to ensure good peptide resolution, spot size was minimized (approximately 3mm in diameter) by repeated applications of less than 0.1ul of sample, and by allowing the spot to dry completely between applications. Drying was assisted by placing a lamp below the plate, at a sufficient distance to warm the plate without without heat damaging the peptides. Back lighting also showed up the position of the application spot.

#### 2.5.3.2 Electrophoresis

Electrophoresis was carried out at room temperature in a Shandon tank fitted with a cooling plate. Electrophoresis buffer consisted of 15% acetic acid and 5% formic acid in distilled water, adjusted to pH 1.4 with additional formic acid <sup>24</sup>. In order to prevent gravitational distortion of the peptide migration

patterns, the cooling plate, on which the TLC plate rested, was carefully levelled before electro-phoresis.

The TLC plate was carefully positioned in the tank and sprayed lightly with electrophoresis buffer to ensure uniform current flow. Electrical contact was made with the aid of buffer-moistened strips of Whatman no.1 paper (20cm x 5cm), laid along opposite sides of the TLC plate and 2cm in from the edges. To prevent dehydration of the plate during electrophoresis, a glass cover plate sprayed with electrophoresis buffer was placed over the TLC plate. The cover plate was supported 2cm above the TLC plate by weights holding the paper wicks in place (fig. 2.4).

Electrophoresis was carried out at 10 watts for 70 minutes using an LKB Bromma 2197 power supply. Electrophoresis was monitored by the progress of the acid fuchsin and orange G dye markers and ended when the lead component of the acid fuchsin reached the sample origin. At a pH of 1.4 the marker dyes moved from the cathode to the anode while the peptides, which are positively charged at this pH, migrated from the anode to the cathode. After electrophoresis, plates were dried overnight at room temperature in a horizontal rack under a fume hood.

#### 2.5.3.3. Ascending chromatography

Ascending chromatography was carried out in the second dimension using the buffer system described by Gentsch and Fields (1981). This consisted of butanol, pyridine, acetic acid and distilled water in the ratio 15:10:3:12. The atmosphere within the chromatography tank was saturated with buffer vapour by lining

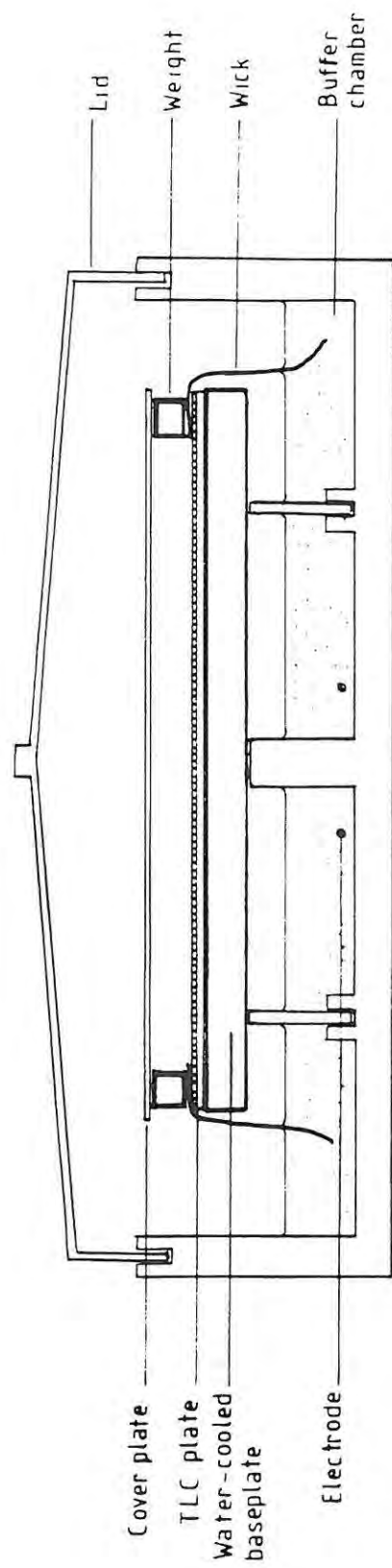


FIGURE 2.4. Cross-section of the thin-layer chromatography apparatus.

the tank with Whatman no.1 paper moistened with buffer.

Chromatography was at right angles to the direction of electrophoresis (figure 2.5.b), with plates placed vertically in the chromatography tank and the buffer reaching 0.5cm up from the lower edge of the plate.

Peptides were chromatographed until the solvent front was 1cm from the top edge of the plate (figure 2.5.b). The chromatogram was removed and dried horizontally under a fume hood overnight at room temperature. Figure 2.5.a shows a photograph of a TLC plate after completion of electrophoresis and chromatography.

#### 2.5.3.4. Autoradiography

A sheet of Cronex-4 medical X-ray film (IE Du Pont de Nemours), 19cm x 20cm, was placed on the TLC plate and held in place by a second glass plate. The assembly was wrapped in two sheets of aluminium foil, and exposure of the film was allowed to proceed for 24 hours to two weeks. Development and fixation of autoradiographs was carried out using Kodak GBx developer and fixer. The film was soaked in each for 5 minutes with periodic agitation and washed for 2 minutes in water before and after fixing. The autoradiograph was then hung to dry in a cool, dust-free environment.

#### 2.5.4. Reversed-Phase High-Performance Liquid-Chromatography (RP-HPLC)

##### 2.5.4.1. Apparatus

Trypsin digests of proteins were separated using a slurry-packed



FIGURE 2.5.a. Photograph of TLC plate after completion of electrophoresis and chromatography.

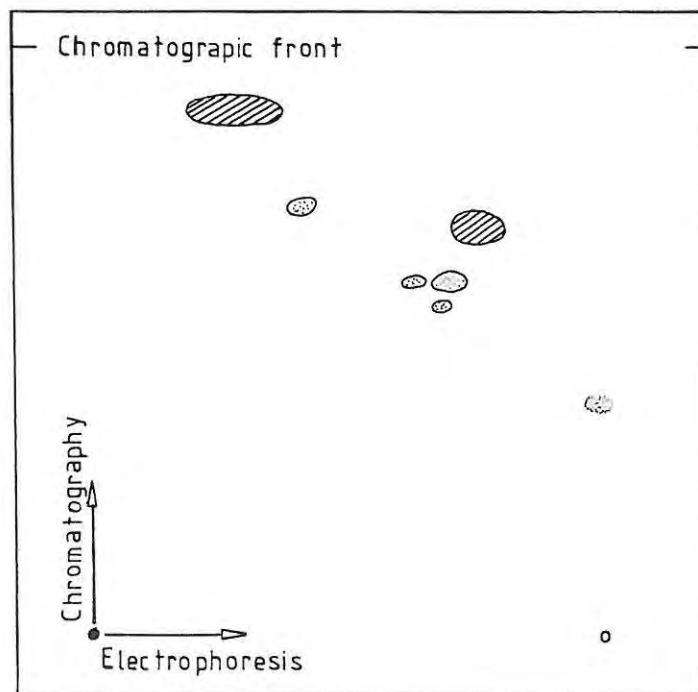


FIGURE 2.5.b. Diagrammatic representation of a TLC plate, showing directions of electrophoresis and chromatography. Dye marker origin indicated by (●), sample origin by (○). Acid fuchsin components shown by [hatched square], orange G components by [dotted square].

stainless steel column 300mm x 3.9mm (internal diameter) protected by a 40mm x 4mm (internal diameter) stainless steel guard column containing 200µ diameter glass beads (Sigma Chemical Co).

The reverse phase consisted of microparticulate octadecyl silane (ODS) packing material (Techsil C-18; HPLC Technology, UK), with an average particle size of 10µm. Packing of both columns was carried out at the Rhodes University School of Pharmaceutical Science.

The high pressure chromatography system consisted of a Phillips Pye Unicam PU 4010 dual-piston pump. Peptide samples were introduced into the system using a Rheodyne injection port with a 100µl sample loop. Eluate was collected in scintillation vials loaded onto an LKB 2112 Redirac fraction collector. The collection time for each fraction was 12 seconds. Total radioactivity, in counts per minute (cpm), of each fraction was determined using a Beckman Model 310 gamma counter fitted with the <sup>125</sup>I isoset.

Absorbance of the eluate at 220 nm was monitored constantly using a Phillips Pye Unicam PU 4020 adjustable UV detector set at a sensitivity of 0.16 AUFS (absorbance units full scale) and recorded using a Hitachi QPD 54 chart recorder.

#### 2.5.4.2. Solvents

Acetonitrile and methanol used during chromatography runs were Hi Per Solv grade (BDH Chemicals Ltd). Phosphoric acid, analysis grade, was purchased from Merck. High grade deionized

"polished" water was produced in the laboratory using a Milli-Q reagent system (Millipore S.A., Molesheim, France).

Solvent solutions were made up freshly on the day of use and filtered under vacuum through a 0.45um Millipore membrane filter prior to use. Vacuum filtration also served to degas solutions, preventing the build up of bubbles in the piston heads. This would result in fluctuations in the pressure of the system and a potential decrease in resolving power of the column due to damage to the ODS packing material.

In order to further protect components of the HPLC system, the delivery tube from the gradient maker was fitted with a 2um stainless steel filter. A 5um in-line stainless steel filter was fitted upstream of the sample injection port.

#### 2.5.4.3. RP-HPLC of trypsin-generated peptides

Tryptic digests of radiolabelled proteins which had been dried under a stream of sterile, dry air, were rehydrated with 25ul of deionized "polished" water and 1ul removed in order to calculate the total radioactivity of the sample. Using a Hamilton series 7000 microsyringe of 25ul capacity the digest was injected into the system and gradient elution initiated. Activity of the sample injected was between  $2.5 \times 10^5$  and  $3.5 \times 10^5$  counts per minute (cpm).

Peptides were eluted at room temperature using a linear gradient. Optimal elution conditions consisted of a gradient of 5% - 40% acetonitrile containing 0.1% phosphoric acid. Gradients were formed using a glass gradient maker constructed



in the laboratory. This consisted of two cylindrical reservoirs each with a capacity of 50ml, connected at their base. A tap between the two reservoirs prevented solvent mixing prior to gradient initiation. Solvent mixing was carried out by the action of a magnetic stirrer bar in the first reservoir, from which a delivery tube led to the HPLC pump. Every attempt was made to ensure standardization of elution conditions but it was not possible to produce identical gradients. Differences between gradients were, however, minor.

The gradient was initiated immediately after the injection of the sample, as was fraction collection. Gradients were run for 60 minutes at a flow rate of  $1.0 \text{ ml min}^{-1}$ , during which time 250 fractions were collected.

After each RP-HPLC run the column was reconditioned by pumping through 40% acetonitrile containing 0.1% phosphoric acid for 5 minutes, followed by 5% acetonitrile with phosphoric acid. The 5% acetonitrile/phosphoric acid was pumped through the column until the absorbance at 220 nm had returned to zero, indicating that all of the 40% acetonitrile (which has a higher UV absorbance than 5% acetonitrile) had been flushed out.

#### 2.5.4.4. Column storage

If the column was to be out of operation overnight or longer, 40% methanol in deionized "polished" water was pumped through the system at  $1.0 \text{ ml min}^{-1}$  for 30 minutes. This ensured that any remaining acetonitrile and phosphoric acid, which could cause deterioration of the ODS packing material, had been fully dis-

placed. Methanol at a concentration of 40% was used rather than pure water to prevent the growth of microorganisms within the system.

## 2.6. RNase T<sub>1</sub> Oligonucleotide Mapping

### 2.6.1. 5'-End Labelling of RNA Oligonucleotides

#### 2.6.1.1. Preparation of RNA

RNA extracted from purified poliovirus and stored in 95% ethanol at -20°C was centrifuged at 27 000g for 30 minutes. The pellet was drained and dried thoroughly under vacuum before in vitro 5'-end labelling using  $\gamma^{32}\text{P}$ -ATP as described by Pederson and Haseltine (1980).

#### 2.6.1.2. Digestion of viral RNA

Dried RNA (approximately 5ug) in a 0.5ml Eppendorf tube was resuspended in 1ul sterile distilled water. To this was added 1ul 40mM tris-HCl (pH 8.0) containing 0.2 units Aspergillus oryzae RNase T<sub>1</sub> (Boehringer Mannheim, Germany) and  $2 \times 10^{-4}$  units Echerichia coli Type III N alkaline phosphatase (BAP; Sigma Chemical Co.) for each microgram of RNA. Incubation was carried out for 30 minutes at 37°C.

#### 2.6.1.3. Radiolabelling of oligonucleotides

Immediately after incubation the polynucleotide kinase (PNK) reaction was initiated by adding 50ul of PNK reaction mix and 5 units of PNK, obtained from E. coli infected with T<sub>4</sub> phage (Bethseda Research Laboratories, USA). The PNK reaction mix was prepared by vacuum drying 50uCi  $\gamma^{32}\text{P}$ -ATP (>4 000 Ci/mmol; ICN Radiochemicals, Irvine, USA) in a 0.5ml Eppendorf tube and

dissolving the labelled ATP in 50ul of the following solution: 10mM  $K_2HPO_4 - K_3PO_4$  (pH 9.5), 10mM magnesium acetate, 5mM dithio-threitol. The 10mM phosphate in the PNK reaction mix inhibited contaminating phosphatase <sup>85</sup>. This eliminated possible charge and/or migration heterogeneity due to partial dephosphorylation.

Labelling was carried out at 37°C for 12 hours and the reaction terminated by the addition of 50ul of 0.6M ammonium acetate and 100ug of carrier RNA (prepared as described in section 2.2.2.).

Precipitation of carrier RNA and oligonucleotides was carried out by adding 300ul cold (-20°C) 95% ethanol and chilling at -20°C for 20 minutes. The precipitate was collected by centrifugation in a Beckman Microfuge B for 15 minutes at 4°C, washed with 400ul of cold 95% ethanol and microfuged for 5 minutes at 4°C. The ethanol was carefully poured off and the cRNA, with radiolabelled oligonucleotides, vacuum dried.

## 2.6.2. Two-Dimensional Electrophoresis of Oligonucleotides

### 2.6.2.1. Apparatus

Gels were cast between 0.3cm-thick glass plates (36cm x 16.5cm and 38cm x 36cm for the first and second dimensions, respectively). One plate of each set had a notch 2.0cm deep cut in it which extended to within 3cm of either end of the top edge. Spacers at either side of the gels consisted of 0.15cm thick "Perspex" strips, 38cm long and 3cm wide.

Wells (0.75cm wide and 1.5cm deep) in the first-dimension gel

were formed using three teeth of a teflon well former from the Laemmli PAGE apparatus.

Plates were assembled with a spacer at each side, and were held together by a plastic clamp running the length of the glass plates. The spacers were lightly coated with grease (for example "Vaseline") before putting them in place. This ensured good sealing of the plates. To prevent leakage of the first-dimension gel during polymerization, the assembly, notched plate uppermost, was tilted at  $15^{\circ}$  and the base of the plates placed in a 1.5cm deep trough which was then filled with 4% agar.

During polymerization of the second-dimension gel, the assembly was placed in the second-dimension electrophoresis tank, notched plate up, at a  $30^{\circ}$  angle. The tank was filled with buffer until the level was almost up to the top of the gel plates. This ensured that hydrostatic pressure prevented leakage of the gel, while the buffer kept the gel cool during polymerization <sup>60</sup>.

Electrophoresis was carried out in two Perspex electrophoresis tanks, built by the Rhodes University Department of Physics and Electronics (see fig. 2.6. and 2.7.). During operation the first-dimension gel assembly was held in place by stainless steel clips, while the second-dimension assembly was held in place by two "G"-clamps which fastened it to the electrophoresis tank.

#### 2.6.2.2. First-dimension gel electrophoresis

##### 2.6.2.2.1. First-dimension polyacrylamide gel preparation

The acrylamide used was Electran grade (BDH Chemicals Ltd.),

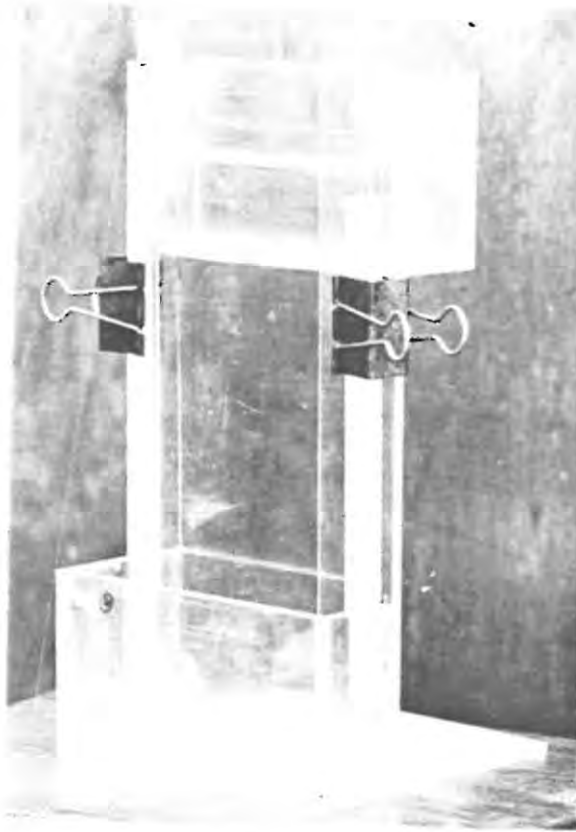


FIGURE 2.6.a. First-dimension electrophoresis apparatus used for RNase T<sub>1</sub> oligonucleotide mapping of poliovirus RNA.

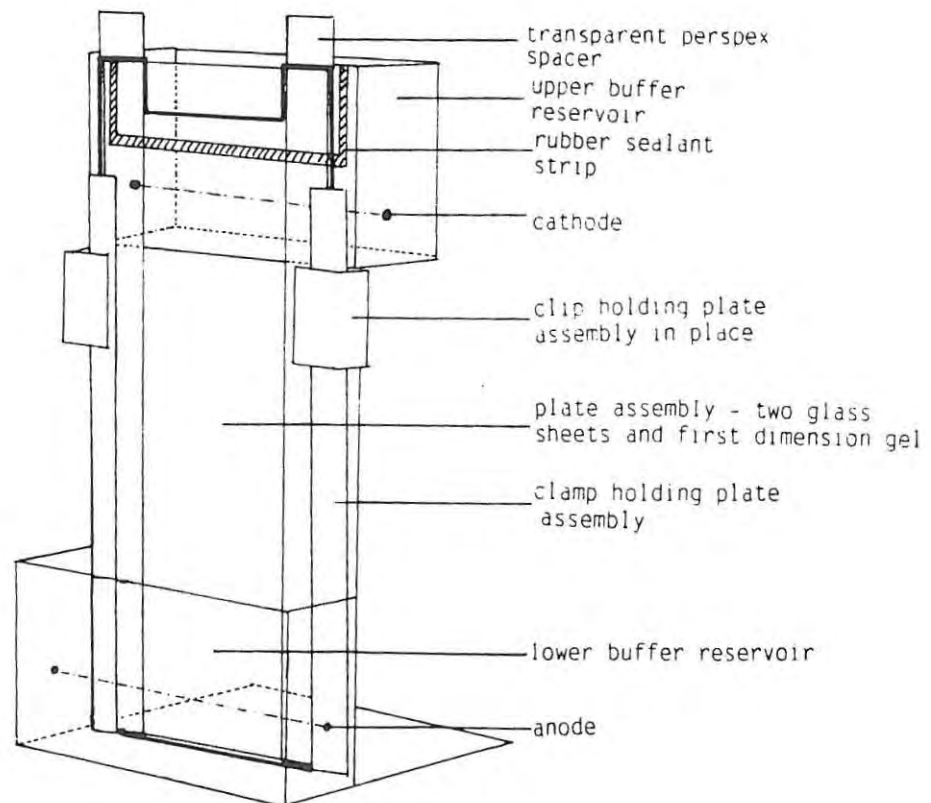


FIGURE 2.6.b. Schematic drawing of electrophoresis apparatus.

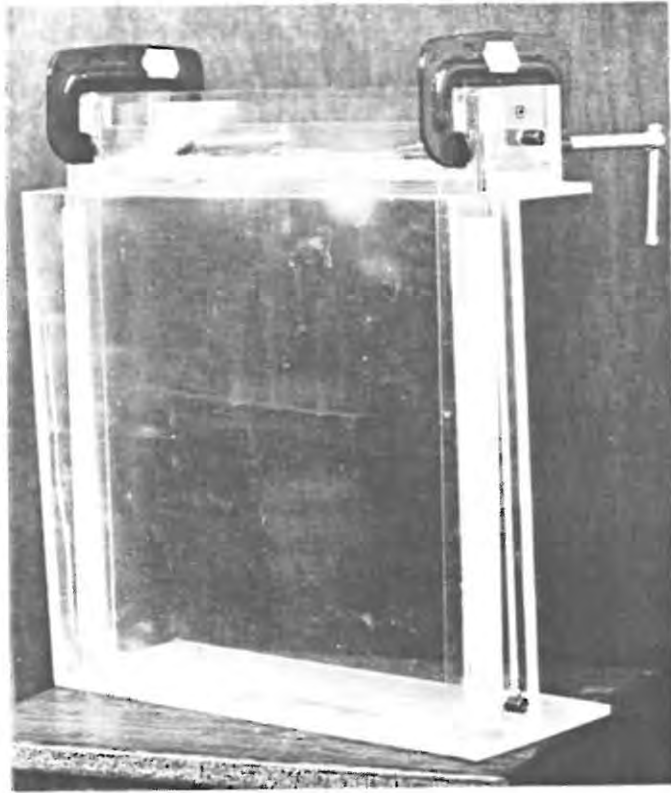


FIGURE 2.7.a. Second-dimension electrophoresis apparatus used for RNase  $T_1$  oligonucleotide mapping of poliovirus RNA.

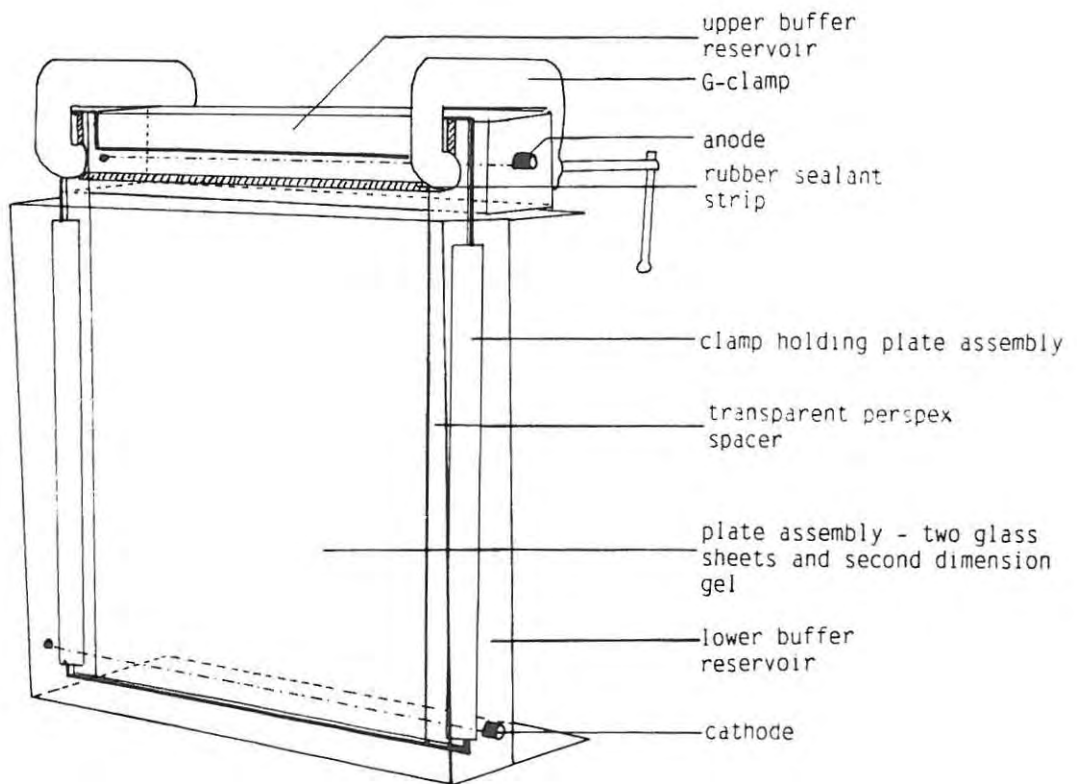


FIGURE 2.7.b. Schematic drawing of electrophoresis apparatus.

while N-N'-bis-methylene acrylamide was Synthesis grade (Merck). All other chemicals were AnalaR (BDH Chemicals Ltd.). De-ionized, "polished" water was obtained in the laboratory using a Milli-Q reagent system (Millipore S.A.).

Gels containing 8% acrylamide were prepared from acrylamide stock (40% acrylamide, 0.5% N-N'-bis-methylene acrylamide), mixed with 9M urea to a final concentration of 6M urea, and the pH adjusted to 3.3 with citric acid, saturated at room temperature.

The catalysts of Jordan and Raymond (1969)(ferrous sulphate, ascorbic acid and hydrogen peroxide) were used for polymerizing the gel (table 2.2.). Care was taken to ensure that the catalysts were added in the order shown in the table.

Table 2.2. Stock solutions for the first-dimension gel system<sup>51</sup>.

COMPONENT	VOLUME REQUIRED FOR ONE GEL
Acrylamide:Bis (40:0.5)	18.0ml
Urea, 9M	60.0ml
Deionized water	8.5ml
Saturated citric acid	0.7-1.0ml
FeSO <sub>4</sub> .7H <sub>2</sub> O (0.16% (w/v))	0.5ml
Ascorbic acid (1% (w/v))	2.0ml
Hydrogen peroxide (30%)	75ul

The FeSO<sub>4</sub>.7H<sub>2</sub>O (in 0.5ml aliquots) and ascorbic acid (in 2ml fractions) were stored at -20°C, after filtration through a 45um Millipore filter. Hydrogen peroxide was stored at 4°C.

Gel was poured into the first-dimension gel assembly, with the liquid level up to the notch in the upper glass plate. A teflon well-forming comb was inserted to a depth of approximately 1cm. Any bubbles present were removed by tapping the glass plate until they floated to the surface.

After polymerization, which took approximately 30 minutes, the well former was removed and the plate assembly removed from the agar-filled trough. Any agar adhering to the bottom of the gel was carefully removed using a sterile syringe needle. The plates were fastened into place and the top and bottom reservoirs of the electrophoresis apparatus filled with electrophoresis buffer (25mM citric acid adjusted to pH 3.3 with solid sodium hydroxide). Care was taken to ensure that no bubbles were trapped at the bottom of the gel, as these could result in poor electrophoresis.

#### 2.6.2.2.2. Sample preparation

Prior to electrophoresis, vacuum dried oligonucleotides and cRNA were resuspended in 20ul of sample buffer (4.5M urea, 50% glycerol (v/v)) containing two dye markers (bromophenol blue (BPB) and xylene cyanol (XC), each at a concentration of 0.5% (w/v)). Protonation of adenine and cytosine residues by urea prevented aggregate formation <sup>19</sup>. Markers were used to monitor the progress of electrophoresis. In order to calculate the radioactivity 1ul of the sample was removed. The remaining sample was carefully layered onto the bottom of the central well using a sterile, silanized disposable 10ul micropipette.



#### 2.6.2.2.3. Electrophoresis

Electrophoresis was carried out at a constant potential of 450V (approximately 7mA) using an LKB Bromma 2197 power supply. The power setting did not exceed 3.2W because of excessive heat production above this wattage. The electrophoresis run was terminated when the bromophenol blue marker dye (green at pH 3.3) had migrated 25cm from the origin. This took 7.5 to 8.25 hours. The XC migrated more slowly than the BPB, moving through the gel with the larger oligonucleotides.

#### 2.6.2.3 Second-dimension gel electrophoresis

##### 2.6.2.3.1. Preparation of the first-dimension gel strip for second-dimension electrophoresis

After electrophoresis in the first dimension was complete, the notched glass plate was removed. Using a 3cm x 38cm perspex template as a guide, a gel strip containing the migration lane of the oligo-nucleotides was cut out with a rotary pastry cutter. The ends of the gel strip were removed 22cm above and 7cm below the lower edge of the BPB marker spot, resulting in a strip 29cm long - the width of the second-dimension gel.

The first-dimension gel strip was removed carefully from the glass plate in order to avoid stretching it and soaked twice for five minutes in 100ml second-dimension electrophoresis buffer (50mM tris-borate, pH 8.2). This served to elute urea which would otherwise inhibit polymerization at the interface of first dimension and connecting gels.

After soaking, the gel strip was drained and placed in position

parallel to, and 1 - 2 mm from, the short (36cm) edge of the un-notched second-dimension electrophoresis plate. After the positioning of a spacer at each end of the strip (in contact with the ends of the strip and perpendicular to it) the second glass plate was put in place. Clamps were attached and the assembly placed upright with the lower edge resting on the bottom of the glass trough.

In order to remove any bubbles between the gel and plate 10ml of second dimension electrophoresis buffer was poured in and the plates pressed against the gel. After 10 minutes the buffer was poured off and the gel strip overlaid with 5ml of connecting gel. The chamber was tipped from side to side to ensure good coverage of the first dimension gel strip. The low cross-linked connecting gel (10% acrylamide (40:0.5 acrylamide:bis stock) 0.1M tris-borate pH 8.2, 0.25% TEMED (v/v) and 0.124% ammonium sulphate (using a 10% w/v stock)) formed a sealant and junction between the first and second dimension gels <sup>51</sup>. Polymerization was complete within 5 minutes.

#### 2.6.2.3.2. Second dimension polyacrylamide gel preparation

The second-dimension gel consisted of 22% polyacrylamide prepared from a stock of 15 : 1 acrylamide : bis in 50mM tris borate pH 8.2. (Electran grade acrylamide; BDH Chemicals Ltd. Synthesis grade bis-acrylamide; Merck. All other chemicals were AnalaR; BDH Chemicals Ltd.) Polymerization was catalysed by the addition of TEMED and fresh 10% ammonium sulphate (table 2.3). The advantage of 50mM tris borate, pH 8.2 is that it produces very little heat at the high voltages used for the second-

dimension electrophoresis. As a result electrophoresis may be carried out at room temperature without the necessity for cooling <sup>60</sup>.

Table 2.3. Stock solutions for the second-dimension gel system <sup>51</sup>.

COMPONENT	VOLUME REQUIRED FOR ONE GEL
Acrylamide:Bis (15:1)	209.0ml
50mM Tris-borate pH 8.2	11.0ml
TEMED	0.1ml
Ammonium sulphate (10% (w/v))	0.4ml

Gel was poured into the chamber till it was approximately 1/3 full and the chamber was tilted in order to mix in any unpolymerized connecting gel. The chamber was placed in the second-dimension buffer reservoir and filled with gel solution which was then overlaid with 75% ethanol. Polymerization was complete within 30 to 40 minutes.

#### 2.6.2.3.3. Electrophoresis

After polymerization had taken place the plate assembly was clamped to the upper reservoir of the electrophoresis apparatus. The upper and lower reservoirs were filled with second-dimension electrophoresis buffer. Electrophoresis was carried out at room temperature and at a constant power of 10 - 12 watts (600 V; about 16mA) using an LKB Bromma 2197 power supply. Regulation

of power allowed the voltage to rise during electrophoresis as resistance increased during the run, without an increase in temperature.

When the major bromophenol blue component had migrated 20cm, which took 14 to 15 hours, electrophoresis was ended. Figure 2.8 shows the relative positions of the BPB and XC spots after electrophoresis.

#### 2.6.2.4. Autoradiography

After second-dimension electrophoresis the notched plate and spacers were removed from the gel. Two layers of "Cling Film" plastic were wrapped round the gel and glass plate to prevent the gel from dehydrating and protect the X-ray film from being damaged by the moist gel. Virtually no radioactivity is absorbed by the plastic film so results were not affected.

A 30cm x 38cm Cronex 4 medical X-ray plate (I.E. Du Pont de Nemours) was laid over the gel, and a second glass sheet fixed over the X-ray plate in order to hold it in place and ensure good contact of the X-ray film with the gel surface. The entire assembly was wrapped in two layers of aluminium foil and autoradiography carried out for 24 hours. If, after 24 hours, the autoradiograph was found to be underexposed, autoradiography was carried out again, for up to 96 hours. Development and fixation of autoradiographs was carried out as described in section 2.5.3.4.

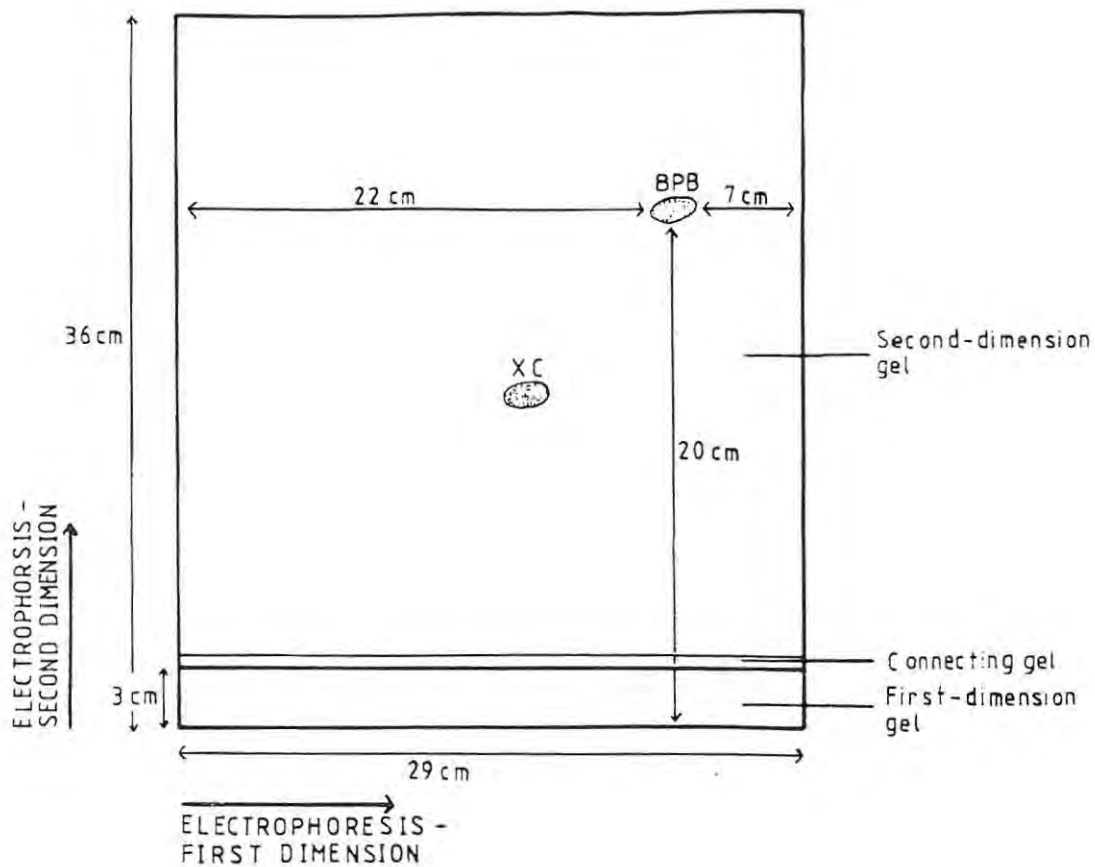


FIGURE 2.8. Diagrammatic representation of a second-dimension oligonucleotide mapping gel. Positions of bromophenol blue dye marker (BPB) and xylene cyanol marker (XC) after electrophoresis are shown.

## CHAPTER THREE

### COMPARISON OF POLIOVIRUS CAPSID PROTEINS USING DISCONTINUOUS SDS-POLYACRYLAMIDE GEL ELECTROPHORESIS

#### 3.1. Introduction

Proteins from different strains of poliovirus generally differ in their amino acid composition. These differences may be reflected in the electrophoretic mobility of the proteins after discontinuous SDS—polyacrylamide gel electrophoresis. Even slight differences can result in variations in mobility <sup>52</sup>.

It was decided to exploit these differences and use SDS-polyacrylamide gel electrophoresis to compare the relative mobilities of capsid proteins from wild-type, vaccine, and Gazankulu outbreak strains of poliovirus. It was hoped that results obtained would indicate the relationship between the Gazankulu outbreak strains and the vaccine and wild-type strains of the virus.

Discontinuous polyacrylamide gel electrophoresis (disc-PAGE) was first introduced in 1964 by Ornstein and Davis, working independently <sup>4</sup>. The polyacrylamide is in two parts, a high porosity "stacking gel" overlaying a low porosity "resolving gel". The system is a multibuffer one, resulting in sharper bands and better sample resolution than conventional continuous phosphate gel electrophoresis.

In 1963 Maizel discovered that sodium dodecyl sulphate (SDS) facilitated the electrophoresis of proteins in polyacrylamide

gels <sup>4</sup>. It was later shown that the binding of SDS to proteins was accompanied by dissociation of oligomeric molecules into sub-units. Migration of these sub-units during electrophoresis depended on their polypeptide chain size <sup>4</sup>. Laemmli (1970) and Neville (1971) combined discontinuous PAGE and SDS-PAGE, and two multiphasic systems for SDS-PAGE were developed. The slightly lower pH method of Laemmli, incorporating tris-glycine and tris-HCl buffers, is most frequently used today.

Once polypeptides have been electrophoresed, several techniques are available for their visualisation. These include precipitation with 2.5M potassium chloride <sup>16</sup>, silver staining <sup>37</sup>, staining with Coomassie brilliant blue <sup>4</sup>, and autoradiography of radiolabelled proteins <sup>81</sup>. Though not the most sensitive technique, staining with Coomassie brilliant blue R250 is widely used <sup>4</sup>. The stain forms electrostatic bonds with ammonium (NH<sub>3</sub><sup>+</sup>) groups and non-covalent bonds with non-polar regions <sup>4</sup>. The detection limit is 0.1ug of protein <sup>4,106</sup>.

Prior to electrophoresis samples to be used in this study were prepared using SDS and  $\beta$ -mercaptoethanol. Treatment with SDS for three minutes at 100°C caused breaking of hydrogen bonds and coated the sample with a blanket negative charge. Simultaneously, treatment with  $\beta$ -mercaptoethanol reduced disulphide bonds and prevented protein aggregation. Complete and uniform binding of SDS to the polypeptides was ensured by the removal of conformational constraints <sup>4</sup>. The overall uniform negative charge densities and lack of tertiary structure allowed electro-

phoretic separation of the polypeptides according to molecular weight.

The electrophoretic mobility of a polypeptide in discontinuous SDS-PAGE is inversely proportional to the logarithm of its molecular weight <sup>4,99</sup>. This has allowed calculation of the molecular weight of many proteins, including those comprising the capsid of poliovirus. Using SDS-PAGE, the three larger capsid proteins of poliovirus give highly consistent results. The smallest protein, VP4, tends to give anomalous results <sup>99</sup>. This is characteristic of polypeptides with a molecular weight of less than 15 000 <sup>106</sup>.

### 3.2. Results

Figures 3.1.a and 3.2.a show the results obtained when phenol-extracted capsid proteins of poliovirus were separated electrophoretically on polyacrylamide gels. By plotting migration of the marker proteins against the logarithm of their molecular weights a standard curve was produced (figures 3.1.b and 3.2.b). Molecular weights of the virus proteins were calculated (table 3.1.) by plotting the distances migrated by the poliovirus capsid proteins on the standard curve.

#### 3.2.1. Comparison of Capsid Proteins of Type 1 Polioviruses

There is a difference in the electrophoretic mobilities of capsid proteins VP1 and VP3 of the Gazankulu outbreak strain 5061 and type 1 vaccine strain LS-c (table 3.1). In contrast, the molecular weights calculated for VP1 and VP3 of the wild-type 1 strain LS-a are identical to those of the Gazankulu



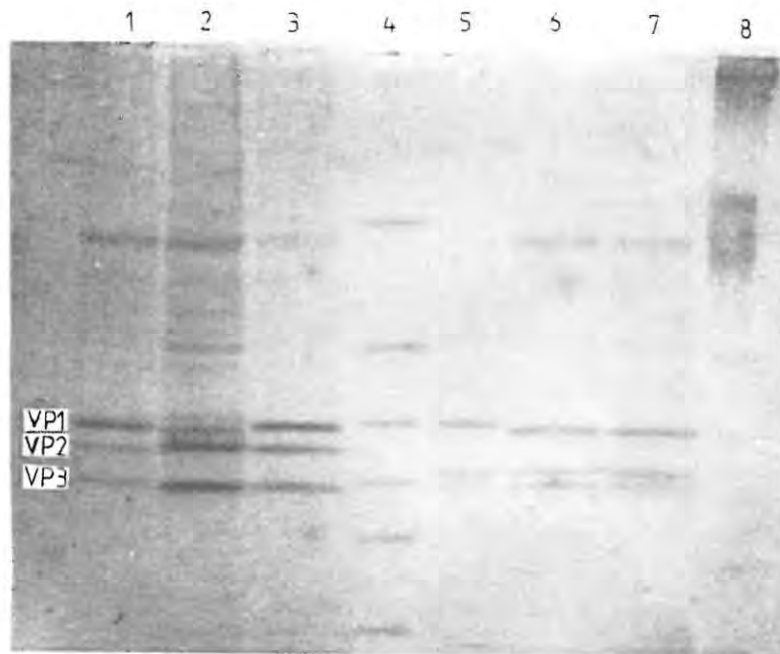


FIGURE 3.1.a. Photograph of SDS-PAGE gel after electrophoresis of type 1 and 2 polioviruses.  
 Tracks 4 and 8 - marker proteins;  
 Tracks 1 to 3 - poliovirus type 1; Wild-type strain LS-a, Sabin vaccine strain LS-c and Gazankulu outbreak strain 5061, respectively;  
 Tracks 5 to 7 - poliovirus type 2; Wild-type strain Lansing, Sabin vaccine strain P712 and Gazankulu outbreak strain 5068, respectively.

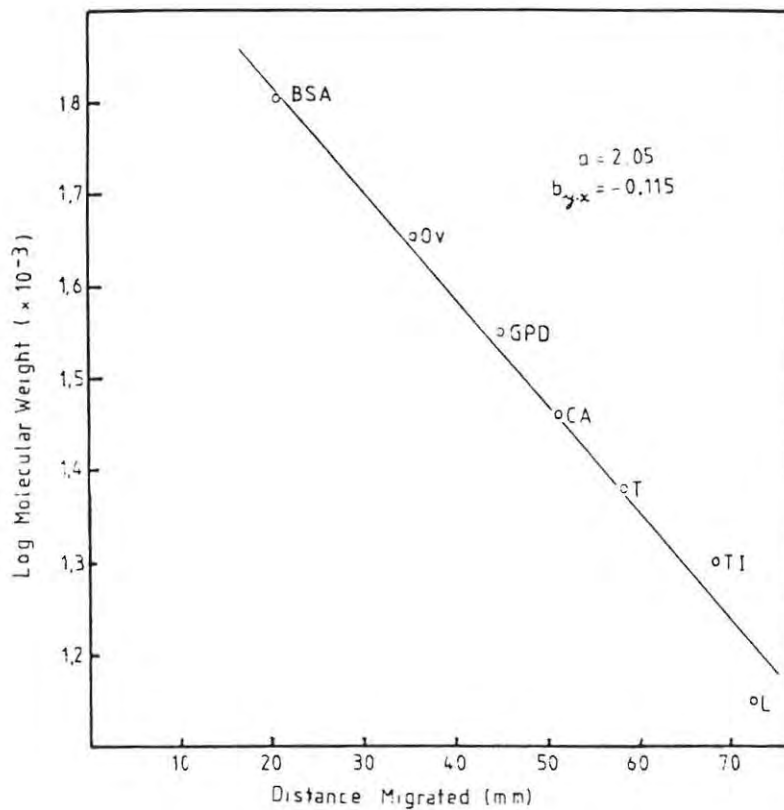


FIGURE 3.1.b. Standard curve obtained by plotting log. molecular weight ( $\times 10^{-3}$ ) of marker proteins against distance migrated.

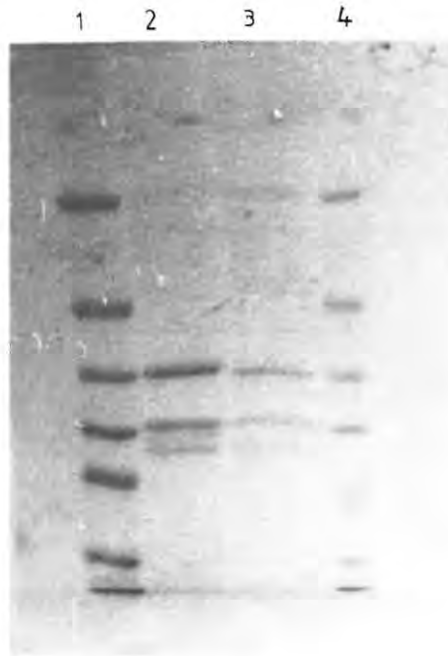


FIGURE 3.2.a. Photograph of SDS-PAGE gel after electrophoresis of type 3 polioviruses.  
 Tracks 1 and 4 - marker proteins;  
 Track 2 - Wild-type strain Leon III;  
 Track 3 - Sabin vaccine strain Leon 3.

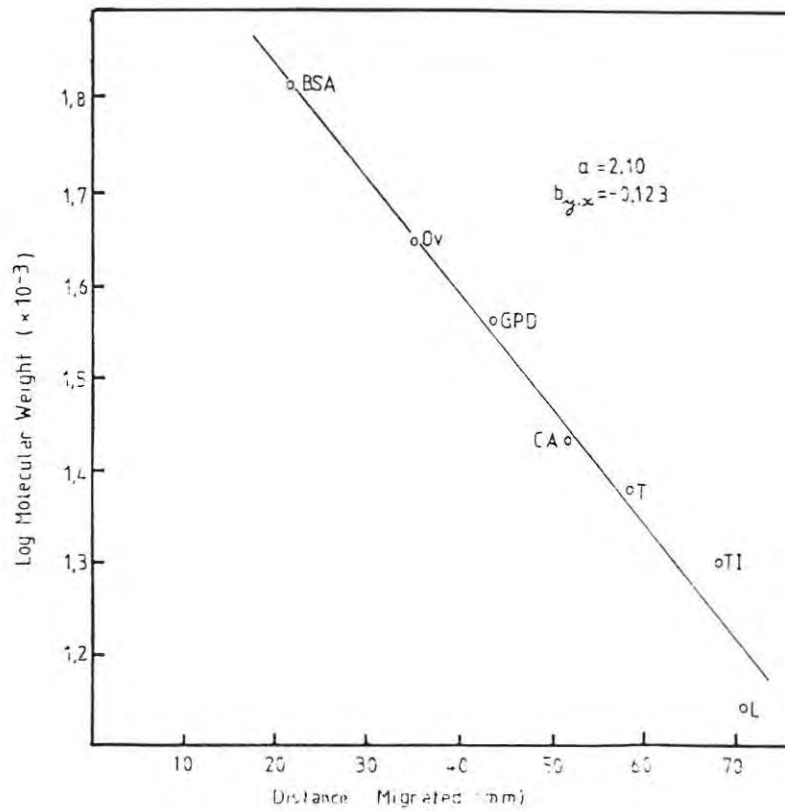


FIGURE 3.2.b. Standard curve obtained by plotting log. molecular weight ( $\times 10^{-3}$ ) of marker proteins against distance migrated.

Table 3.1. Molecular weight of poliovirus capsid proteins calculated after SDS-PAGE by plotting protein migration on standard curve.

VIRUS TYPE	VIRUS STRAIN	MOLECULAR WEIGHTS OF CAPSID PROTEINS		
		VP1	VP2	VP3
1	5061	36 300	31 600	26 600
	LS-c	34 400	31 600	26 100
	LS-a	36 300	30 200	26 600
2	5068	36 300	29 200	26 900
	P712	36 300	29 200	26 900
	Lansing	36 900	28 500	26 900
3	Leon 3	37 200	30 000	27 200
	Leon III	38 000	30 000	27 200

outbreak strain of poliovirus type 1.

An apparent similarity in electrophoretic mobility exists between the VP2 of both vaccine and Gazankulu outbreak strains. This cannot, however, be taken as an indication of relatedness because conservation of VP2 usually occurs between poliovirus strains <sup>52,104</sup>. The results obtained thus suggest that there is little relationship between Gazankulu outbreak strain 5061 and Sabin vaccine strain LS-c.

Although various workers <sup>52,68</sup> have reported anomalous migration characteristics of capsid proteins from poliovirus type 1 vaccine strain LS-c, these were not apparent. Figure 3.1.a shows that separation of capsid proteins VP1, VP2 and VP3 of LS-c has occurred. The electrophoretic mobilities of VP1 and VP2 are similar, due to the characteristic increase in mobility of VP1 displayed by LS-c <sup>80</sup>.

Little or no degradation of capsid proteins is apparent, despite the finding by Kew et al (1980) of an unexplained and poorly reproducible tendency towards degradation of LS-c VP1 during SDS-PAGE. A faint additional protein band, molecular weight  $37.1 \times 10^3$ , is present. This may be due to incomplete dissociation of capsid proteins or aggregation of dissociated proteins. As this protein was not always present it was assumed to be artefactual and no analysis of it was carried out.

### 3.2.2. Comparison of Capsid Proteins of Type 2 Polioviruses

In the case of the type 2 virus strains, the capsid proteins of

the Gazankulu outbreak strain, 5068, and those of the vaccine strain, P712, display identical electrophoretic mobilities (table 3.1). The similarity between VP1 of the two poliovirus strains is surprising - Yoneyama et al (1981) found that in 14 out of 17 vaccine-related isolates of poliovirus tested, electrophoretic mobility of VP1 differed from that of the vaccine strain.

The mobilities on SDS-PAGE of the capsid proteins of both type 2 Gazankulu outbreak strain 5068 and type 2 vaccine strain P712 differ from those of wild-type 2 strain Lansing. This suggests that the relationship between the Gazankulu and vaccine strains of type 2 poliovirus is closer than that between the Gazankulu outbreak strain and the wild-type strain.

### 3.2.3. Comparison of Capsid Proteins of Type 3 Polioviruses

Electrophoretic mobilities of the capsid proteins of the two type 3 poliovirus strains tested are very similar. Capsid proteins VP2 and VP3 of the attenuated Sabin vaccine strain, Leon 3, display electro-phoretic mobilities identical to those of the neurovirulent wild-type strain Leon III. There is a difference in apparent molecular weight of 800 between VP1 of the two virus strains (table 3.1.). This noticeable difference in electrophoretic mobility between vaccine and wild-type VP1 capsid protein has also been reported by Minor (1982).

### 3.3. Discussion

Although Martin (1984, unpublished data) detected small amounts of VP4 from the Sabin type 2 and 3 vaccine strains of poliovirus

(P712 and Leon 3), this capsid protein was not detected for any of the virus samples. This was not surprising, for VP4 is known to stain poorly if at all.

Because no VP4 was detected it was not possible to compare VP4 of the poliovirus strains under study. Unpublished studies carried out by Kew using radiolabelled poliovirus proteins (cited in Kew et al, 1980) have indicated that electrophoretic mobility of VP4 on SDS-PAGE is much less variable than that of VP1 and VP3. This is hardly unexpected, for VP4 is not a surface protein of the viral capsid. Consequently it would not be expected to be as prone to mutation as the surface proteins are.

Comparison of electrophoretic mobilities of poliovirus capsid proteins (table 3.1.), shows that type 1 Gazankulu poliovirus outbreak strain 5061 differs from type 1 vaccine strain LS-c. In contrast, the electrophoretic mobilities of capsid proteins from type 2 Gazankulu outbreak strain 5068 are identical to those of poliovirus type 2 vaccine strain P712. Comparison of electrophoretic mobilities of capsid proteins indicate that the two outbreak strains have been correctly identified as type 1 and type 2 polioviruses. Neither appears to bear any relationship to the type 3 polioviruses studied.

As expected, variability between capsid proteins of vaccine and wild-type poliovirus strains was found to be greatest within VP1, which is the major surface protein and is the type-specific neutralizing antigen <sup>16,25,29</sup>. A surprising conservation of electrophoretic mobility existed within VP3 of the type 2 and

type 3 vaccine and wild-type strains. VP3 lies in close proximity to VP1<sup>52</sup> and forms complexes with it when treated with bifunctional cross-linking agents<sup>109</sup>. Because of its exposed position and association with VP1, VP3 will probably also be considerably altered during attenuation<sup>52,94</sup>. It is likely that, while differences between VP3 of the vaccine and wild-type strains do exist, SDS-PAGE was not sufficiently sensitive to detect them.

Within a poliovirus type, variability between capsid proteins is possibly due to relatively minor changes in the capsid proteins, probably amino acid substitutions<sup>52</sup>. In the case of type 1 polioviruses Mahoney (the neurovirulent parent strain to which strain LS-a is closely related) and vaccine strain LS-c 2ab, amino acid substitutions represent approximately 1% to 2% of all the residues<sup>52</sup>. Between types, however, differences in molecular weight of the capsid proteins may be due to amino acid deletions or additions as well as to substitutions<sup>104</sup>.

Unfortunately SDS-PAGE is a fairly crude technique, only capable of indicating differences in electrophoretic mobility between proteins. Such differences are not necessarily directly related to differences in the composition of the proteins<sup>52</sup>. This applies particularly if closely related proteins differ due to slight chemical modification or due to artefactual proteolysis during preparation<sup>14</sup>. Consequently, unambiguous identification of the relationship between specific proteins cannot be made on the basis of electrophoretic mobility alone.

## CHAPTER FOUR

### COMPARISON OF POLIOVIRUS CAPSID PROTEINS BY MAPPING TRYPTIC PEPTIDES USING THIN-LAYER CHROMATOGRAPHY (TLC) AND REVERSED-PHASE HIGH-PERFORMANCE LIQUID-CHROMATOGRAPHY (RP-HPLC)

#### 4.1. Introduction

SDS-PAGE indicated that similarities existed between the Gazankulu isolate and vaccine strain of poliovirus type 2 but not between those of poliovirus type 1. In an attempt to find a more sensitive method of comparing virus strains, tryptic peptide mapping of capsid proteins was carried out.

Mapping of peptides produced after proteolytic digestion of purified proteins is an important technique used to characterise proteins, to compare amino acid sequences and to detect small differences in their primary structure <sup>12</sup>. Because the peptide composition of a protein can be studied, an analysis of tryptic peptides should be considerably more sensitive than a comparison of molecular weights by discontinuous SDS-PAGE.

Most polypeptide changes resulting from alterations in the RNA during attenuation of poliovirus strains occur in the capsid proteins <sup>52,104</sup>. These proteins determine the ability of virus particles to bind to recognition sites on the surface of susceptible cells, initiating infection <sup>88</sup>. Pathogenic reversion of vaccine strains is thus generally reflected in the capsid protein amino acid sequence. Consequently it was decided to use tryptic peptide mapping of poliovirus capsid proteins for



comparing vaccine and Gazankulu outbreak strains of poliovirus.

Several chromatographic techniques are available for the analysis of peptides. These include thin-layer chromatography (TLC), reversed-phase high-performance liquid-chromatography (RP-HPLC), ion-exchange chromatography (IEC), affinity chromatography and size-exclusion chromatography <sup>28,90</sup>. Thin-layer chromatography and reversed-phase high-performance liquid-chromatography were used in this study.

Obtaining large enough amounts of protein for analysis was difficult. As a result, purification to homogeneity of each of the poliovirus capsid proteins was not feasible. To circumvent this problem, individual capsid proteins separated by SDS-PAGE were radiolabelled within gel slices as described in section 2.5.1.2. of "Materials and Methods" <sup>24</sup>. This was followed by modified tryptic digestion as described by Elder et al (1977).

<sup>125</sup>I-iodine has a half-life of 60 days and a considerably higher specific activity than many other radioisotopes. This allows rapid and easy detection of picogram amounts of protein <sup>10</sup>. Because <sup>125</sup>I is a high energy  $\gamma$ -emitter, no special sample preparation was required for counting <sup>10</sup>. This was important because large numbers of samples were collected.

Because no iodine is present in poliovirus proteins, in vitro incorporation of <sup>125</sup>I using the chloramine-T reaction was chosen as the method of protein labelling. In vivo labelling using <sup>3</sup>H or <sup>35</sup>S-methionine was not used because these isotopes have a lower activity than <sup>125</sup>I (75 times lower and 35 000 times lower,

respectively <sup>10</sup>) and are more costly than <sup>125</sup>I.

Chloramine-T is the sodium salt of the N-monochloro derivative of *p*-toluene sulphonamide and oxidises radioactive sodium iodide (Na<sup>125</sup>I). In the presence of the protein to be labelled this results in highly efficient incorporation of <sup>125</sup>I into tyrosine residues (figure 4.1.). Addition of sodium metabisulphite reduces excess chloramine-T, and free iodine is reduced to iodide. This is removed by adding excess unlabelled sodium iodide or potassium iodide <sup>10</sup>. In addition to tyrosine, histidine, tryptophan and sulphhydryl groups (such as cysteine) may be labelled to a certain extent <sup>10</sup>. Phenylalanine may also be labelled <sup>24</sup>.

Trypsin, the enzyme used for digestion of the capsid proteins, selectively catalyses hydrolysis of peptide bonds on the carboxyl side of the basic amino acids lysine and arginine <sup>59</sup>. It is not an enzyme of first attack, and in several cases can only digest proteins after denaturation such as that resulting from SDS-PAGE <sup>40</sup>.

#### **4.2. Comparison of Poliovirus Capsid Proteins by Two-Dimensional Thin-Layer Chromatography of Tryptic Peptides**

Polyacrylamide gel electrophoresis has been used for the mapping of peptides both in one-dimension <sup>14</sup> and two-dimensions <sup>9,81</sup>. A more sensitive test of polypeptide identity involves peptide mapping using a thin layer of cellulose or alumina a few hundred microns thick <sup>87</sup>.

Separation of tryptic digests in two dimensions on either paper or thin-layers was originally developed by Ingram (1956). Electrophoresis was carried out in one direction and chromatography in the other. Using a combination of techniques along the two axes of the plate, two-dimensional separation gives more information than single dimension chromatography. Such a technique may be very sensitive, with less than 10ug of  $^{125}\text{I}$ -labelled protein giving a very satisfactory result <sup>4</sup>. Generally, horizontal electrophoresis is carried out in the first dimension and ascending chromatography in the second. Electrophoretic migration in the first dimension is dependant on the charge of the samples to be separated. Separation during ascending chromatography is due to sample solubility in the solvents used <sup>4</sup>.

Thin-layer chromatography (TLC) of  $^{125}\text{I}$  and ( $^{35}\text{S}$ )-methionine labelled proteins on cellulose has been used by Gentsch and Fields (1981). These workers carried out analysis of the outer capsid proteins of mammalian reovirus serotypes 1,2 and 3. Lamb and Choppin (1978) also used TLC of ( $^{35}\text{S}$ )-methionine labelled tryptic peptides for comparison of the viral polypeptides of Sendai virus. Polypeptides were labelled, then separated using SDS-PAGE, and digested. Peptide separation was carried out using electrophoresis followed by ascending chromatography. Similar techniques of two-dimensional TLC were used in this study for mapping radiolabelled peptides of poliovirus capsid proteins.

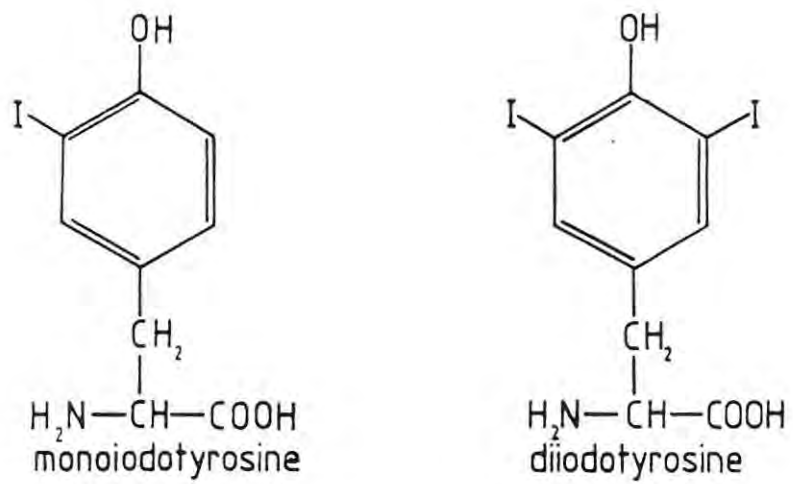


FIGURE 4.1. Incorporation of  $^{125}\text{I}$  into tyrosine residues, forming either monoiodotyrosine or diiodotyrosine.

#### 4.2.1. Results

Photographs were taken of the autoradiographs produced after individual capsid proteins of the poliovirus strains were subjected to peptide mapping. Drawings were then made and used for comparing the tryptic peptide maps of the different viral capsid proteins.

##### 4.2.1.1. Comparison of tryptic peptide maps of capsid proteins from poliovirus type 1

Figure 4.2.a shows photographs of the tryptic peptide maps generated after radiolabelling and tryptic digestion of VP1 from Gazankulu outbreak strain 5061, Sabin vaccine strain LS-c and wild-type strain LS-a. A diagrammatic representation of the photographs is shown in figure 4.2.b, with only the major peptide spots indicated.

When the maps of VP1 from type 1 Gazankulu outbreak strain 5061 and that of vaccine strain LS-c are compared, several differences are apparent. Two novel peptide spots are present on the LS-c map, while four of the tryptic peptides present on the map of 5061 VP1 have been lost. Two peptide spots on the map of VP1 from 5061 (spots 9 and 10) appear to have shifted on the map of LS-c. Such "shifting" is the result of minor alterations in amino acid composition and refers to slight changes in the position of peptide spots. Horizontal shift reflects a change in electrophoretic mobility, vertical shift a change in chromatographic mobility.

From a comparison of the tryptic peptide maps of the three virus

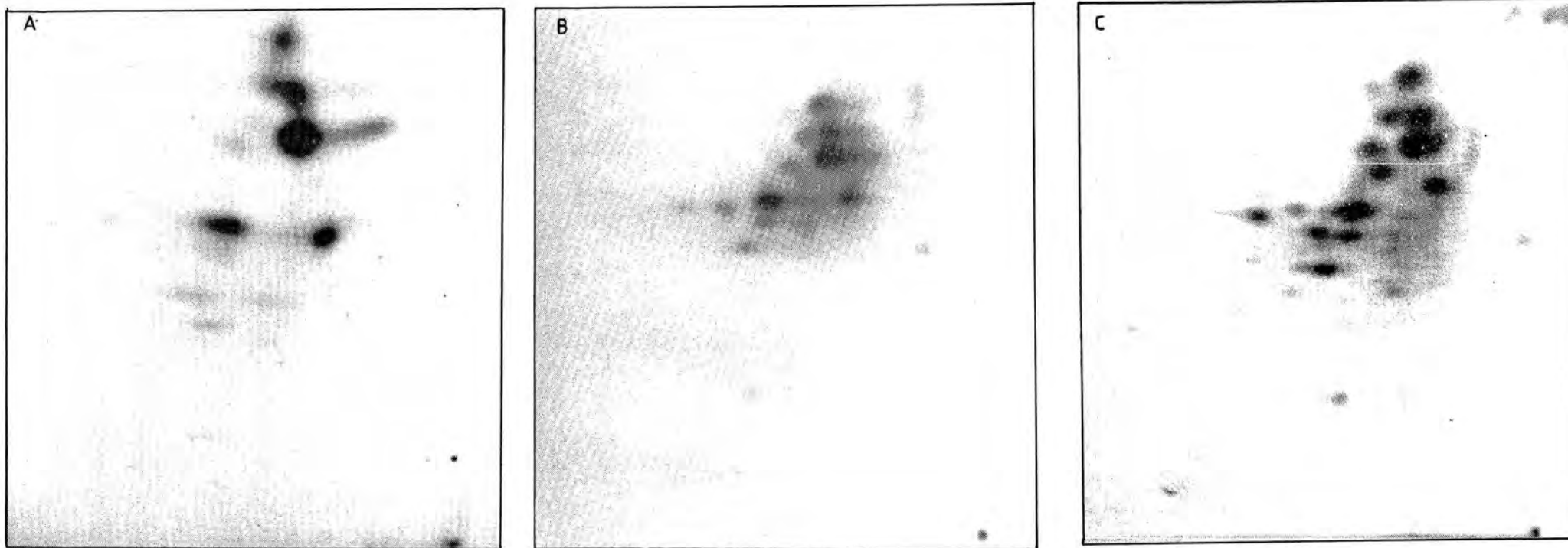


FIGURE 4.2.a. Maps produced after TLC of peptides from VP1 of poliovirus type 1 strains. A - Gazankulu outbreak strain 5061; B - Sabin vaccine strain LS-c; C - wild-type strain LS-a.

712

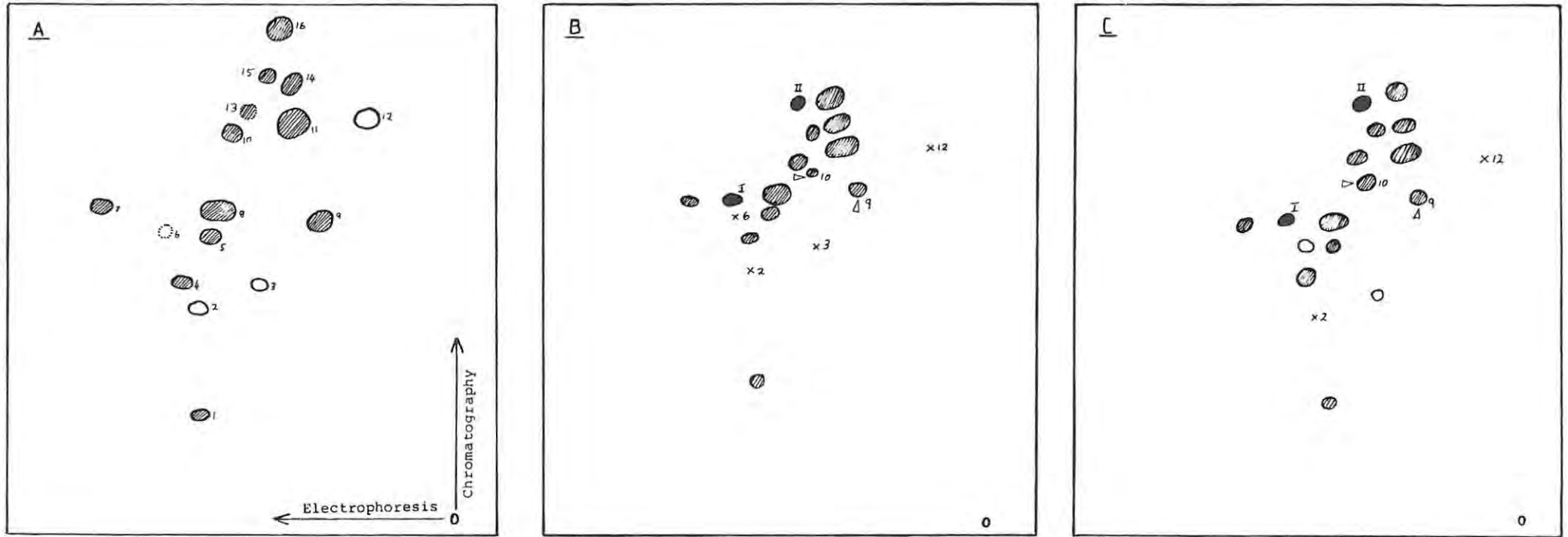


FIGURE 4.2.b.

Diagrammatic representation of the peptide maps of VP1 from 5061 (A), LS-c (B) and LS-a (C). Numbering of spots on the map of 5061 is arbitrary. On maps of LS-c and LS-a only missing spots (x) are numbered. Novel spots are indicated by (●), shifted spots by (▷), with the arrow showing the direction of shift. Roman numerals indicate spots common to vaccine and wild-type strains only. Spots common to all strains are shown by (⊙). Faint spots are indicated by a dotted outline. Sample origin (o) is in lower right-hand corner.

strains it may be seen that the greatest similarities exist between VP1 of type 1 vaccine strain LS-c and wild-type strain LS-a. Two peptides missing when VP1 of type 1 Gazankulu outbreak strain 5061 is compared with vaccine strain LS-c are also missing from wild-type LS-a. Additionally, both of the novel peptides apparent on the map for LS-c are shared with reference strain LS-a. The two peptides which have shifted on the tryptic peptide map of LS-c VP1 have also shifted on the map of LS-a.

Variability between the VP2 peptide maps of the three type 1 poliovirus strains (figure 4.3.a and b) is more pronounced than that between the VP1 peptide maps. VP2 of vaccine strain LS-c lacks two of the peptides apparent on the map for type 1 Gazankulu outbreak strain 5061 and has gained six new peptide spots. Six differences between VP2 of 5061 and vaccine strain LS-c are common to wild-type reference strain LS-a. Of the novel LS-c peptides, four are shared with LS-a VP2, while the two peptides missing from the LS-c map are also missing from the LS-a map.

Variations are also apparent upon comparison of the tryptic peptide map of VP3 of each of the viral strains (figure 4.4.a and b). VP3 of the Gazankulu outbreak strain, 5061, displays several differences from that of vaccine strain LS-c. Three tryptic peptides are apparent on the 5061 map but not that of LS-c, which has three new peptides. Of the novel features apparent on the tryptic peptide map for type 1 vaccine strain LS-c, three are common to wild-type reference strain LS-a. The shared differences (loss of two peptides and the gain of one novel peptide) comprise all of the differences between LS-a and



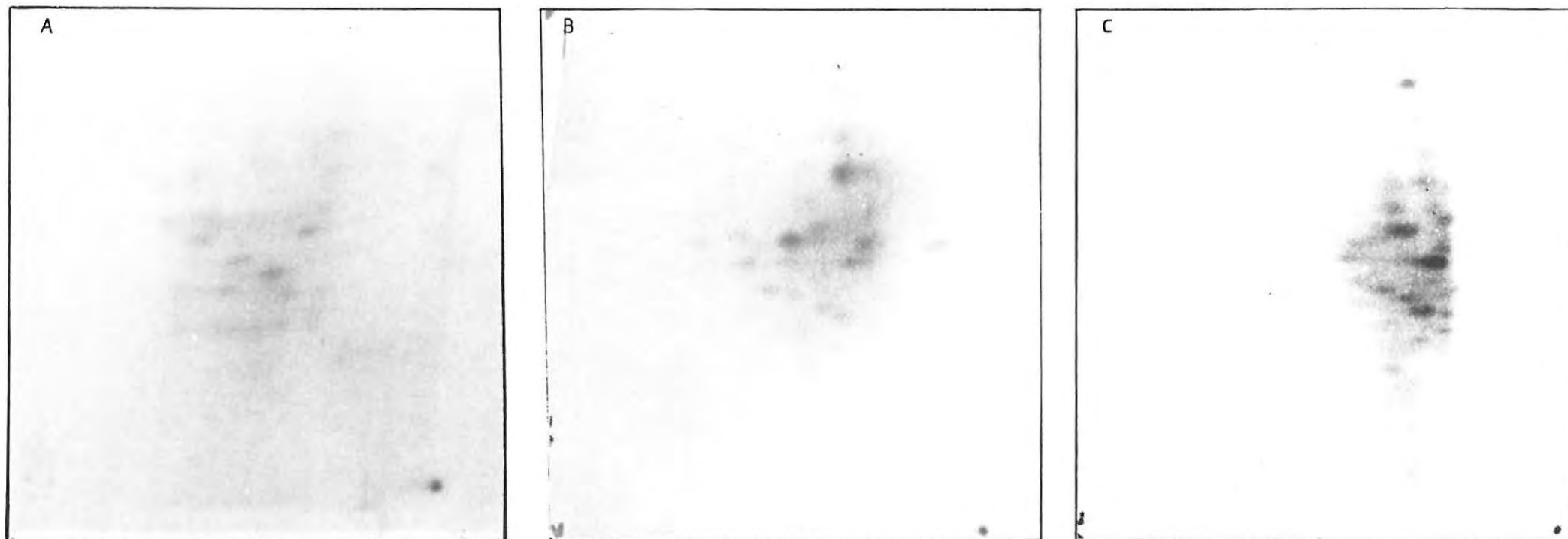


FIGURE 4.3.a. Maps produced after TLC of peptides from VP2 of poliovirus type 1 strains. A - Gazankulu outbreak strain 5061; B - Sabin vaccine strain LS-c; C - wild-type strain LS-a.

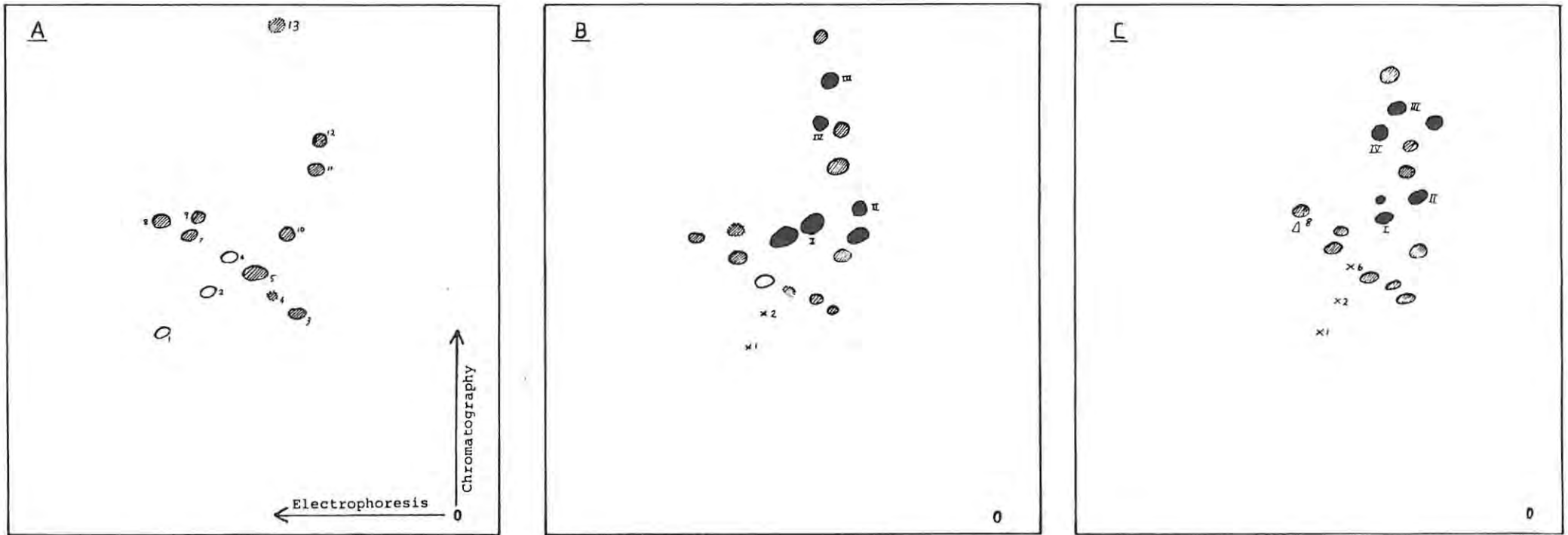


FIGURE 4.3.b. Diagrammatic representation of the peptide maps of VP2 from 5061 (A), LS-c (B) and LS-a (C). Numbering of spots on the map of 5061 is arbitrary. On maps of LS-c and LS-a only missing spots (x) are numbered. Novel spots are indicated by (●), shifted spots by (▷), with the arrow showing the direction of shift. Roman numerals indicate spots common to vaccine and wild-type strains only. Spots common to all strains are shown by (⊙). Faint spots are indicated by a dotted outline. Sample origin (o) is in lower right-hand corner.

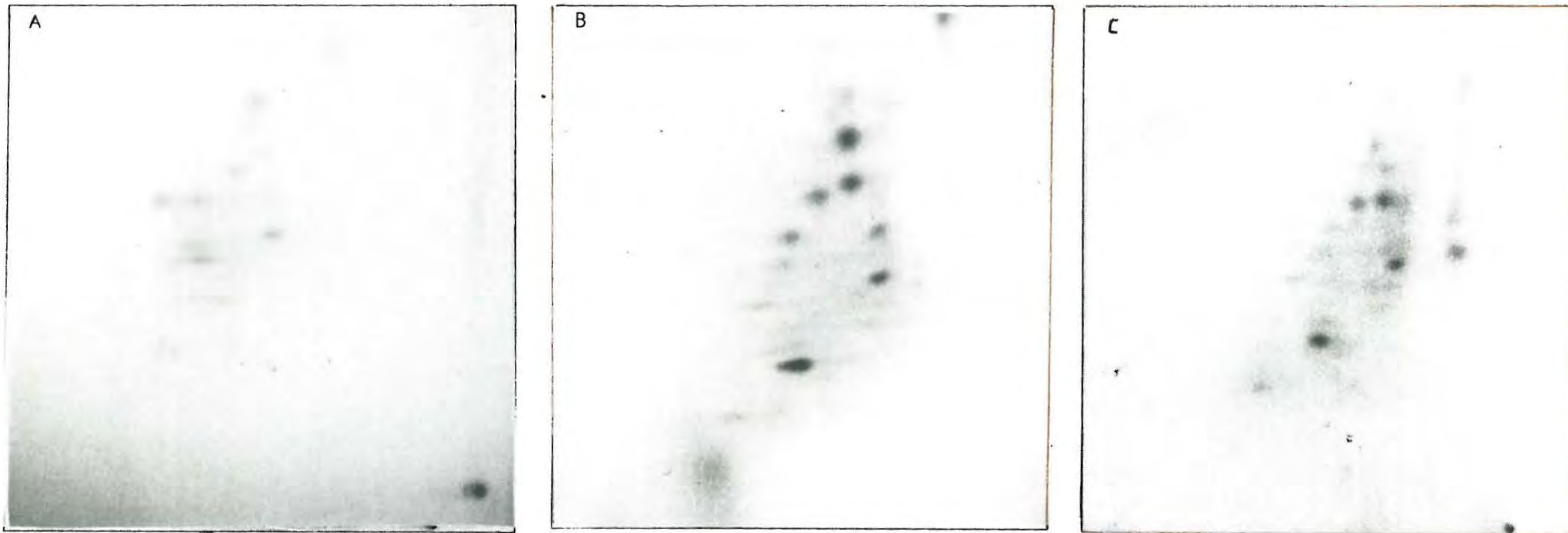


FIGURE 4.4.a. Maps produced after TLC of peptides from VP3 of poliovirus type 1 strains. A - Gazankulu outbreak strain 5061; B - Sabin vaccine strain LS-c; C - wild-type strain LS-a.

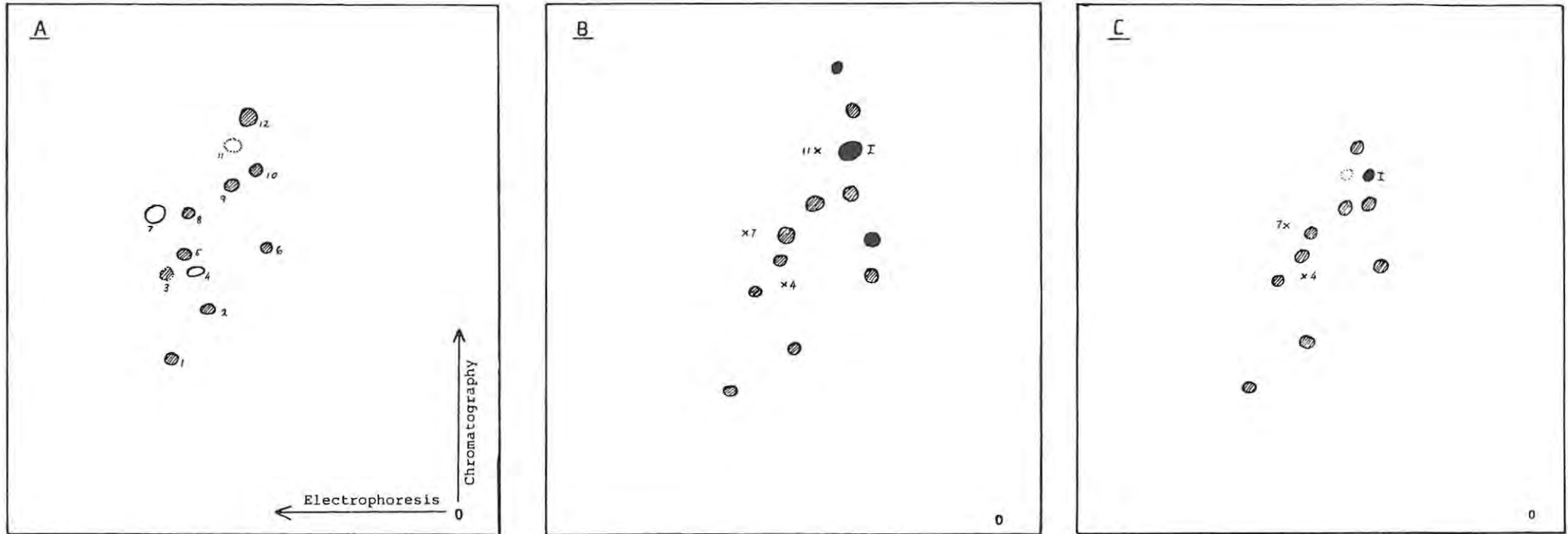


FIGURE 4.4.b. Diagrammatic representation of the peptide maps of VP3 from 5061 (A), LS-c (B) and LS-a (C). Numbering of spots on the map of 5061 is arbitrary. On maps of LS-c and LS-a only missing spots (x) are numbered. Novel spots are indicated by (●). Roman numerals indicate spots common to vaccine and wild-type strains only. Spots common to all strains are shown by (⊗). Faint spots are indicated by a dotted outline. Sample origin (o) is in lower right-hand corner.

5061. Several apparent tryptic peptides (fig. 4.4.a) are not shown on the drawn representations (fig. 4.4.b). These were not reproducible and were presumably artefactual.

Variability between VP1 and VP3 of the Gazankulu outbreak strain and the vaccine strain is considerably greater than that between the outbreak strain and the wild-type strain. Differences between the Gazankulu outbreak strain and vaccine strain are frequently shared by the vaccine and wild-type reference strain (see table 4.1). This suggests that there is little relationship between the poliovirus type 1 outbreak strain and Sabin vaccine strain. In contrast, relationship appears to exist between the vaccine strain and the wild-type strain.

#### 4.2.1.2. Comparison of tryptic peptide maps of the capsid proteins of type 2 polioviruses

Photographs of the autoradiographs resulting from TLC mapping of tryptic peptides of the capsid proteins from the type 2 polioviruses used in this study (Gazankulu strain 5068, Sabin vaccine strain P712 and reference strain Lansing) are shown in figures 4.5.a, 4.6.a and 4.7.a. Diagrammatic representations of the photographs are shown in figure 4.5.b, 4.6.b and 4.7.b.

A clearly visible pattern is apparent between the tryptic peptide maps of VP1, with maps from all three strains having a similar appearance (fig. 4.5.a and b). Differences do, however, exist. Type 2 vaccine strain P712 displays one novel peptide when compared with Gazankulu outbreak strain 5068, and lacks four others.

Table 4.1. Comparison of tryptic peptide maps of capsid proteins 1,2 and 3 of poliovirus type 1 Gazankulu outbreak strain 5061 with similar maps of vaccine strain LS-c and wild-type 1 strain LS-a.

CAPSID PROTEIN	VIRUS STRAIN	TOTAL SPOTS*	NOVEL SPOTS	LOST SPOTS	MOVED	TOTAL DIFF'S**	SHARED <sup>+</sup>
VP1	5061	16	-	-	-	-	
	LS-c	14	2	4	2	8	6
	LS-a	16	2	2	2	6	
VP2	5061	13	-	-	-	-	
	LS-c	17	6	2	0	8	6
	LS-a	16	6	3	1	10	
VP3	5061	12	-	-	-	-	
	LS-c	12	3	3	0	6	3
	LS-a	11	1	2	0	3	

\* Number of dominant spots used for comparison of peptide maps.

\*\* Total number of differences apparent between peptide maps of outbreak strain poliovirus capsid proteins and vaccine/wild-type strain maps.

+ Number of differences from outbreak strain map that are common to vaccine and wild-type strains of poliovirus.

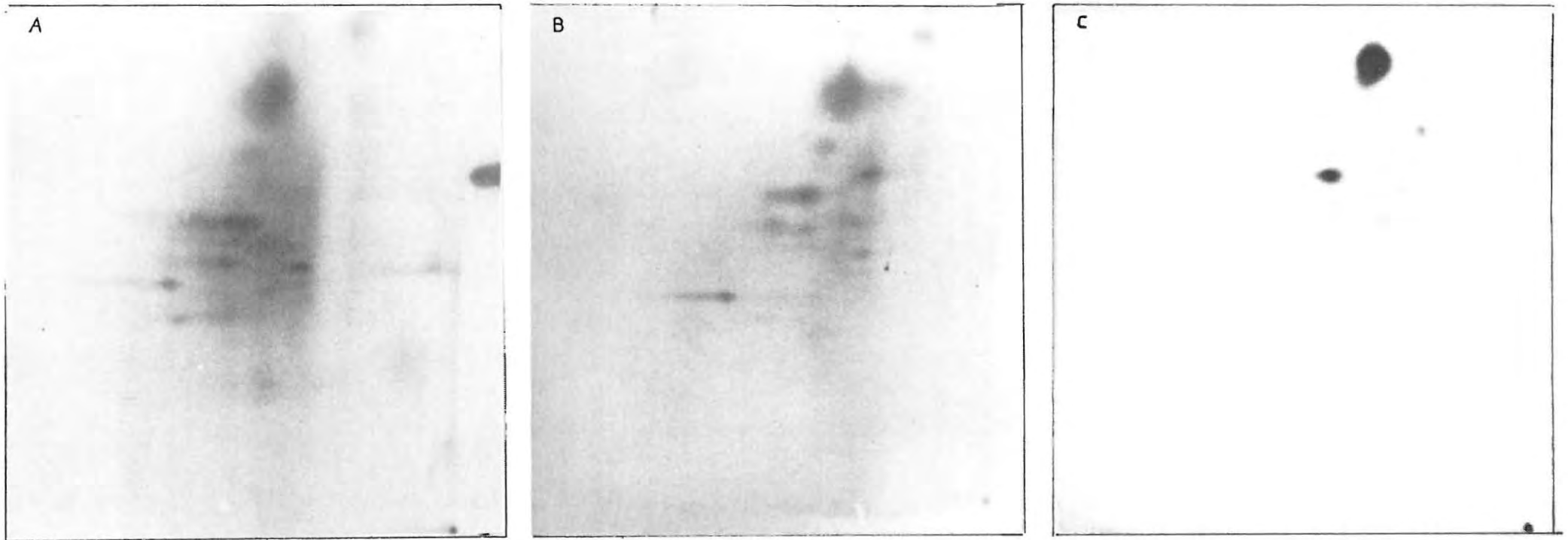


FIGURE 4.5.a Maps produced after TLC of peptides from VP1 of poliovirus type 2 strains. A - Gazankulu outbreak strain 5068; B - Sabin vaccine strain P712; C - wild-type strain Lansing.

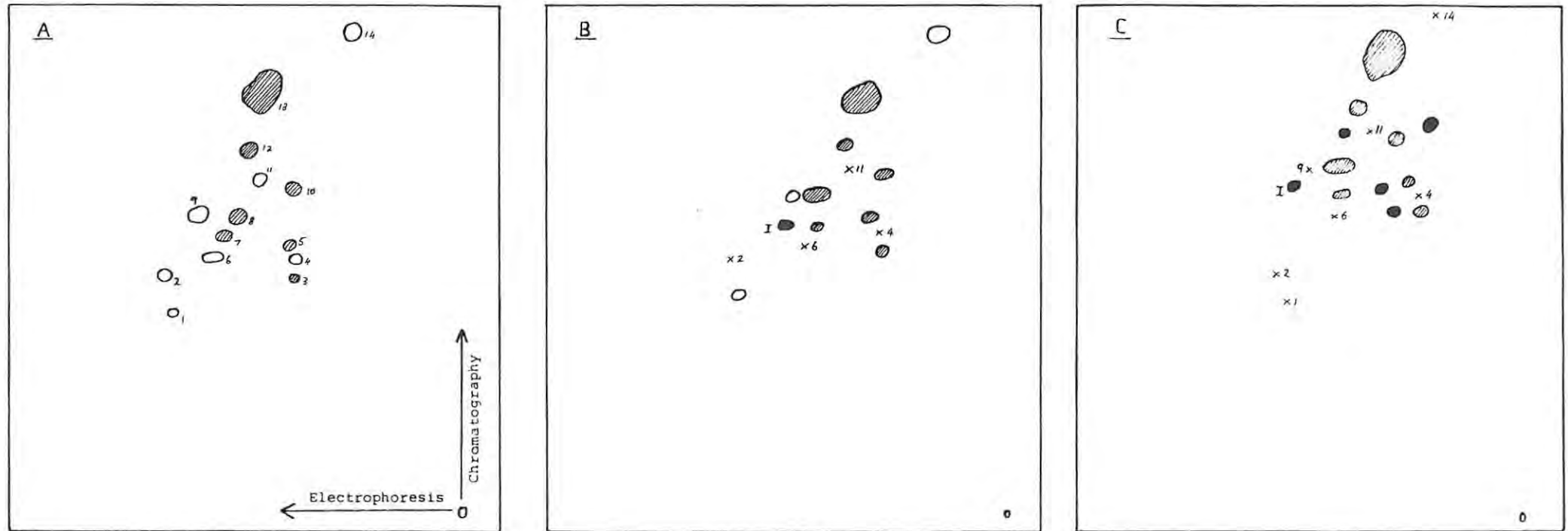


FIGURE 4.5.b. Diagrammatic representation of the peptide maps of VP1 from 5068 (A), P712 (B) and Lansing (C). Numbering of spots on the map of 5068 is arbitrary. On maps of P712 and Lansing only missing spots (x) are numbered. Novel spots are indicated by (●). Roman numerals indicate spots common to vaccine and wild-type strains only. Spots common to all strains are shown by (⊙). Sample origin (o) is in lower right-hand corner.



The differences between peptide maps of VP1 of 5068 and vaccine strain P712 are all common to both P712 and wild-type Lansing. There are, however, several features unique to the VP1 tryptic peptide map of Lansing. These include four spots shared with neither P712 nor 5068, and the absence of three peptide spots present on both the outbreak and vaccine strain maps. The similarity between the VP1 tryptic peptide maps of Gazankulu outbreak strain 5068 and vaccine strain P712 is thus greater than that between 5068 and wild-type Lansing.

Comparison of the tryptic peptide maps for VP2 of the three type 2 poliovirus strains (fig.4.6.a and b), shows that considerable similarity exists between type 2 Gazankulu outbreak strain 5068 and vaccine strain P712. Three peptide spots present on the map of 5068 VP2 have disappeared from that of P712. Two spots (numbers 16 and 18) have shifted their positions slightly, but no new peptide spots are apparent on the map for VP2 of vaccine strain P712. This contrasts strongly with the differences apparent between type 2 Gazankulu outbreak strain 5068 and wild-type strain Lansing. Four novel peptides have appeared on the Lansing map, while seven peptides are missing. The chromatographic mobility of spot 22 appears to have increased, resulting in a vertical shift of that peptide. Of the differences between VP2 of Gazankulu outbreak strain 5068 and vaccine strain P712, only the loss of peptides 2 and 19 are shared by P712 and Lansing.

Greater differences exist between VP2 of Gazankulu outbreak strain 5068 and wild-type 2 strain Lansing than between 5068 and

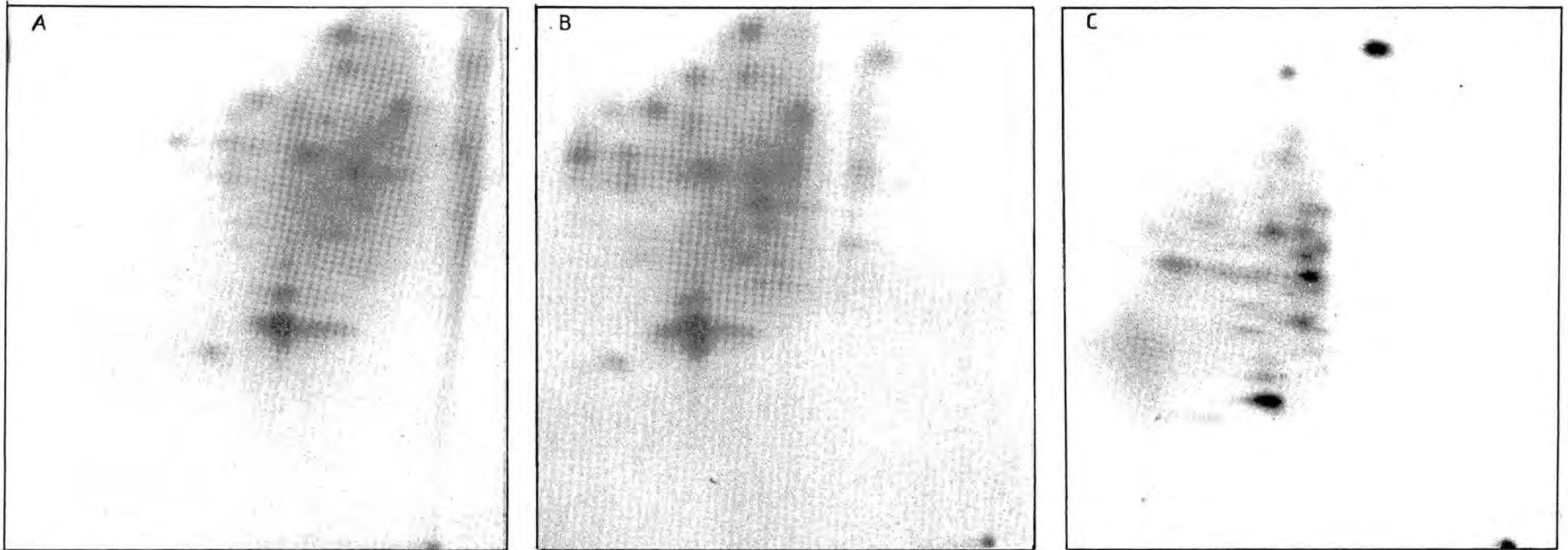


FIGURE 4.6.a Maps produced after TLC of peptides from VP2 of poliovirus type 2 strains. A - Gazankulu outbreak strain 5068; B - Sabin vaccine strain P712; C - wild-type strain Lansing.

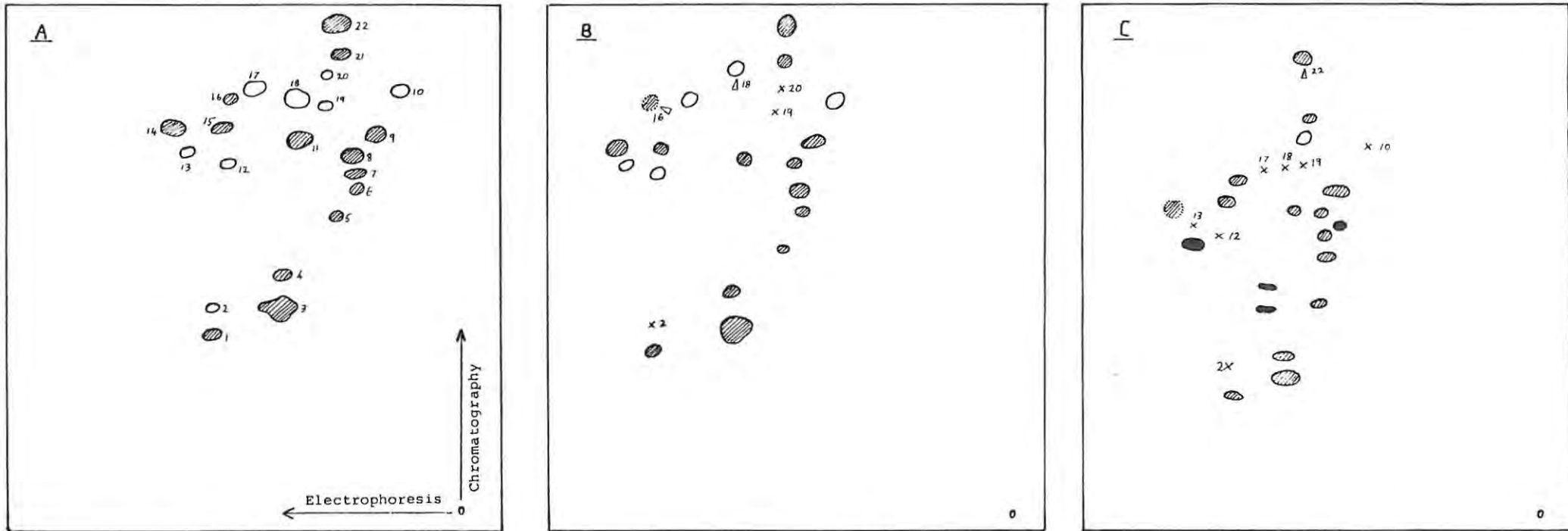


FIGURE 4.6.b. Diagrammatic representation of the peptide maps of VP2 from 5068 (A), P712 (B) and Lansing (C). Numbering of spots on the map of 5068 is arbitrary. On maps of P712 and Lansing only missing spots (x) are numbered. Novel spots are indicated by (●), shifted spots by (▷), with the arrow showing the direction of shift. Spots common to all strains are shown by (○). Faint spots are indicated by a dotted outline. Sample origin (o) is in lower right-hand corner.

vaccine strain P712. This indicates that the VP2 proteins of P712 and 5068 have a number of common sequences not shared by the wild-type strain, Lansing.

The peptide sequence of VP3 of all three of the type 2 poliovirus strains appears to be more conserved than either VP1 or VP2. All of the 15 major peptide spots appearing on the map for VP3 of Gazankulu outbreak strain 5068 are shared by vaccine strain P712, with no shifting of spots (fig. 4.7.a and b). There is, however, one new peptide spot apparent on the P712 map. This spot is also apparent on the VP3 map for wild-type strain Lansing, which differs from the maps of both 5068 and P712 in the loss of two peptides. The tryptic peptide maps thus indicate a greater similarity between VP3 of Gazankulu outbreak strain 5068 and vaccine strain P712 than between 5068 and wild-type strain Lansing.

From table 4.2 it may be seen that for all three of the capsid proteins mapped there are similarities between Gazankulu outbreak strain 5068 and vaccine strain P712. At the same time, considerable differences exist between the Gazankulu outbreak strain and the wild-type 2 poliovirus strain.

#### 4.2.1.3. Comparison of tryptic peptide maps of the capsid proteins of type 3 polioviruses

Few differences exist between the tryptic peptide maps of VP1 from poliovirus type 3 vaccine strain Leon 3 and the wild-type strain Leon III (fig. 4.8.a and b). Only one spot is unaccounted for on the map of VP1 from the wild-type strain, Leon III, while

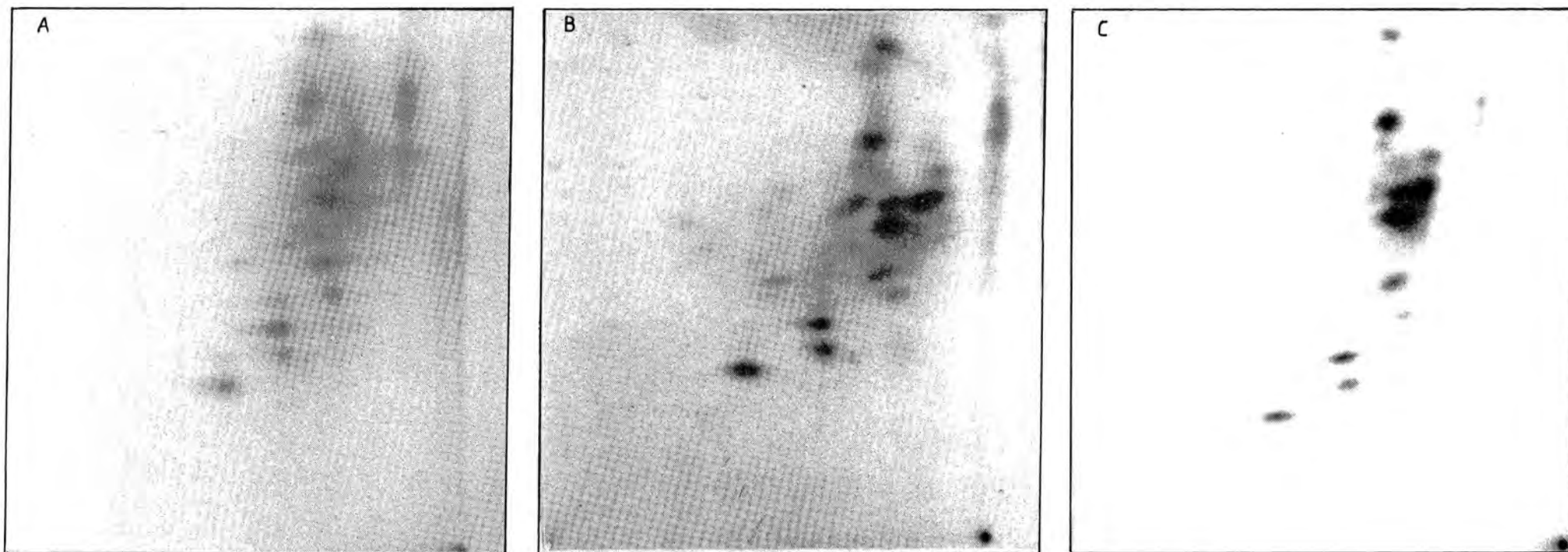


FIGURE 4.7.a Maps produced after TLC of peptides from VP3 of poliovirus type 2 strains. A - Gazankulu outbreak strain 5068; B - Sabin vaccine strain P712; C - wild-type strain Lansing.

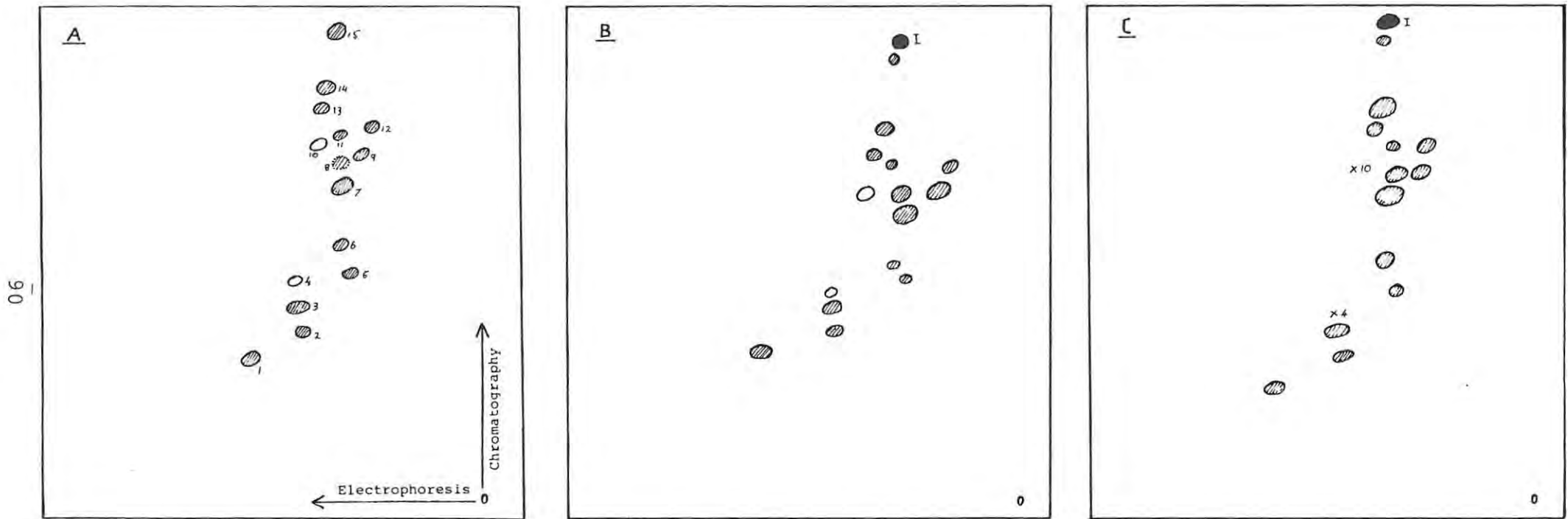


FIGURE 4.7.b. Diagrammatic representation of the peptide maps of VP3 from 5068 (A), P712 (B) and Lansing (C). Numbering of spots on the map of 5068 is arbitrary. On maps of P712 and Lansing only missing spots (x) are numbered. Novel spots are indicated by (●). Roman numerals indicate spots common to vaccine and wild-type strains only. Spots common to all strains are shown by (⊙). Faint spots are indicated by a dotted outline. Sample origin (o) is in lower right-hand corner.

Table 4.2. Comparison of tryptic peptide maps of capsid proteins 1,2 and 3 of poliovirus type 2 Gazankulu outbreak strain 5068 with similar maps of vaccine strain P712 and wild-type 1 strain Lansing.

CAPSID PROTEIN	VIRUS STRAIN	TOTAL SPOTS*	NOVEL SPOTS	LOST SPOTS	MOVED SPOTS	TOTAL DIFF'S**	SHARED <sup>+</sup>
VP1	5068	14	-	-	-	-	
	P712	13	1	4	0	5	5
	5068	14	7	7	0	14	
VP2	5068	22	-	-	-	-	
	P712	19	0	3	2	5	2
	Lansing	19	4	7	1	12	
VP3	5068	15	-	-	-	-	
	P712	16	1	0	0	1	1
	Lansing	14	1	2	0	3	

\* Number of intense peptide spots used for comparison of peptide maps.

\*\* Total number of differences apparent between peptide maps of outbreak poliovirus capsid proteins and vaccine/wild-type strain maps.

+ Number of differences from outbreak strain map shared by vaccine and wild-type strains of poliovirus.

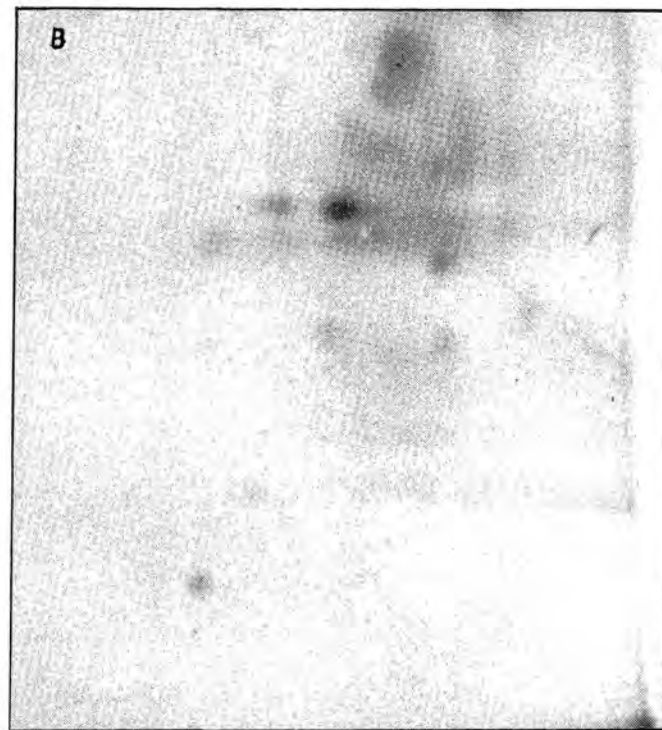
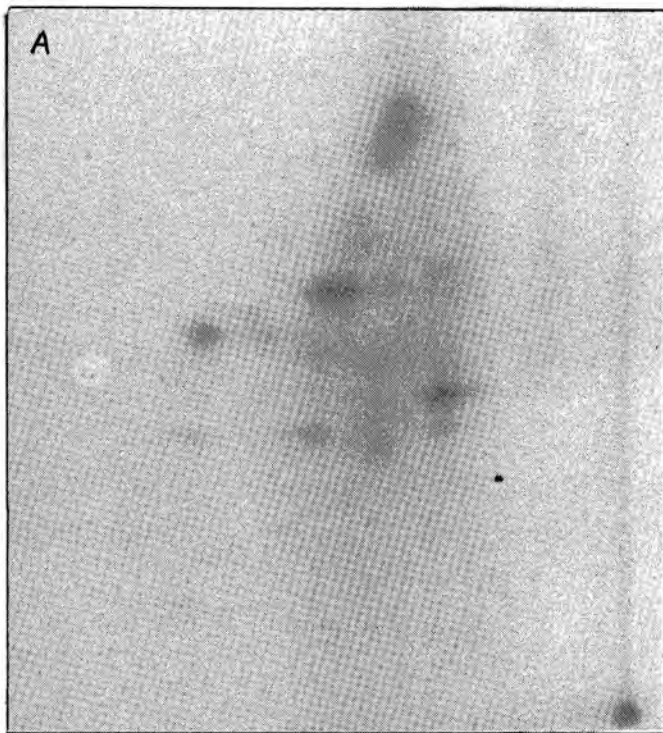


FIGURE 4.8.a Maps produced after TLC of peptides from VP1 of poliovirus type 3 strains. A - Sabin vaccine strain Leon 3; B - wild-type strain Leon III.

20



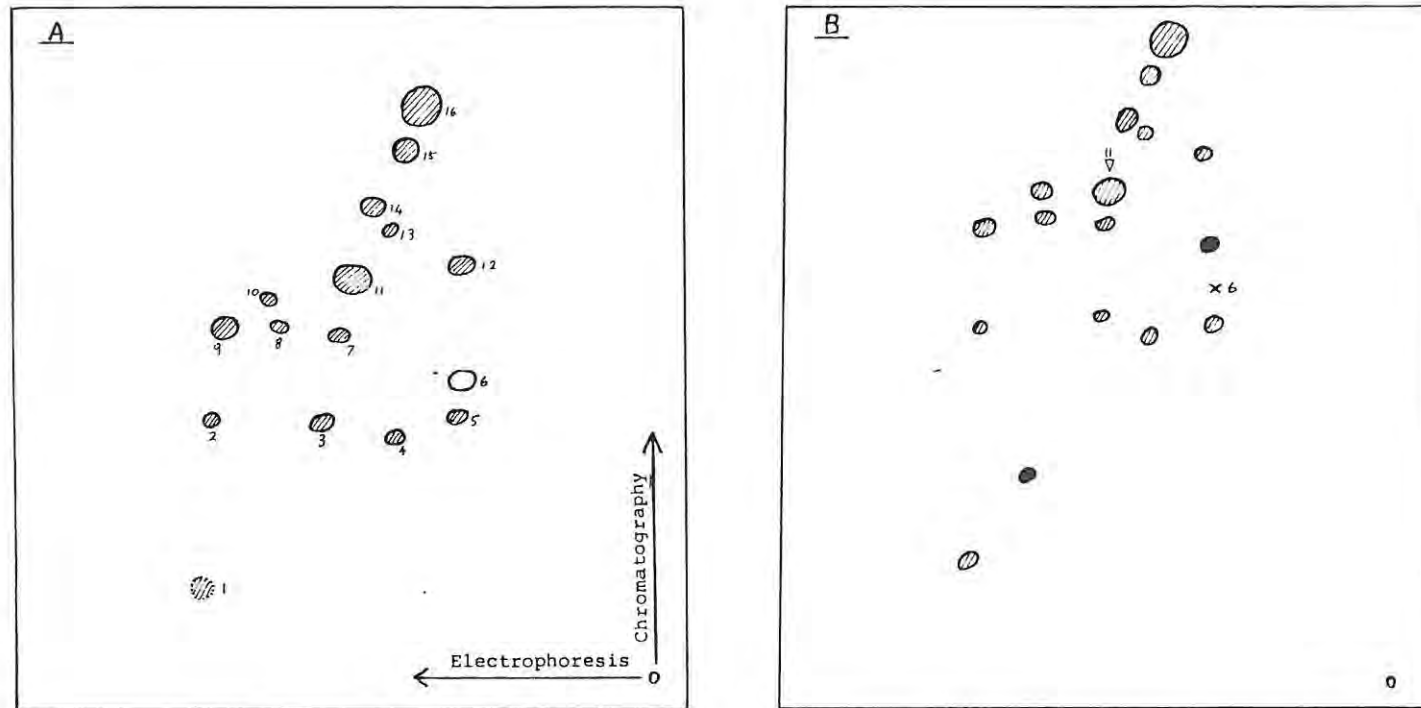


FIGURE 4.8.b. Diagrammatic representation of the peptide maps of VP1 from Leon 3 (A), and Leon III (B). Numbering of spots on the map of Leon 3 is arbitrary. On the map of Leon III only missing spots (x) are numbered. Novel spots are indicated by (●), shifted spots by (▷), with the arrow showing the direction of shift. Spots common to both strains are indicated by (◐). Faint spots are indicated by a dotted outline. Sample origin (o) is in lower right-hand corner.

two novel peptides have appeared. One spot, 11, has shifted vertically, indicating a decrease in chromatographic mobility.

The tryptic peptide maps for VP2 of the two virus strains show that this protein is also highly conserved. One peptide spot has disappeared from the map of VP2 from wild-type strain Leon III and a single new peptide spot is present (fig.4.9.a and b).

Within the VP3 of type 3 vaccine strain Leon 3 and wild-type strain Leon III, changes have also taken place at a low frequency. Two novel spots are apparent on the map of wild-type reference strain Leon III and a single peptide has disappeared. One peptide spot, number 5, displays an altered electrophoretic mobility, being displaced away from the origin (fig.4.10.a and b).

As shown by comparison of table 4.3 with tables 4.1 and 4.2, conservation between the two type 3 poliovirus strains is considerably greater than that between any other wild-type and vaccine strains. With respect to the type 1 poliovirus strains, conservation is greatest between vaccine strain LS-c and wild-type strain LS-a. Between the type 2 poliovirus strains considerable similarity exists between Gazankulu outbreak strain 5068 and vaccine strain P712.

As expected, no similarity exists between tryptic peptide maps of the two outbreak strains and those of the type 3 poliovirus strains, indicating that neither has been mis-identified.

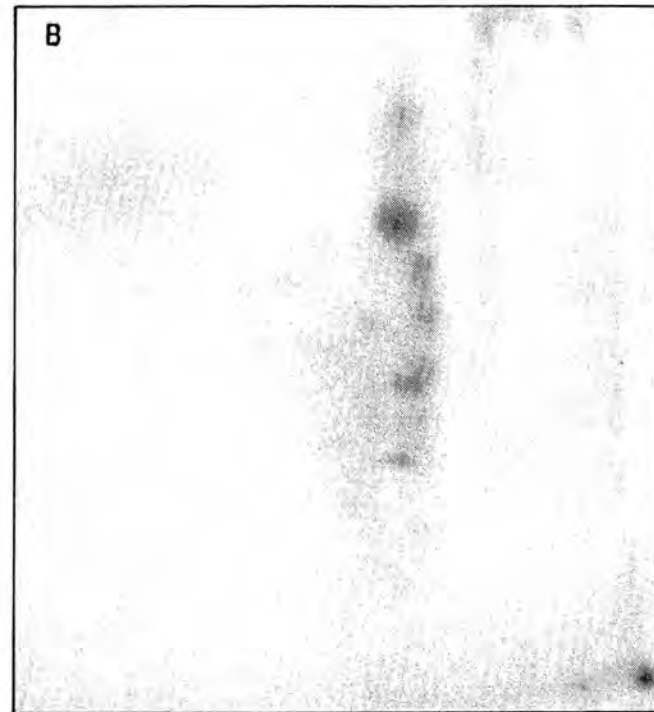
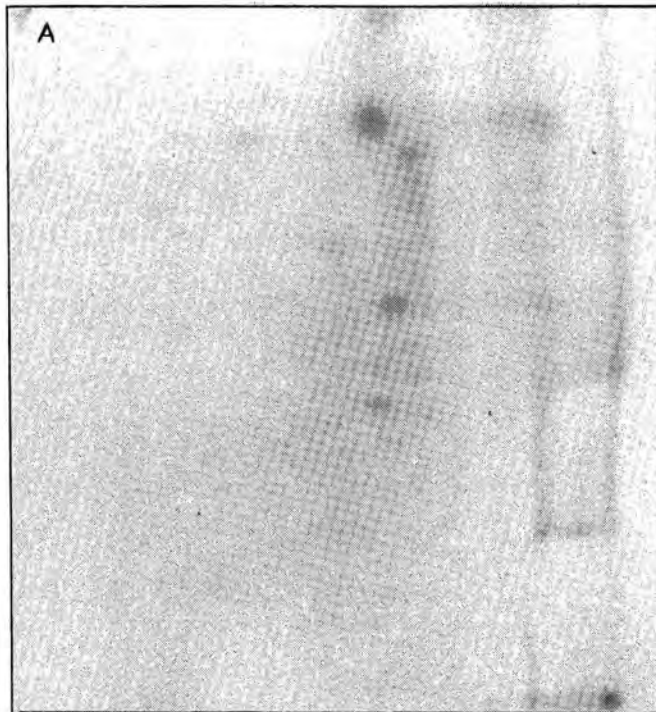


FIGURE 4.9.a Maps produced after TLC of peptides from VP2 of poliovirus type 3 strains. A - Sabin vaccine strain Leon 3; B - wild-type strain Leon III.

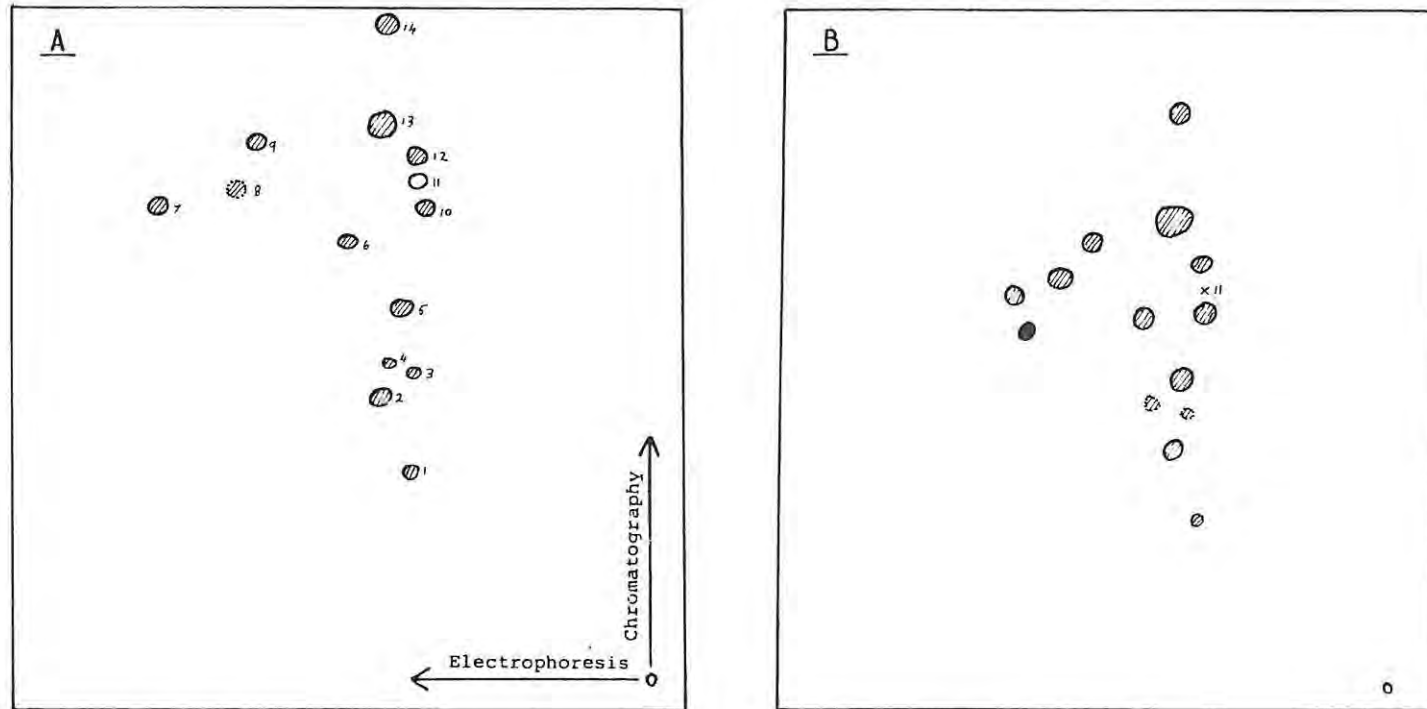


FIGURE 4.9.b. Diagrammatic representation of the peptide maps of VP2 from Leon 3 (A), and Leon III (B). Numbering of spots on the map of Leon 3 is arbitrary. On the map of Leon III only missing spots (x) are numbered. Novel spots are indicated by (●). Spots common to both strains are indicated by (◐). Faint spots are indicated by a dotted outline. Sample origin (o) is in lower right-hand corner.

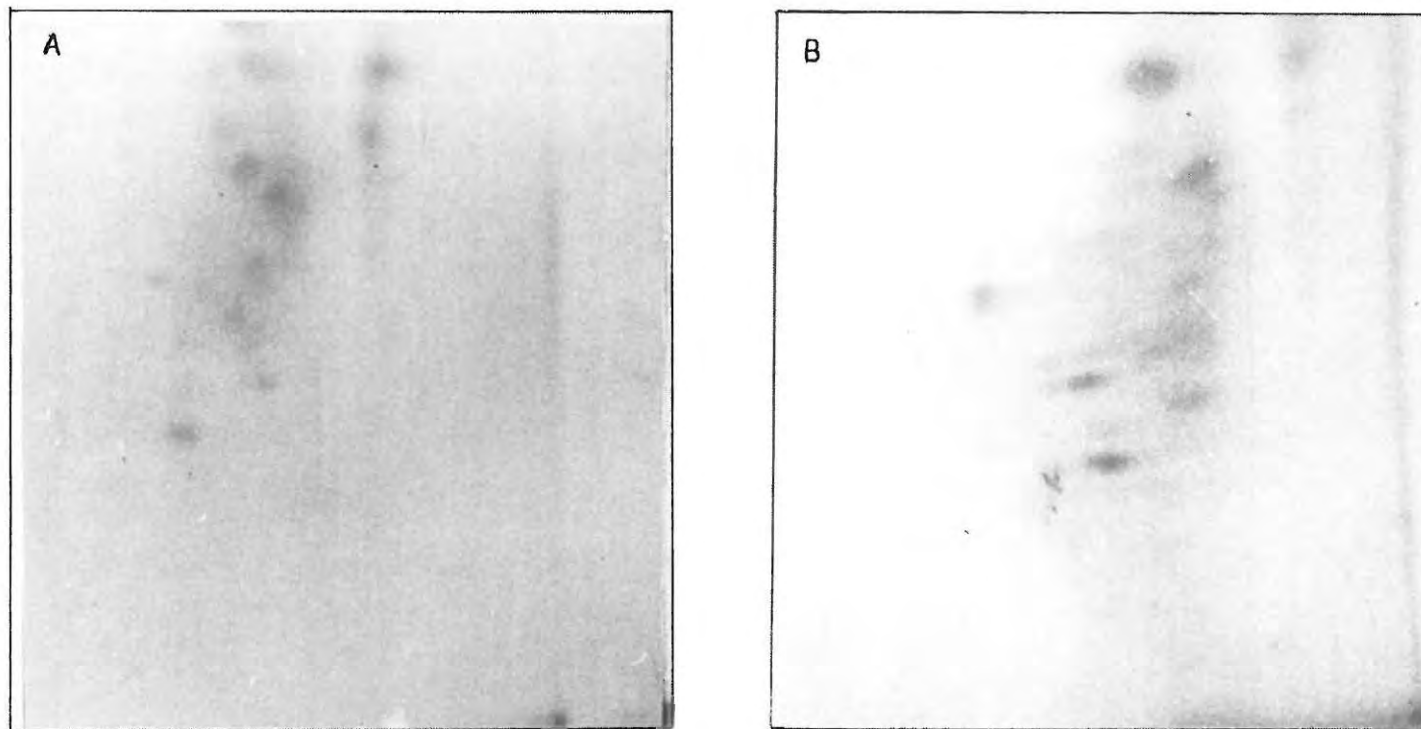


FIGURE 4.10.a Maps produced after TLC of peptides from VP3 of poliovirus type 3 strains. A - Sabin vaccine strain Leon 3; B - wild-type strain Leon III.

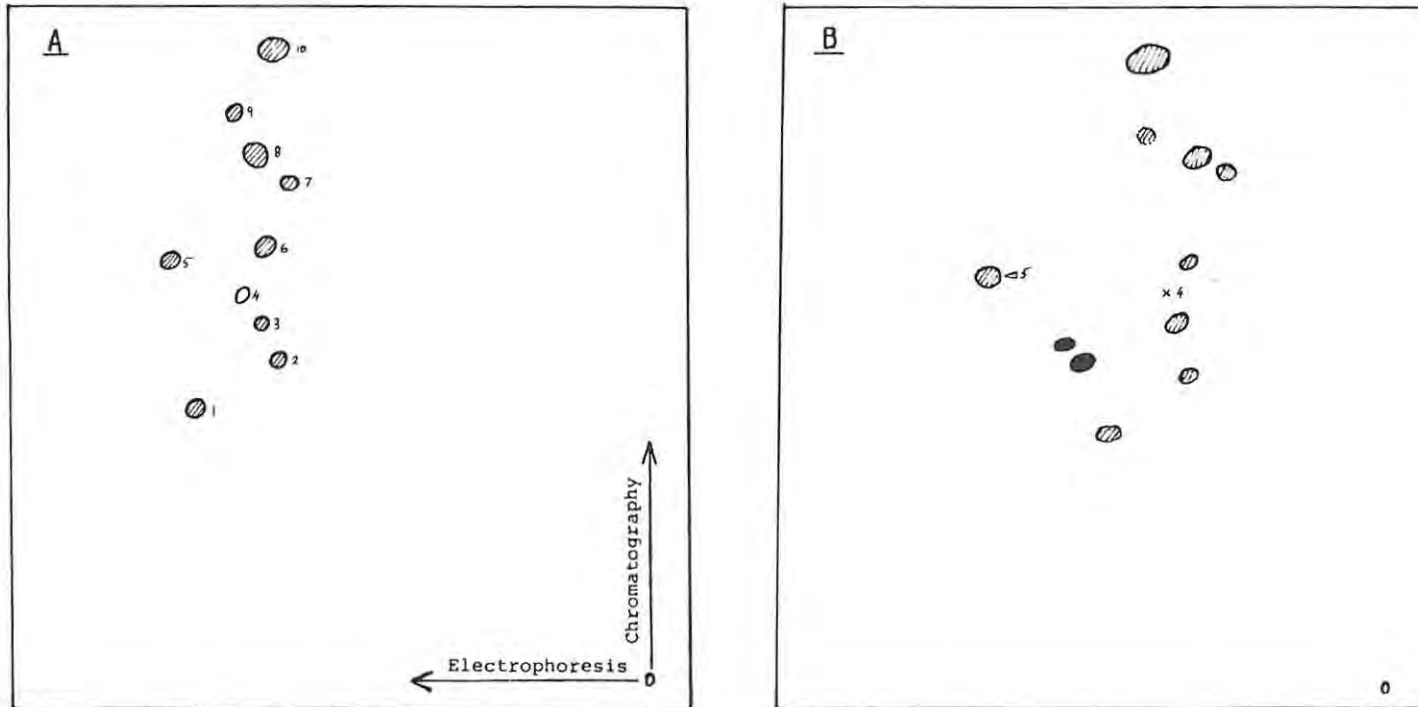


FIGURE 4.10.b. Diagrammatic representation of the peptide maps of VP3 from Leon 3 (A), and Leon III (B). Numbering of spots on the map of Leon 3 is arbitrary. On the map of Leon III only missing spots (x) are numbered. Novel spots are indicated by (●), shifted spots by (▷), with the arrow showing the direction of shift. Spots common to both strains are indicated by (⊙). Faint spots are indicated by a dotted outline. Sample origin (o) is in lower right-hand corner.

Table 4.3. Comparison of tryptic peptide maps of capsid proteins 1,2 and 3 of poliovirus type 3 vaccine strain Leon 3 with similar maps of wild-type 3 strain Leon III.

CAPSID PROTEIN	VIRUS STRAIN	TOTAL SPOTS	NOVEL SPOTS	LOST SPOTS	MOVED SPOTS	TOTAL DIFF'S
VP1	Leon 3	16	-	-	-	-
	Leon III	17	2	1	1	4
VP2	Leon 3	14	-	-	-	-
	Leon III	14	1	1	0	2
VP3	Leon 3	10	-	-	-	-
	Leon III	11	2	1	1	4

\* Number of intense peptide spots used for comparison of peptide maps.

\*\* Total number of differences apparent between peptide maps of vaccine strain capsid proteins and wild-type strain maps.

#### 4.2.2. Results of Control Experiments Carried Out to Determine Accuracy and Reproducibility of Two-Dimensional TLC of Tryptic Peptides

As may be seen from figure 4.11., no peptides were present after TLC mapping of a blank gel slice. This indicates that neither the trypsin used for protein digestion nor components within the gel were labelled. Maps obtained after digestion and mapping of two ovalbumin samples (fig.4.12.) show the reproducibility of TLC peptide mapping.

Figure 4.13.a shows the tryptic peptide map obtained after digesting a radiolabelled sample of trypsin, resolved using SDS-PAGE. The pattern of peptides (fig.4.13.b) does not correlate with any of the maps for capsid proteins of the poliovirus strains studied. This further indicates that trypsin was not radiolabelled during digestion of virus capsid proteins.

Only the most intense spots apparent on photographs of the tryptic peptide maps were used for comparing the maps. Faint peptide spots were not always reproducible, and may have been artefactual. The original autoradiographs were referred back to if photographs were not clear.

On some maps a series of 1 to 3 spots is visible, arranged vertically in line with, or close to, the sample origin. These had a poor reproducibility and were probably artefactual. It is possible that they were caused by some contaminant, or even peptide aggregates, with a poor electrophoretic mobility.



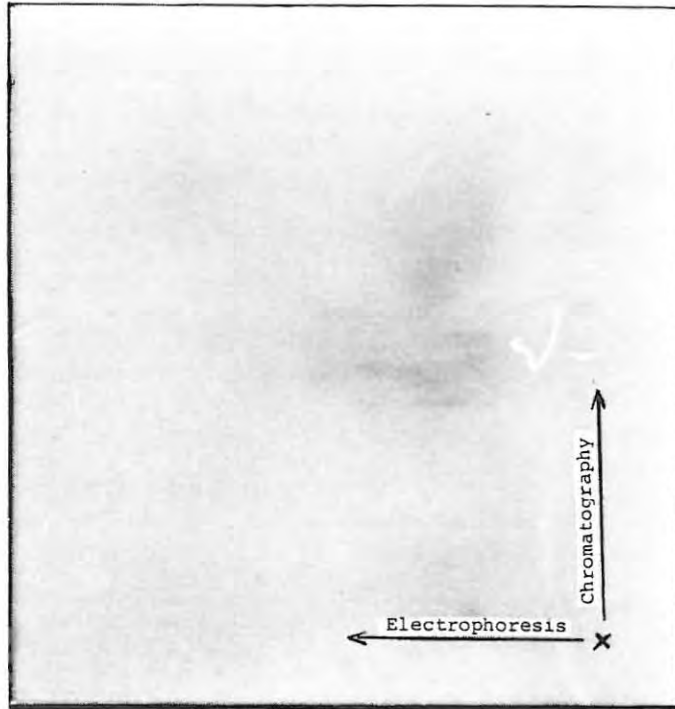


FIGURE 4.11. Photograph showing autoradiograph after radiolabelling, trypsin treatment and TLC mapping of a gel slice containing no protein. Sample origin indicated by (x).

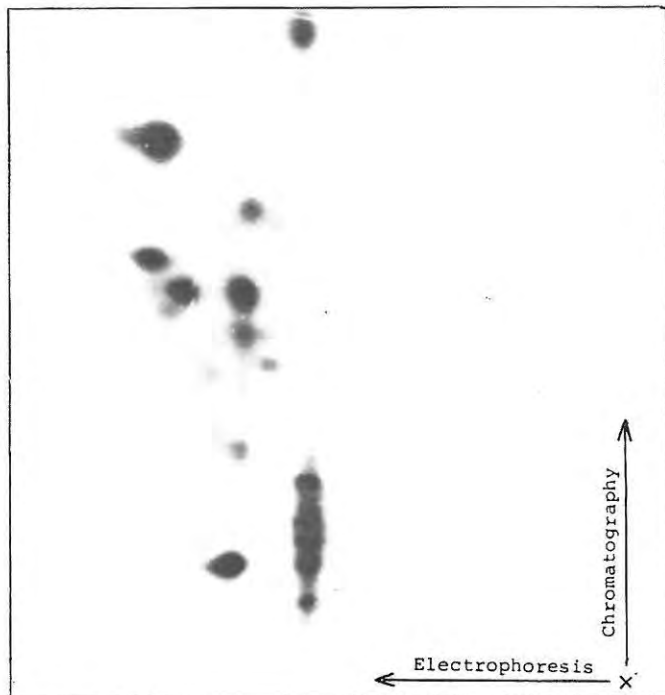
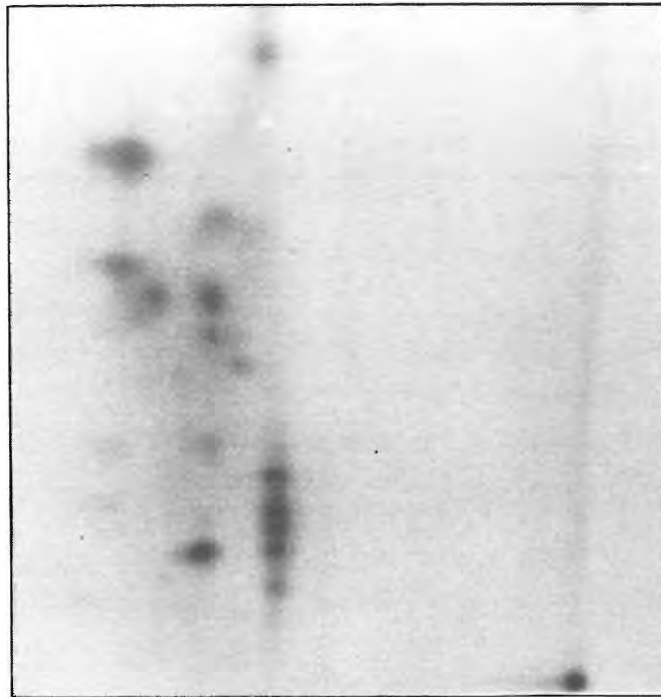


FIGURE 4.12. Maps produced after TLC of peptides from two samples of ovalbumin resolved using SDS-PAGE and labelled with  $^{125}\text{I}$ , showing reproducibility of peptide maps. Origin indicated by (x).

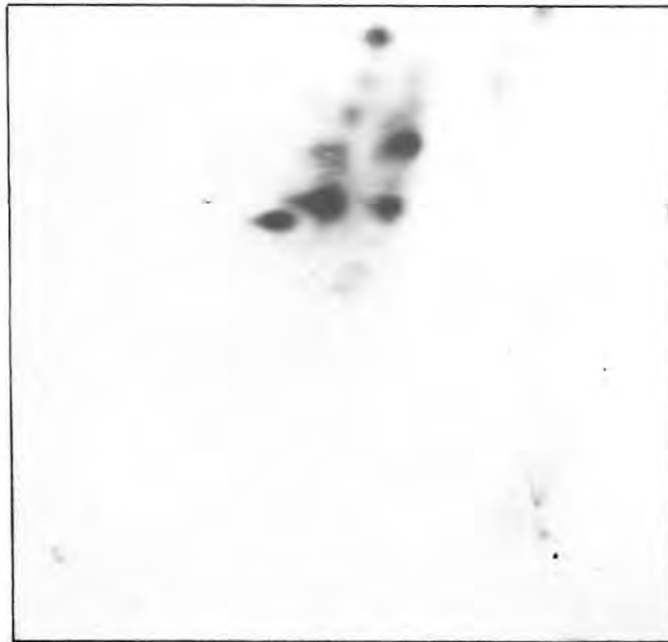


FIGURE 4.13.a. Map produced after a sample of trypsin, resolved using SDS-PAGE, was radiolabelled with  $^{125}\text{I}$  and digested with trypsin.

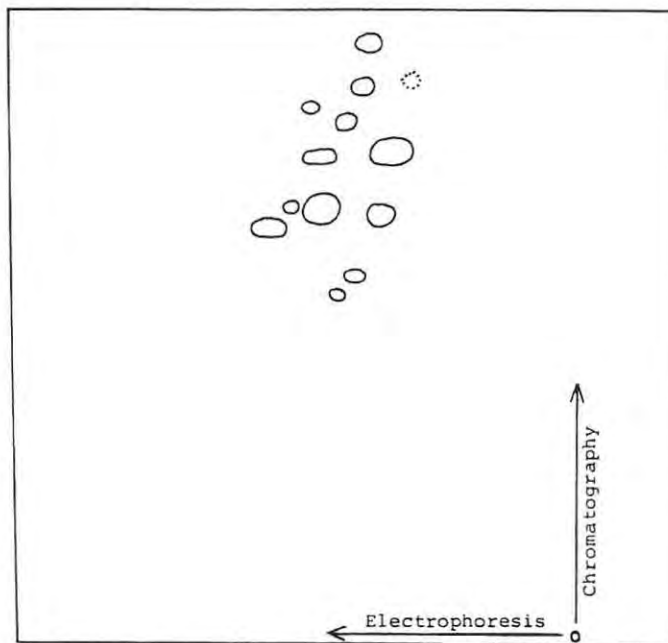


FIGURE 4.13.b. Diagrammatic representation of intense spots on peptide map of trypsin. Sample origin (o) is in lower right hand corner.

#### 4.3. Comparison of Poliovirus Capsid Proteins by Reversed-Phase High-Performance Liquid-Chromatography of Tryptic Peptides

Two-dimensional TLC proved to be an effective means of mapping tryptic peptides of poliovirus capsid proteins. Problems lay in the interpretation of the data obtained, and deciding which peptide spots were significant. Consequently, an alternative technique of tryptic peptide mapping, using reversed-phase high-performance liquid-chromatography (RP-HPLC), was tried. It was hoped that the results would support those obtained using TLC, although RP-HPLC results were expected to be more precise and conclusive. RP-HPLC and TLC results would be similar in that only peptides susceptible to labelling with  $^{125}\text{I}$  by the chloramine-T reaction could be mapped.

RP-HPLC is a highly sensitive and rapid technique. Sample separation may be achieved within 10 to 60 minutes and detection of picogram amounts of peptides is possible <sup>34</sup>. During chromatography continuous partitioning of the solute between the rigid stationary phase and the liquid mobile phase occurs. Separation is dependant on the hydrophobicity of the solute relative to the polarity of the two phases <sup>90</sup>. Hydrophobic compounds bind reversibly to the hydrophobic stationary phase and, as a result, move more slowly than hydrophilic compounds <sup>74</sup>.

The system is "reversed-phase" because the stationary phase is non-polar while the mobile phase is polar (generally consisting of an organic solvent in buffer or water). This is in contrast to the polarity of the older solid-liquid chromatography

systems.

Because chromatographic runs are rapid, high pressures (36 - 360 atmospheres) are generated. Consequently the stationary phase must be highly stable. Stationary phase materials consist of an inorganic (generally silica) backbone to which organic groups (frequently carbon chains of specific length) are bound (fig.4.14.). Octadecyl silica (ODS) stationary phases, consisting of C<sub>18</sub> chains bonded onto microparticulate silica beads, are widely used.

Chromatography may either be isocratic (i.e. the composition of the eluting solvent remains constant), or the percentage of the organic phase can be increased, resulting in a solvent gradient. This progressively elutes more tightly bound fractions from the stationary phase. Isocratic elution profiles are ideal because of the ease of duplication and because column reconditioning is unnecessary between chromatographic runs. Nevertheless, linear gradients are frequently used <sup>34</sup>.

Elution of hydrophobic solutes requires a reduction in polarity of the mobile phase and/or increase in polarity of the solute. Generally polarity of the mobile phase is decreased by increasing the concentration of the organic solvent. One of the most widely used solvents for RP-HPLC of peptides and proteins is the non-polar solvent, acetonitrile <sup>90</sup>. Ion-pairing agents bind with solute molecules and alter their hydrophobicities, improving resolution and sample recovery <sup>41</sup>.

Phosphate and perchlorate are both very powerful ion-pairing

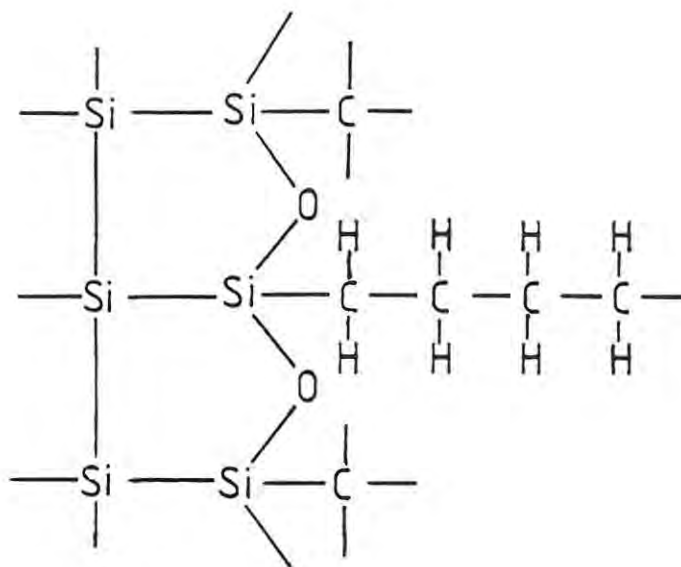


FIGURE 4.14. Structure of silica - organic stationary phase used for RP-HPLC.

agents <sup>74</sup>. Retention times of peptides containing free amino groups may be drastically reduced by addition of 0.1% phosphoric acid to water-acetonitrile gradients <sup>38</sup>. Because phosphoric acid is non-absorbent in the range of 195 - 220nm, it is compatible with the sensitive variable wavelength UV monitors used in RP-HPLC.

RP-HPLC has recently emerged as a significant technique for the analysis and separation of un-derivatized amino acids and peptides <sup>41</sup>. Peptide mapping often detects subtle differences in the primary structure of closely related proteins. Application of RP-HPLC with hydrophilic ion-pairing agents allows rapid and reproducible peptide "fingerprints" using only picomole amounts of peptide <sup>41</sup>. Analysis times may be kept short by using small columns (typically 4mm x 300mm) and small particle sizes (less than 10um in diameter). Use of closed, reusable columns allows hundreds of samples to be resolved without column re-packing <sup>39</sup>.

While fingerprint analysis of peptides (including tryptic peptides) using RP-HPLC has been carried out <sup>5,21,75,76,111</sup>, RP-HPLC is still a relatively novel technique in virus research. Virus proteins studied to date include those of herpes simplex virus <sup>107</sup>, Sendai virus <sup>108</sup>, influenza virus <sup>86</sup>, murine leukaemia virus <sup>42</sup> tick borne encephalitis virus <sup>110</sup>, and poliomyelitis virus <sup>43,44</sup>. Little work has been carried out using RP-HPLC for finger-printing tryptic peptides of viral proteins. Kinney and Trent (1982), however, have reported mapping the tryptic peptides of viruses in the Venezuelan equine encephalitis complex.

The extremely high hydrophobicity of polioviral proteins, coupled with the compactness of the virus, makes RP-HPLC of poliovirus difficult. Work carried out to date has tended to make use of high concentrations (60%) of formic acid for virus dissociation, and large-pore disposable HPLC columns <sup>43,44</sup>. Because disposable HPLC columns are costly, a reusable chromatography column was used in this study. Mapping of poliovirus capsid proteins was carried out by producing trypsin-generated peptides of the proteins and subjecting them to RP-HPLC.

#### 4.3.1. Results

After RP-HPLC of the tryptic peptides produced by digesting radiolabelled poliovirus capsid proteins, radioactivity traces were plotted. These were used for comparing the different viral capsid proteins.

##### 4.3.1.1. Comparison of tryptic peptide maps of capsid proteins of type 1 polioviruses

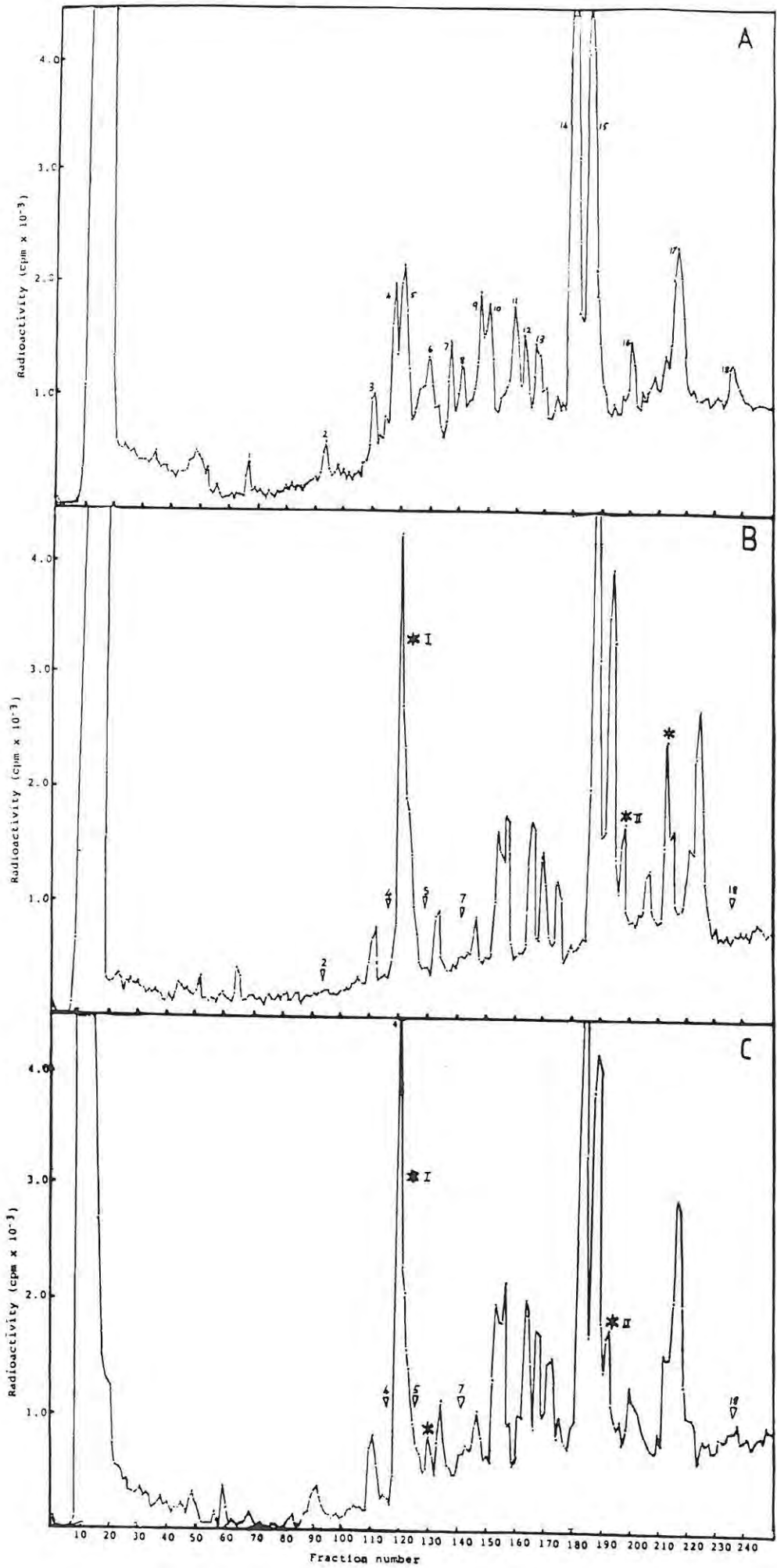
Figure 4.15. shows the radioactivity traces for tryptic peptides of VP1 from the three type 1 poliovirus strains. There are 18 major peptides present on the radioactivity trace for VP1 from Gazankulu outbreak strain 5061. The majority of these peptides are clearly differentiated. The peptides labelled 4 and 5, and those labelled 9 and 10 occur close together, overlapping to a certain extent.

Differences are apparent between VP1 of Gazankulu outbreak strain 5061 and Sabin vaccine strain LS-c. Five peptides are missing from the map of LS-c VP1 when compared to 5061 while



FIGURE 4.15.

Radioactivity traces obtained after RP-HPLC of tryptic peptides of radiolabelled VP1 from poliovirus type 1 strains. A - Gazankulu outbreak strain 5061; B - Sabin vaccine strain LS-c; C - wild-type strain LS-a. On maps of LS-c and LS-a VP1 only missing peptides, indicated by (∇) are numbered, while novel peptides are indicated by (\*). Roman numerals indicate peptides common to vaccine and wild-type strains only.



three novel peptides are present. Comparison of VP1 tryptic peptide maps from Gazankulu outbreak strain 5061 and wild-type strain LS-a shows that four peptides are absent from the LS-a map and three new peptides are present. Two of the new peptides are common to vaccine type 1 strain LS-c and wild-type strain LS-a. All of the peptides absent from the map of LS-a VP1 are also missing from that of vaccine strain LS-c. Clearly, greater similarity exists between vaccine strain LS-c and wild-type LS-a than between outbreak strain 5061 and LS-c.

Upon comparison of the RP-HPLC maps of  $^{125}\text{I}$  labelled tryptic peptides of VP2 of the type 1 poliovirus strains (figure 4.16.) a pattern is again apparent, although the similarity between the three strains is reduced. On the map obtained for 5061 VP2, 13 peptides are present. The majority of these appear on the VP2 map for vaccine strain LS-c.

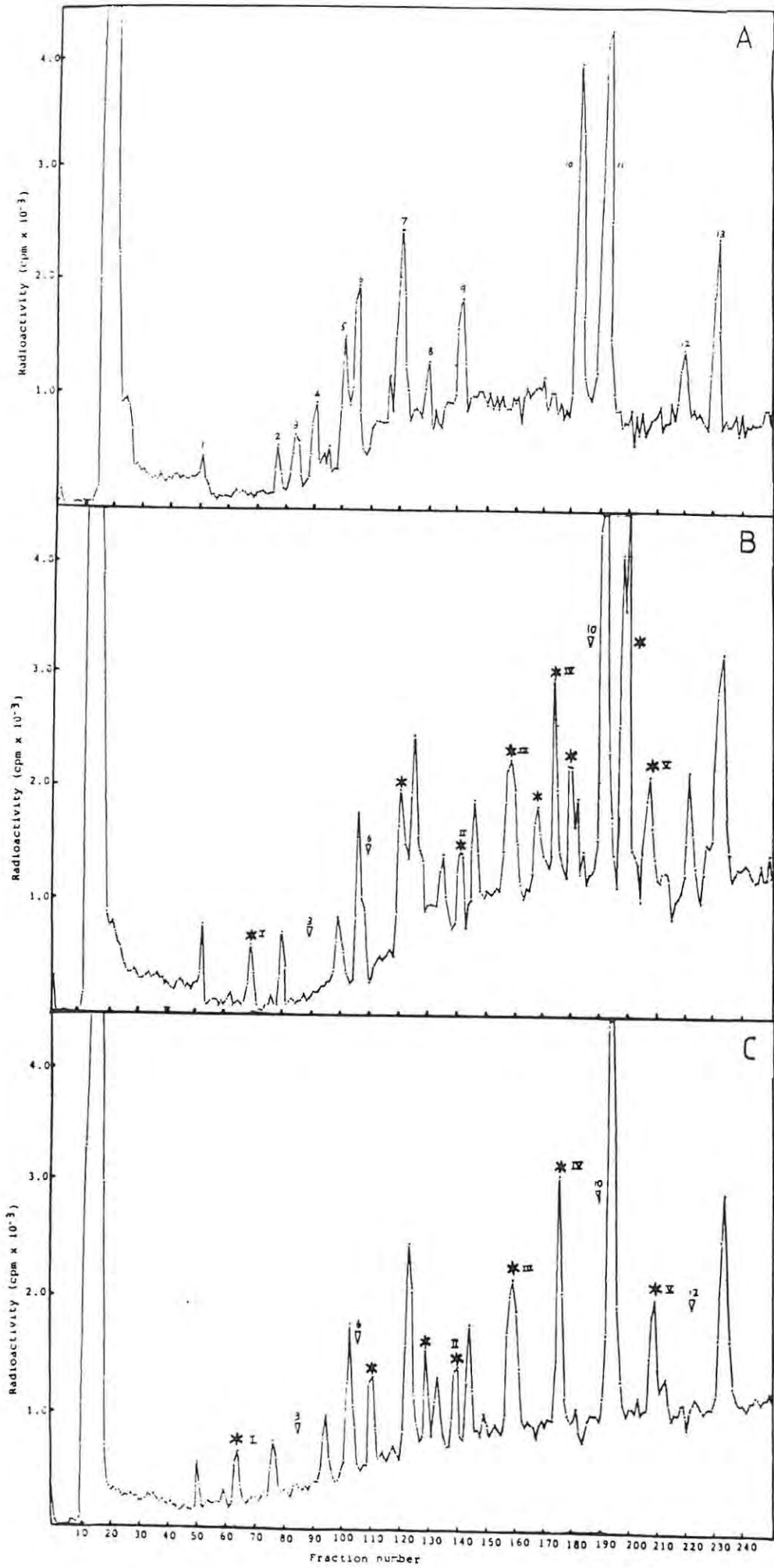
Three tryptic peptides present on the VP2 map of Gazankulu outbreak strain 5061 are missing from the map of the vaccine strain LS-c. Nine new peptide peaks, including one very large one, are apparent. The large peptide is probably the result of internal substitutions increasing the number of amino acids susceptible to labelling.

Several differences exist between the peptide maps obtained after RP-HPLC of VP2 from the Gazankulu outbreak strain and wild-type strain LS-a. The map for wild-type strain LS-a is missing four peptides present on the map for Gazankulu outbreak strain 5061 while seven additional peptides are present.

110a

FIGURE 4.16.

Radioactivity traces obtained after RP-HPLC of tryptic peptides of radiolabelled VP2 from poliovirus type 1 strains. A - Gazankulu outbreak strain 5061; B - Sabin vaccine strain LS-c; C - wild-type strain LS-a. On maps of LS-c and LS-a VP2 only missing peptides, indicated by (∇) are numbered, while novel peptides are indicated by (\*). Roman numerals indicate peptides common to vaccine and wild-type strains only.



There is a considerable degree of similarity between the VP2 tryptic peptide maps of vaccine strain LS-c and wild-type strain LS-a. Five peptides are exclusive to LS-c and LS-a, while all of the peptides missing from the LS-c map are also absent from that of LS-a. Such similarity is not shared by 5061 and LS-c - only peptide 12 is exclusive to their VP2 maps.

Differences are also apparent when the radioactivity traces for the eluted peptides of VP3 of the different strains are compared (fig.4.17.). Of the 12 peptides present on the VP3 map for type 1 Gazankulu outbreak strain 5061, nine are shared with the vaccine strain LS-c. Five new peptides have appeared on the map for LS-c. Comparison of the VP3 tryptic peptide map obtained for Gazankulu outbreak strain 5061 with that of wild-type LS-a shows that two peptides are missing. The two missing peptides are also absent from the map of VP3 from vaccine strain LS-c. Two new tryptic peptides are present on the wild-type LS-a map, both of which are common to vaccine strain LS-c.

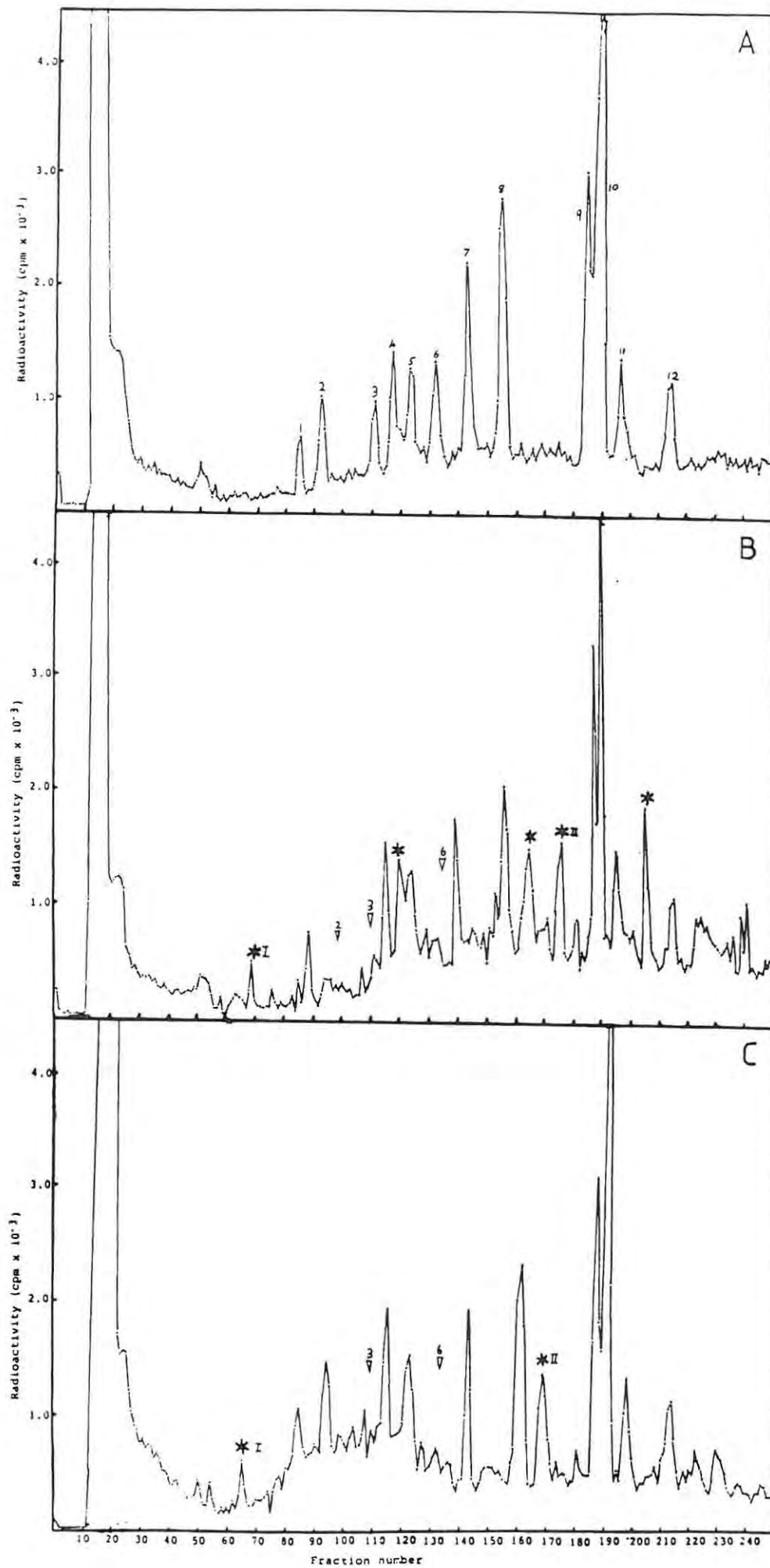
The Gazankulu outbreak strain of type 1 poliovirus, 5061, differs from vaccine strain LS-c in all three of the capsid proteins compared. These differences are considerably greater than those between vaccine strain LS-c and wild-type strain LS-a. This indicates that relationship between type 1 Gazankulu outbreak strain 5061 and Sabin vaccine strain LS-c is unlikely.

#### 4.3.1.2. Comparison of tryptic peptide maps of capsid proteins of type 2 polioviruses

Similarities exist between the tryptic peptide maps obtained by

FIGURE 4.17.

Radioactivity traces obtained after RP-HPLC of tryptic peptides of radiolabelled VP3 from poliovirus type 1 strains. A - Gazankulu outbreak strain 5061; B - Sabin vaccine strain LS-c; C - wild-type strain LS-a. On maps of LS-c and LS-a VP3 only missing peptides, indicated by (V) are numbered, while novel peptides are indicated by (\*). Roman numerals indicate peptides common to vaccine and wild-type strains only.





RP-HPLC of VP1 of the type 2 poliovirus strains studied (figure 4.18.). Of the 16 peptides on the map for VP1 of Gazankulu outbreak strain 5068, all but four are shared with the VP1 map of vaccine strain P712. There are four peptides on the P712 map which do not appear on the map for 5068.

Some of the differences between 5068 and vaccine strain P712 are shared by P712 and wild-type reference strain Lansing. Three tryptic peptides are exclusive to VP1 from P712 and Lansing, while three of the peptides missing from the P712 map are absent from that of Lansing. Several additional features are unique to Lansing. These include four novel peptides and the loss of three peptides present on both the outbreak and vaccine strain maps.

The results indicate that greater similarities exist between VP1 tryptic peptide maps of Gazankulu outbreak strain 5068 and Sabin vaccine strain P712 than between either strain and the wild-type reference strain, Lansing.

Differences between the tryptic peptide maps of VP2 of the three type 2 virus strains also exist (fig.4.19.). Of the 21 peptides appearing on the map for VP2 of type 2 Gazankulu outbreak strain 5068, 16 are common to vaccine strain P712. Two new peptides are present on the peptide map of P712 VP2.

Differences between VP2 tryptic peptide maps of Gazankulu outbreak strain 5068 and type 2 reference strain Lansing are greater than those between 5068 and vaccine strain P712. There are five new peptides on the map for Lansing, while seven

FIGURE 4.18.

Radioactivity traces obtained after RP-HPLC of tryptic peptides of radiolabelled VP1 from poliovirus type 2 strains. A - Gazankulu outbreak strain 5068; B - Sabin vaccine strain P712; C - wild-type strain Lansing. On maps of P712 and Lansing VP1 only missing peptides, indicated by (∇) are numbered, while novel peptides are indicated by (\*). Roman numerals indicate peptides common to vaccine and wild-type strains only.

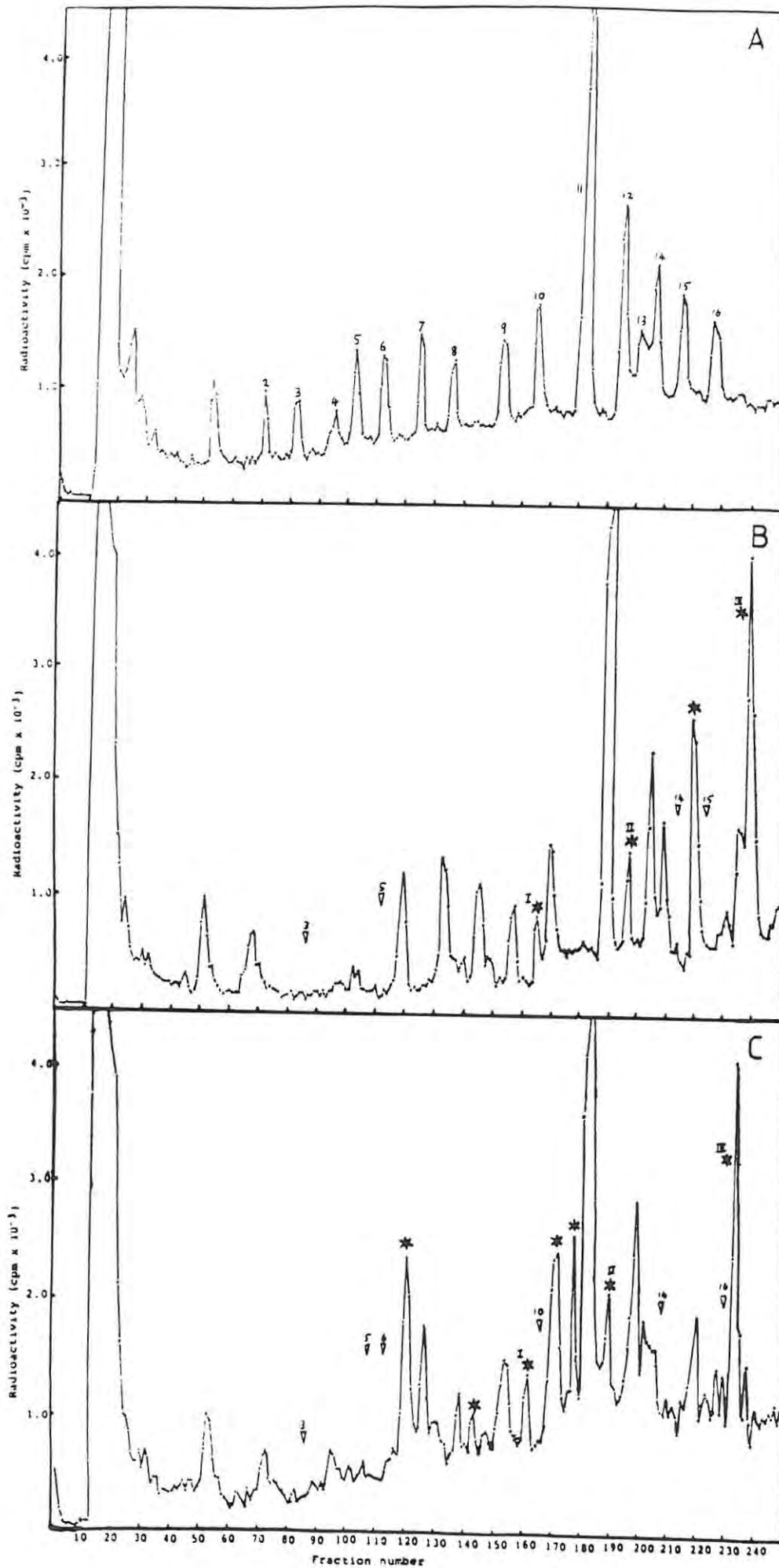
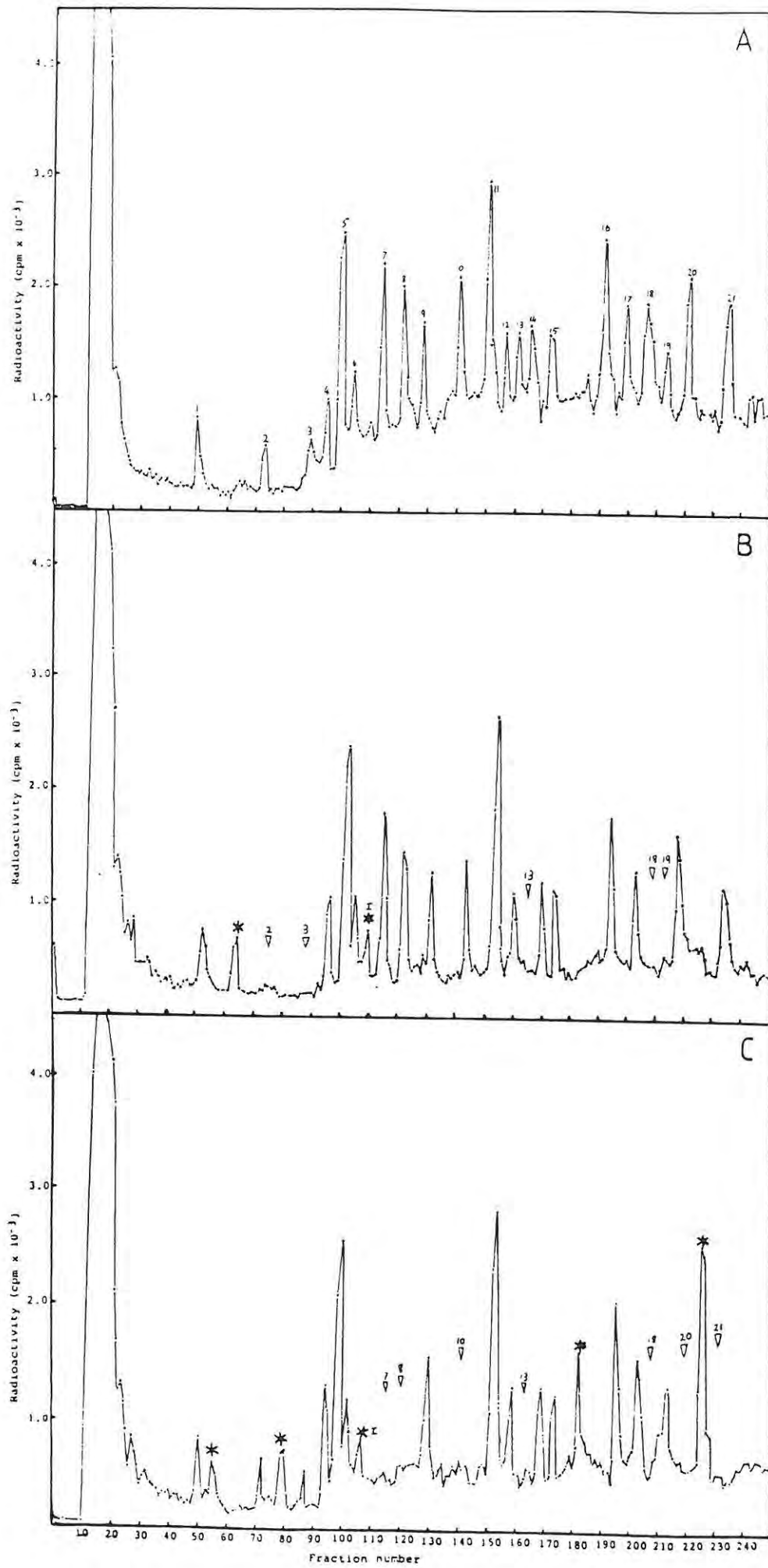


## FIGURE 4.19.

Radioactivity traces obtained after RP-HPLC of tryptic peptides of radiolabelled VP2 from poliovirus type 2 strains. A - Gazankulu outbreak strain 5068; B - Sabin vaccine strain P712; C - wild-type strain Lansing. On maps of P712 and Lansing VP2 only missing peptides, indicated by (∇) are numbered, while novel peptides are indicated by (\*). Roman numerals indicate peptides common to vaccine and wild-type strains only.



peptides present on the 5068 map have been lost.

Few features are exclusive to vaccine strain P712 and reference strain Lansing alone. One of the two novel peaks on the P712 VP2 map is shared, as is the loss of peptides 13 and 18. From this it is clear that greater similarities in VP2 exist between 5068 and P712 than between either strain and wild-type strain Lansing.

Of the three capsid proteins, VP3 shows the least variation between the three virus strains. There are 17 radiolabelled peptides on the tryptic peptide map for type 2 Gazankulu outbreak strain 5068 (fig 4.20.). All but one of these peptides are apparent on the VP3 map for vaccine strain P712. There is one new peptide present on the P712 map. Comparison of the VP3 map of type 2 Gazankulu outbreak strain 5068 with that of wild-type reference strain Lansing shows that two peptides have been lost while one new peptide is present. The new peptide is the only feature which is exclusive to vaccine strain P712 and wild-type strain Lansing.

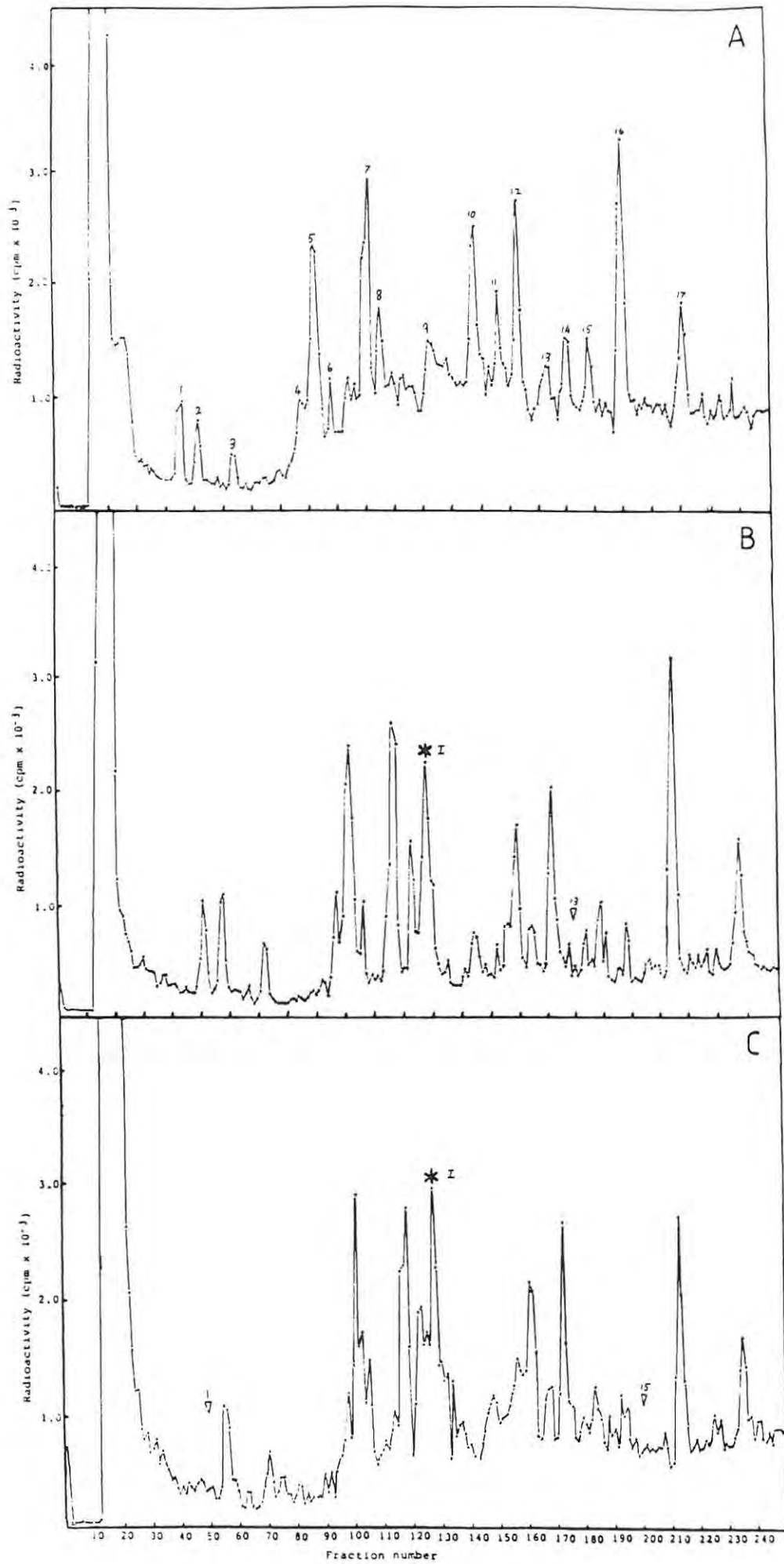
Within the type 2 poliovirus strains studied, the greatest similarity in capsid proteins occurs between type 2 vaccine strain P712 and type 2 Gazankulu outbreak strain 5068. This indicates that 5068 may be vaccine related.

#### 4.3.1.3. Comparison of the tryptic peptide maps of capsid proteins of type 3 polioviruses

The radioactivity traces obtained after RP-HPLC of tryptic peptides of VP1 from Sabin vaccine strain Leon 3 and wild-type Leon

## FIGURE 4.20.

Radioactivity traces obtained after RP-HPLC of tryptic peptides of radiolabelled VP3 from poliovirus type 2 strains. A - Gazankulu outbreak strain 5068; B - Sabin vaccine strain P712; C - wild-type strain Lansing. On maps of P712 and Lansing VP3 only missing peptides, indicated by (∇) are numbered, while novel peptides are indicated by (\*). Roman numerals indicate peptides common to vaccine and wild-type strains only.





III are shown in figure 4.21. The peptide composition appears to be highly conserved, with only three differences between the maps for VP1 of the two strains. On the tryptic peptide map of wild-type Leon III one peptide has disappeared, while a single new peptide is present.

Comparison of maps of VP2 from vaccine and wild-type strains (Fig.4.22.) shows that there is little variability between the two strains. Wild-type strain Leon III is missing one peptide present on the VP2 map for vaccine strain Leon 3, while three new peptides have appeared.

A similar degree of conservation is apparent between VP3 of the two type 3 poliovirus strains (fig.4.23.). Two peptides present on the VP3 tryptic peptide map for vaccine strain Leon 3 have disappeared from the map for wild-type strain Leon III. Two novel peptide peaks are present on the map for the wild-type strain.

The degree of conservation between the two type 3 poliovirus strains is extremely high in all three of the capsid proteins compared. Only within VP3 of the type 2 poliovirus Gazankulu outbreak and vaccine strains does greater peptide conservation exist.

#### 4.3.2. Results of Control Experiments Carried Out to Determine Accuracy and Reproducibility of RP-HPLC of Tryptic Peptides

Figure 4.24. shows the radioactivity trace obtained when a polyacrylamide gel slice containing no protein was radiolabelled

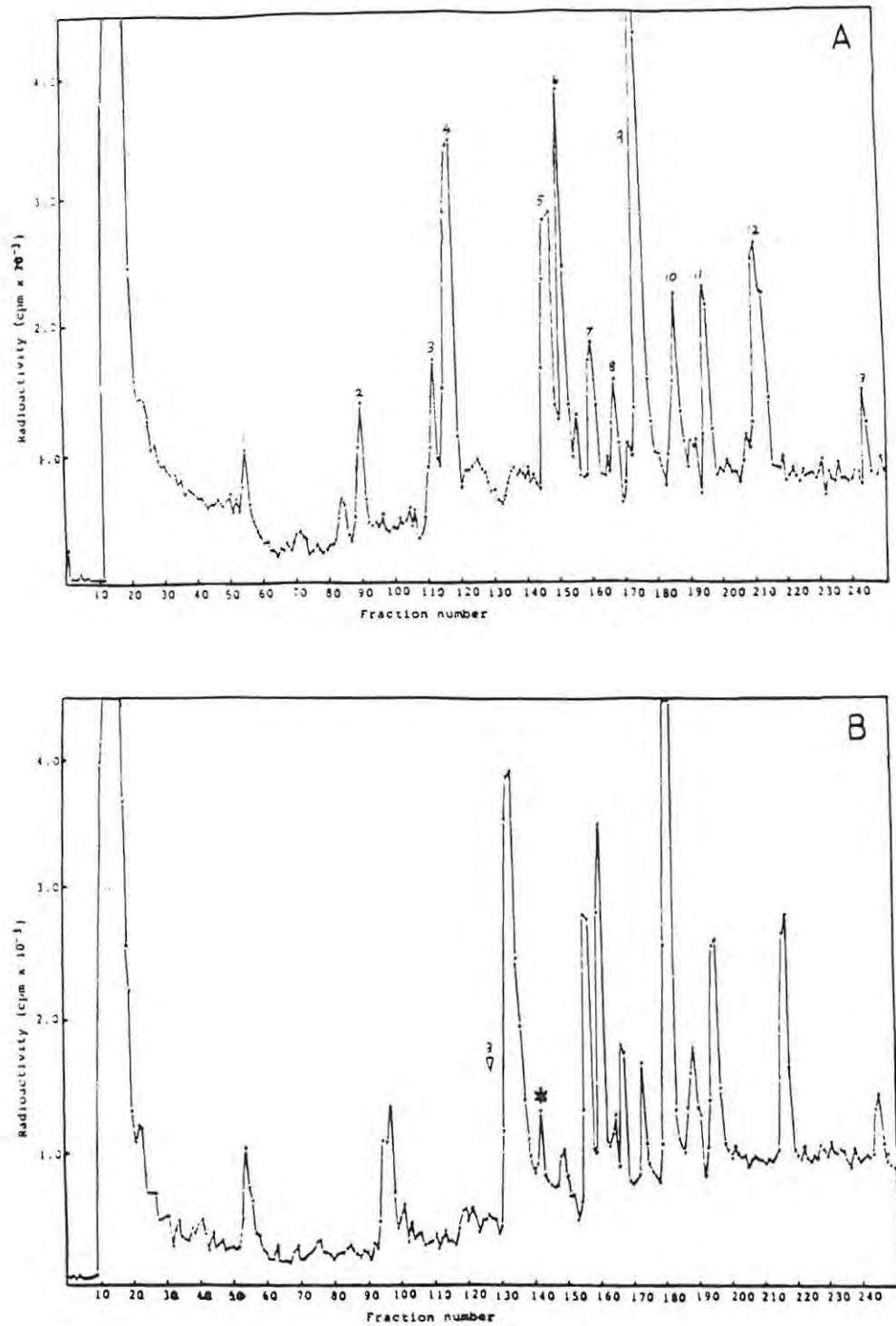


FIGURE 4.21.

Radioactivity traces obtained after RP-HPLC of tryptic peptides of radiolabelled VP1 from poliovirus type 3 strains. A - Sabin vaccine strain Leon 3; B - wild-type strain Leon III. On the map of Leon III VP1 only missing peptides, indicated by (∇) are numbered, while novel peptides are indicated by (\*).

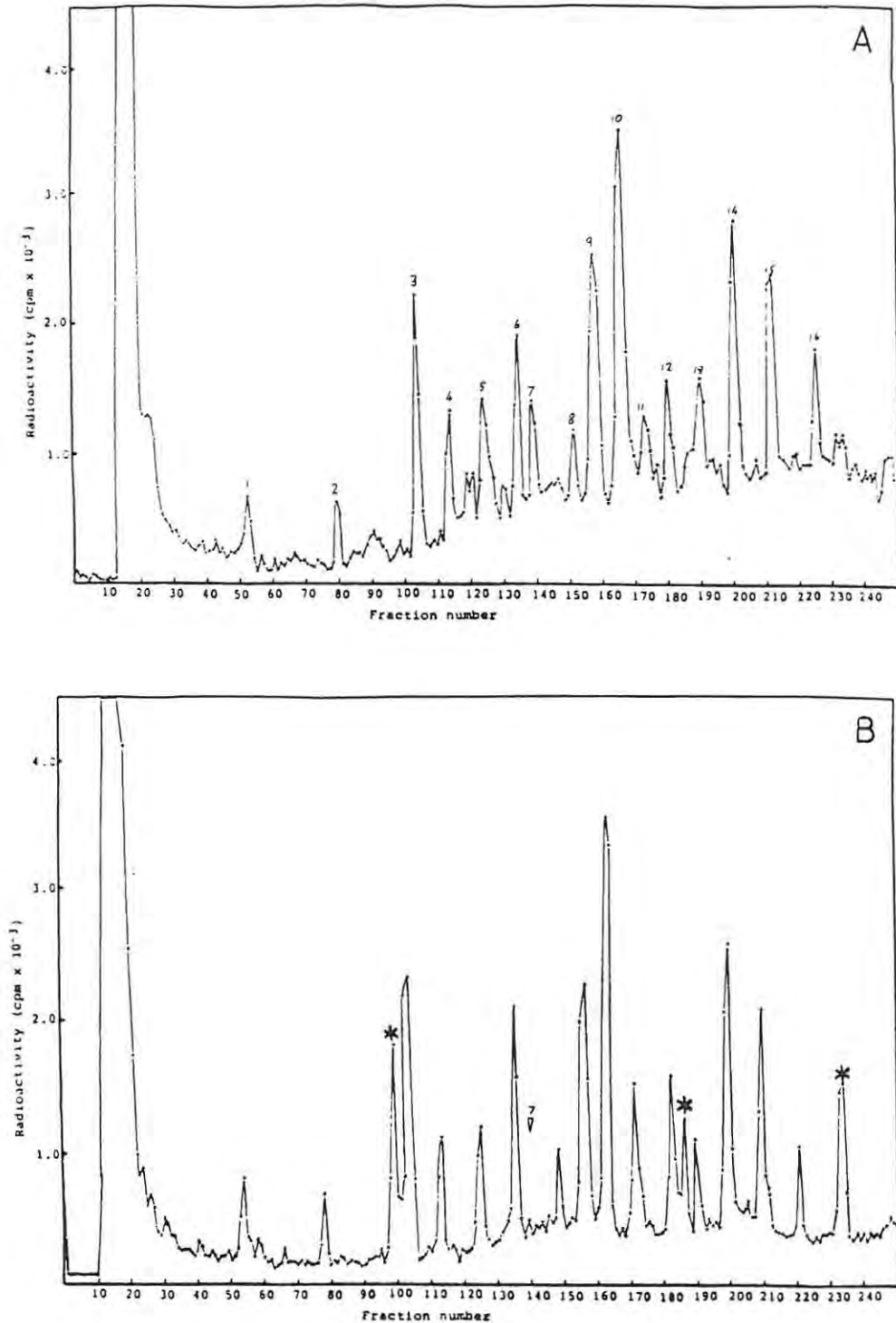


FIGURE 4.22.

Radioactivity traces obtained after RP-HPLC of tryptic peptides of radiolabelled VP2 from poliovirus type 3 strains. A - Sabin vaccine strain Leon 3; B - wild-type strain Leon III. On the map of Leon III VP2 only missing peptides, indicated by (∇) are numbered, while novel peptides are indicated by (\*).

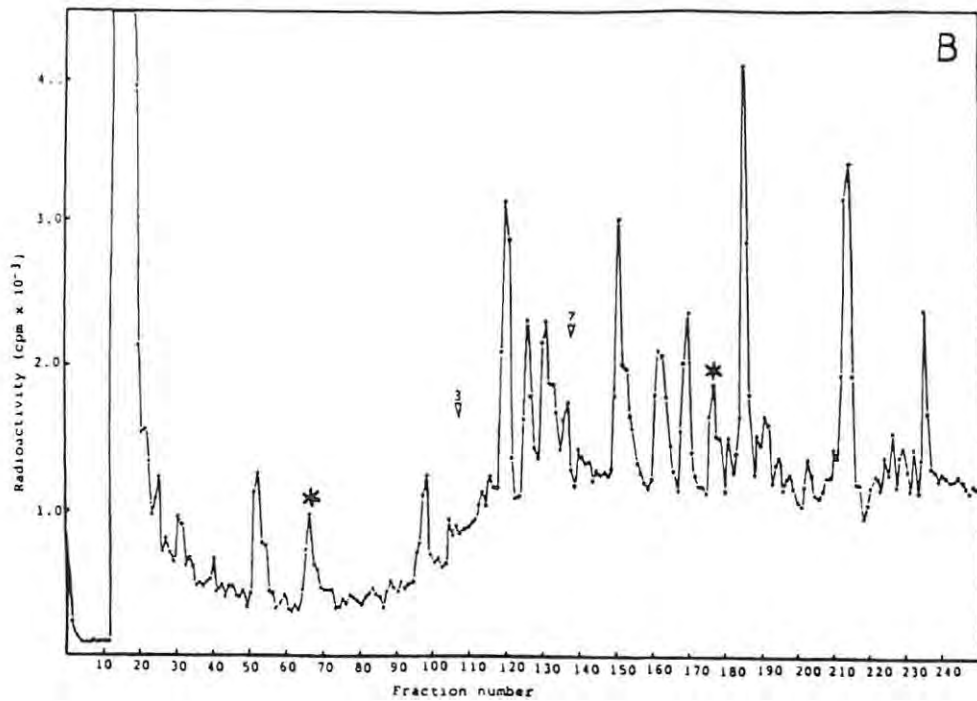
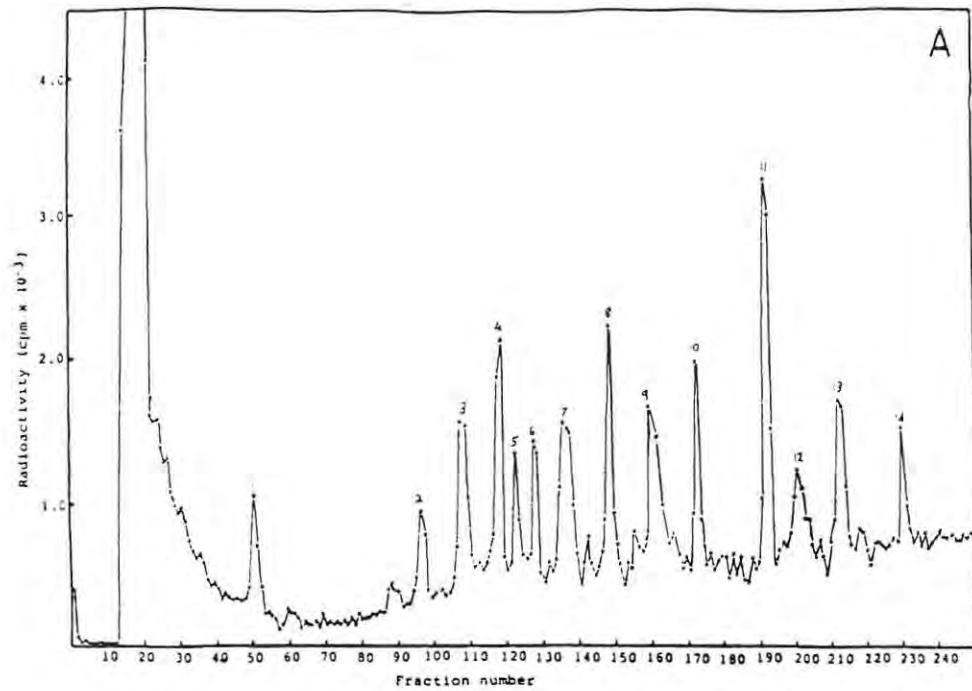


FIGURE 4.23.

Radioactivity traces obtained after RP-HPLC of tryptic peptides of radiolabelled VP3 from poliovirus type 3 strains. A - Sabin vaccine strain Leon 3; B - wild-type strain Leon III. On the map of Leon III VP3 only missing peptides, indicated by (∇) are numbered, while novel peptides are indicated by (\*).

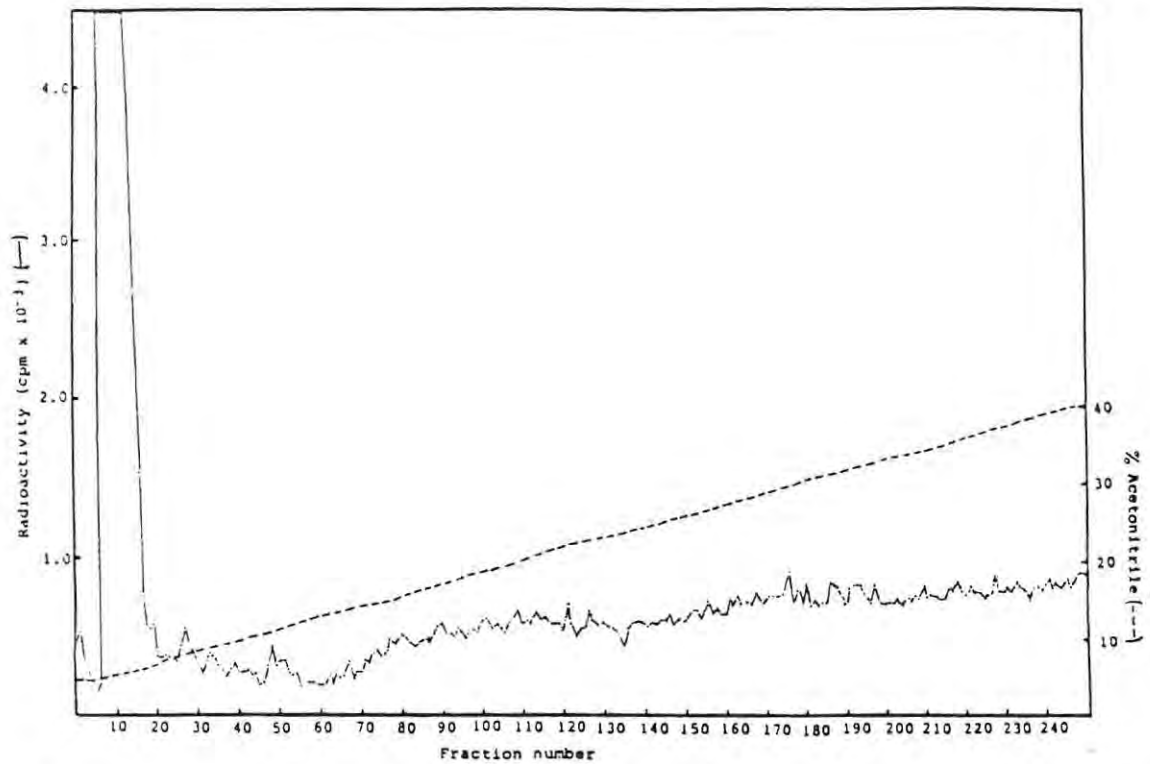


FIGURE 4.24. Radioactivity trace obtained after radiolabelling, trypsin treatment and RP-HPLC mapping of a gel slice containing no protein.

with  $^{125}\text{I}$  and treated with trypsin. Over 95% of the radioactivity recovered did not bind to the stationary phase and was eluted in the first 20 fractions after the void volume.

The remaining radioactivity forms a constant low level background, with no significant radioactive peaks appearing. Elder et al (1977) have noted that certain lots of acrylamide contain a diffusible contaminant which is radioiodinated at low levels. This was probably the reason for the background radioactivity.

In order to check the reproducibility of the results obtained using RP-HPLC, two different samples of bovine serum albumin (BSA) were resolved using SDS-PAGE and digested. The two traces obtained after mapping the digests are shown in figure 4.25. As expected, both traces display the same pattern of peptide peaks. The good peptide separation indicates an efficient solvent system. There are slight differences in elution times between the two traces due to the fact that a home-made gradient maker was used. These differences are not great, and do not seriously affect the maps obtained.

The trace obtained when a radiolabelled and digested sample of trypsin was mapped using RP-HPLC (figure 4.26.a) shows clearly defined peaks of radioactivity. These do not correspond to patterns obtained for the viral capsid proteins, indicating that viral protein digests were not contaminated by radioactive peptides of trypsin.

A close correlation exists between the traces of radioactivity

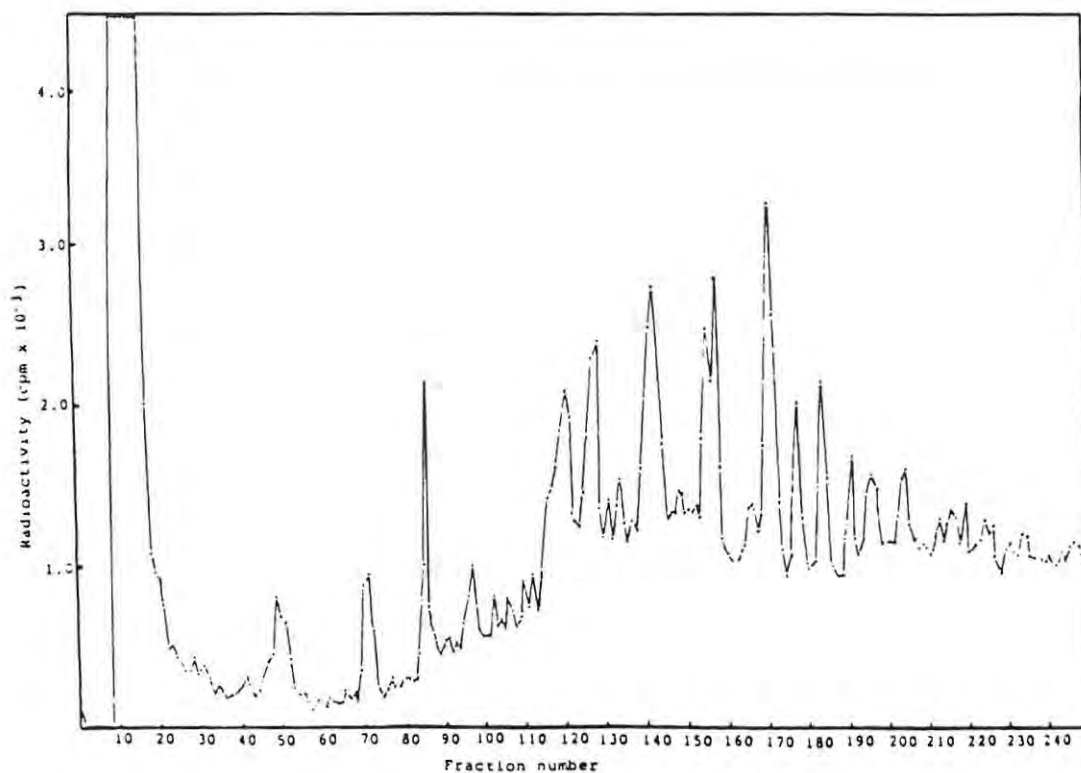
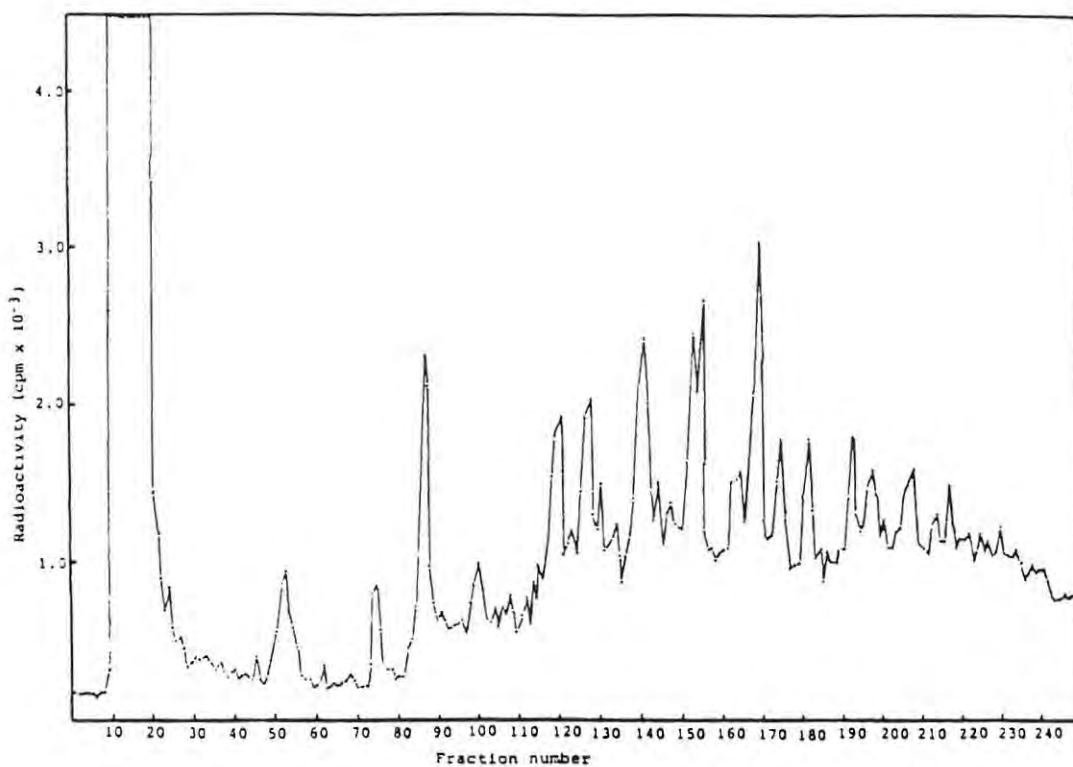


FIGURE 4.25. Radioactivity traces obtained after RP-HPLC of individual samples of BSA labelled with <sup>125</sup>I and trypsin digested, showing reproducibility of results.

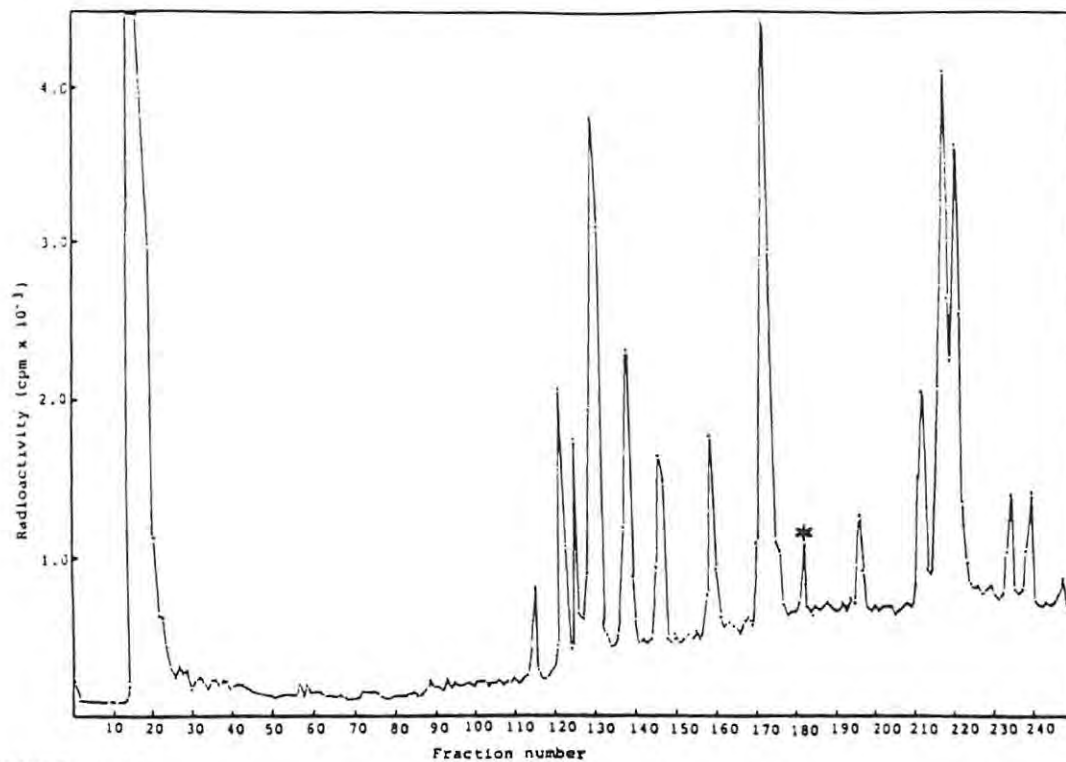


FIGURE 4.26.a. Radioactivity trace obtained after RP-HPLC of a radiolabelled tryptic digest of trypsin. Peak unique to radioactivity trace indicated by (\*).

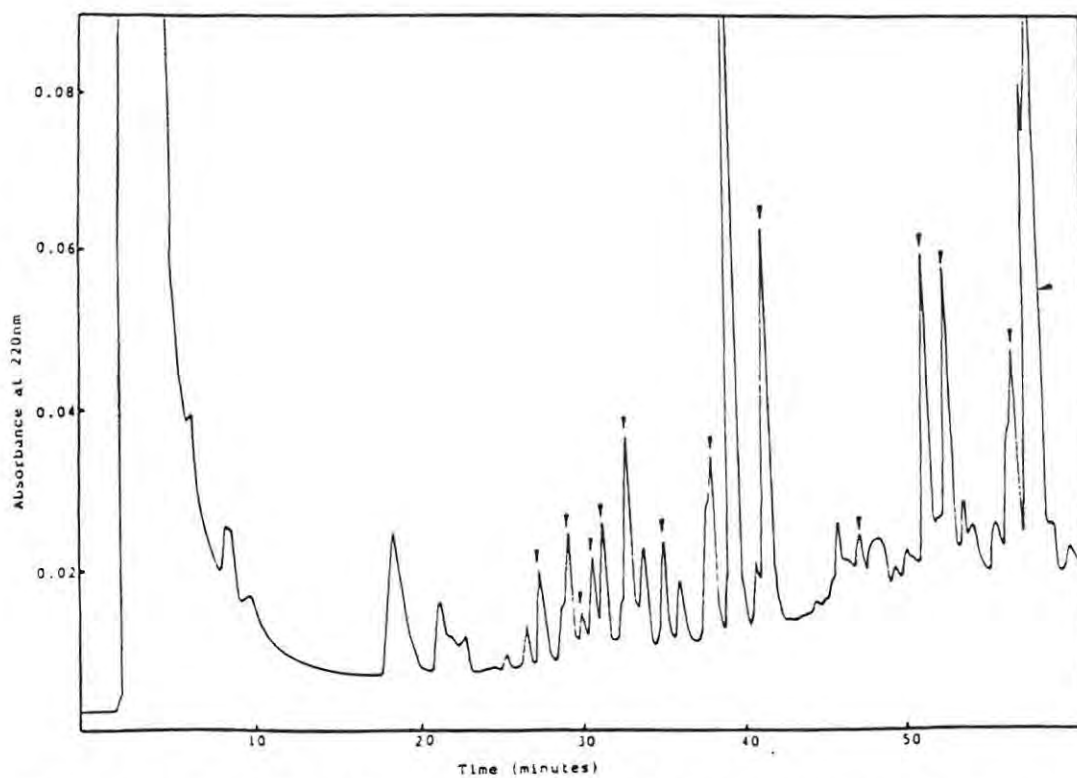


FIGURE 4.26.b. Trace of absorbance at 220nm of peptide sample used in fig.4.26.a. Peaks common to both traces indicated by (►).



and eluate absorbance at 220nm for the digest of trypsin (fig. 4.26.a and b). Of the 15 peptide peaks obtained after plotting radioactivity of the eluate, all but one appear on the trace of absorbance at 220nm. There are 15 peptides which are present on the absorbance trace only. This indicates that 47% of the tryptic peptides were labelled, i.e. contained amino acids that were labelled during the chloramine-T reaction. Differences in the height of the peptide peaks were presumably due to differing amounts of labelled amino acids within the peptides.

Approximately 50% of the recovered radioactivity elutes immediately after the void volume - the first 12-13 fractions (a volume of 2.5ml) (fig.4.26.a). This peak probably contains hydrophilic amino acids, such as lysine, which readily elute from the column <sup>53</sup>. The quantity of radioactivity eluted is, however, too great for this to be the only explanation. Possibly <sup>125</sup>I has been cleaved off the peptides, or peptides have not adsorbed to the column efficiently.

The low level of background radioactivity indicates that peptide degradation has not occurred <sup>52</sup>, implying that the elution conditions are not excessively harsh. Cleavage of <sup>125</sup>I from the peptides is thus unlikely. The second explanation is more likely, for the trace of UV absorbance at 220nm (figure 4.26.b) shows that a large amount of material, optically dense at 220nm, has eluted immediately after the void volume.

SDS contamination of the tryptic digest due to incomplete removal of SDS from proteins after SDS-PAGE probably caused the

excessive peptide elution. Because of its properties as an anionic detergent, SDS alters the hydrophobicity of those peptides to which it remains bound. Resultant "masking" of tryptic peptides may have prevented their adsorption to the RP-HPLC column. Evidence for this is provided by figure 4.27. This shows the peptide map of trypsin which was not prepared using SDS-PAGE. A digestion mixture was prepared in the normal manner, but no gel slice was included. After incubation, the mixture was air dried and the trypsin autodigestion products mapped using RP-HPLC. As can be seen, on the plot of absorbance at 220nm the initial peak is considerably reduced in size.

In the case of all proteins separated using SDS-PAGE before peptide mapping by RP-HPLC, between 50% and 75% of the radio-label elutes immediately after the void volume. As may be seen from the two radioactivity traces of BSA peptides (fig.4.25.) the effect is not selective, and causes a variable but minor reduction in the height of the radioactivity peaks. The overall pattern of the tryptic peptide map is not affected.

#### 4.4. Discussion of Results Obtained After Mapping Tryptic Peptides of Poliovirus Capsid Proteins

Various workers <sup>56,89,104</sup> have carried out sequence studies. These allow calculation of the theoretical number of radio-labelled peptides generated after tryptic digestion of proteins labelled with <sup>125</sup>I by the chloramine-T method. Figure 4.28. shows the amino acid sequence for the capsid proteins of the Sabin virus strains. Sites at which trypsin cleaves, and

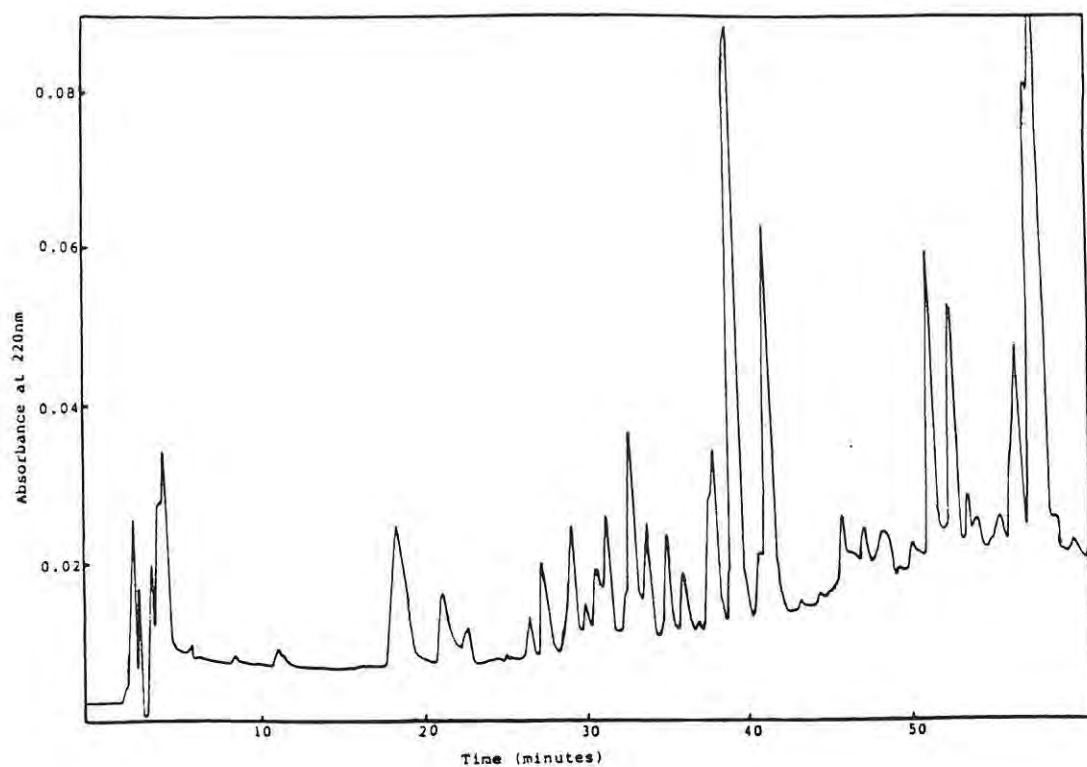
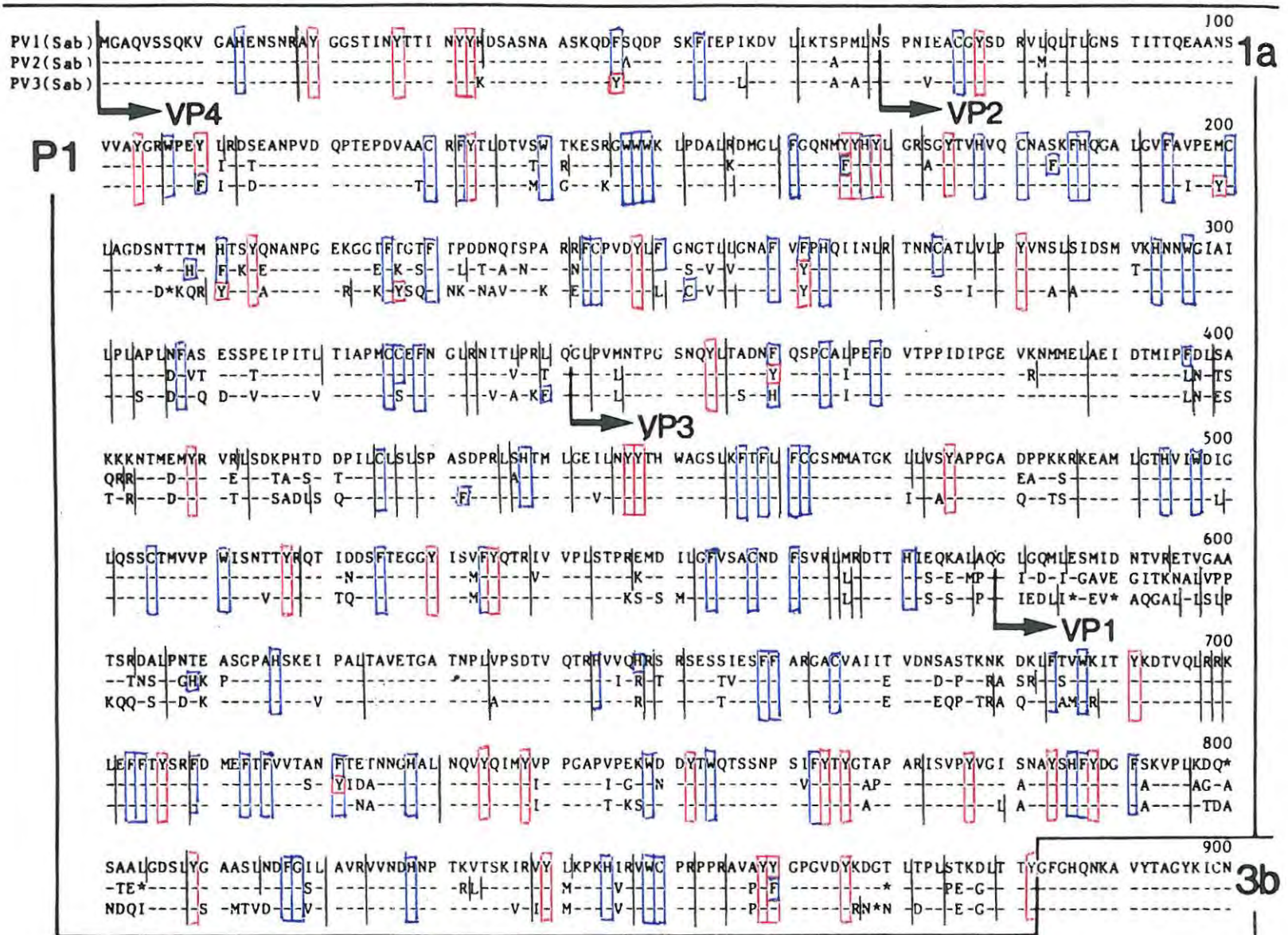


FIGURE 4.27. RP-HPLC map of autodigestion products of trypsin showing trace of absorbance at 220nm. Sample not prepared using SDS-PAGE. Note absence of large initial peak present on peptide maps of proteins resolved using SDS-PAGE.

FIGURE 4.28. Amino acid sequences for capsid proteins of all three Sabin vaccine strains of poliovirus. Only amino acids differing from LS-c are shown on the sequences for P712 and Leon 3. Shared amino acids are indicated by short horizontal bars (Toyoda *et al* 1984). Tyrosine residues (Y) are indicated in red, histidine (H), cysteine (C), tryptophan (W) and phenylalanine (F) in blue. Trypsin cleavage sites are shown in black.



residues labelled with  $^{125}\text{I}$  after chloramine-T treatment, are marked.

Table 4.4 shows theoretical results following  $^{125}\text{I}$ -labelling and trypsin digestion of capsid proteins from wild-type and Sabin vaccine poliovirus strains. Also indicated are the number of radiolabelled peptides expected to be resolved after mapping the digests using TLC or RP-HPLC.

In most TLC peptide maps the number of intense spots (i.e. those used for comparison) exceeded the theoretical number of tryptic peptides. The same applies to the number of peptides generated after RP-HPLC. Protein digestion may have been carried out for an excessive period of time, allowing peptide degradation. This degradation may have been caused by low levels of contaminating proteases. Alternatively, hydrolysis of capsid proteins may have been incomplete. This is unlikely because of the high concentration of trypsin and the length of digestion time.

Generally the number of peptides resolved using RP-HPLC exceeded the number of dominant spots present on TLC maps. These additional peptides probably correlated to spots on the TLC maps which were not judged to be intense enough to be used for peptide comparison. Control experiments show that the additional peptides were not due to either radiolabelled impurities in the gel or to the trypsin becoming labelled and digested. The map produced after a gel slice containing no protein was labelled, treated with trypsin and mapped shows no labelled peptides after TLC (fig.4.11.) or RP-HPLC (fig.4.24.). Tryptic peptide maps

Table 4.4. Radiolabelled peptides expected for each radiolabelled virus capsid protein after digestion by trypsin, determined using sequence data (Toyoda et al, 1984<sup>+</sup>; La Monica et al, 1986<sup>\*</sup>; Racaniello and Baltimore, 1981<sup>++</sup>; Stanway et al, 1984<sup>\*\*</sup>).

VIRUS TYPE	VIRUS STRAIN	CAPSID PROTEIN	PEPTIDE NUMBER <sup>a</sup>	TOTAL TYR <sup>b</sup>	PEPTIDES WITH: H,C,W,F <sup>c</sup>	WITH: TYR	EXPECTED RADIO-ACTIVE PEPTIDES
	5061	No sequence data available					
1	LS-c <sup>+</sup>	1	32	16	8	9	17
		2	17	11	4	9	13
		3	21	8	5	6	11
	Mahoney <sup>++</sup>	1	31	16	8	9	17
		2	18	11	4	8	12
		3	19	8	4	6	10
	5068	No sequence data available					
2	P712 <sup>+</sup>	1	32	16	9	9	18
		2	19	11	6	9	15
		3	17	9	4	6	10
	Lansing <sup>*</sup>	1	31	16	8	9	17
		2	20	11	6	9	15
		3	16	9	3	6	9
3	Leon 3 <sup>+</sup>	1	31	16	8	9	17
		2	21	14	4	10	14
		3	15	8	4	6	10
	Leon III <sup>**</sup>	1	31	16	8	9	17
		2	21	14	4	10	14
		3	15	8	4	6	10

<sup>a</sup> - number of peptides produced by complete trypsin digestion of capsid protein i.e. the number of sites at which arginine or lysine appear.

<sup>b</sup> - total number of tyrosine residues occurring in sequence

<sup>c</sup> - number of peptides which are labelled at a low level due to the presence of histidine (H), cysteine (C), phenylalanine (F) and tryptophan (W).



produced after labelling and digesting trypsin (fig.4.13.a and 4.26.a) correspond to none of the peptide maps of virus capsid proteins.

In the case of VP1 from poliovirus type 2 vaccine strain P712 and wild-type Lansing, TLC peptide maps show fewer than the expected number of radio-labelled peptides. A large spot (labelled 13) is present (fig.4.5.b), and may contain two or more co-migrating peptides. Evidence is provided by the RP-HPLC maps of VP1 from Lansing and P712 (fig.4.18.), where the number of tryptic peptides obtained corresponds closely to the expected number. Additionally, no single peptide on the RP-HPLC map contains the very high levels of radioactivity expected if one peptide constitutes spot 13.

Changes on RP-HPLC maps of capsid protein tryptic peptides generally correlate well with those on TLC maps. In some cases a tentative identification of specific peptides may be made. For example, all the RP-HPLC maps of VP1 of the type 1 polioviruses contain one very large peptide peak, designated 14 (fig.4.15.). This peak probably contains the same peptides as spot number 11, the most intense spot on the poliovirus type 1 TLC maps for VP1 (fig.4.2.b).

Results obtained by both TLC and RP-HPLC mapping of radio-labelled tryptic peptides of poliovirus capsid proteins are similar. There are fewer similarities between the type 1 Gazankulu outbreak strain 5061 and type 1 vaccine strain LS-c than between LS-c and wild-type LS-a. In contrast, similarity within

TABLE 4.5. Number of peptides found to be shared by capsid proteins of poliovirus strains within poliovirus types 1 and 2. Results obtained using both TLC and RP-HPLC for peptide mapping are given.

VIRUS TYPE	CAPSID PROTEIN	NO. OF PEPTIDES SHARED BETWEEN OUTBREAK STR. AND				NO. OF PEPTIDES SHARED BY VACCINE STRAIN AND WILD-TYPE STRAIN	
		VACCINE STR.		WILD-TYPE STR.			
1	1	<b>12</b>	13	<b>14</b>	14	<b>14</b>	15
	2	11	10	10	9	16	14
	3	9	9	<b>10</b>	10	<b>10</b>	11
2	1	<b>10</b>	12	7	10	8	12
	2	19	16	15	14	14	12
	3	<b>15</b>	16	<b>13</b>	15	<b>14</b>	15

**bold face** - results obtained using thin-layer chromatography (TLC).

normal type - results obtained using reversed-phase high-performance liquid chromatography (RP-HPLC).

the type 2 poliovirus strains studied appears to be greatest between Gazankulu outbreak strain 5068 and vaccine strain P712.

Table 4.5. shows a comparison of tryptic peptides shared between the Gazankulu outbreak and vaccine strain of poliovirus and between these two strains and the wild-type strains of poliovirus. These results indicate that while it is unlikely that type 1 Gazankulu outbreak strain 5061 is related to vaccine strain LS-c, type 2 outbreak strain 5068 is probably related to vaccine strain P712.

Comparison of the tryptic peptide maps shows that the general pattern of peptides for a particular capsid protein is apparently type specific. Consequently, each peptide map provides identification of the poliovirus type to which the strain under study belongs. Comparison of all of the tryptic peptide maps indicates that outbreak strains 5061 and 5068 have been correctly identified as being type 1 and type 2 polioviruses, respectively.

Wild-type strains are included in the comparison of poliovirus strains primarily to show whether the Gazankulu outbreak and wild-type strains are related. Additionally, comparison of wild-type and vaccine strains gives an idea of the relative "distance" between a vaccine strain and the neurovirulent wild-type strain. This acts as a reference when determining the importance of differences between Gazankulu outbreak and vaccine strains.

The need for such a reference becomes clear when comparing the

type 2 poliovirus strains. Several differences exist between the capsid proteins of outbreak strain 5068 and vaccine strain P712. These differences could lead to the belief that there is only limited relatedness between the Gazankulu isolate and vaccine strain. Comparison of the Gazankulu and vaccine strains with wild-type 2 strain Lansing shows that the differences between 5068 and P712 are less than those between either strain and Lansing. This indicates that Gazankulu strain 5068 is related to vaccine strain P712.

## CHAPTER FIVE

### COMPARISON OF POLIOVIRUS RNA BY RNase T<sub>1</sub> OLIGONUCLEOTIDE

#### MAPPING

##### 5.1. Introduction

Mapping capsid proteins by TLC and RP-HPLC of <sup>125</sup>I-labelled peptides was a sensitive means of comparing poliovirus strains. The technique was limited in that only capsid proteins could be compared, and during attenuation numerous changes occur in regions of the RNA not coding for capsid proteins<sup>56,89,100,104</sup>. It is probable that biochemical determinants of attenuation are not restricted to the coat protein<sup>8</sup>, which only represents approximately 40% of the genome<sup>94</sup>. In the case of poliovirus type 3 vaccine strain Leon 3, for example, pathogenic reversion results from a single change, from uridine to cytosine, at position 472 in the non-coding region<sup>26</sup>.

In order to detect changes in both the non-coding and coding regions of the viral RNA, comparison of viral strains at a genetic level was carried out. This entailed two-dimensional mapping ("fingerprinting") of oligonucleotides generated by Ribonuclease T<sub>1</sub> (RNase T<sub>1</sub>).

Because highly characteristic RNase T<sub>1</sub> oligonucleotide maps may be prepared, fingerprinting has been used in several lines of virus research. Examples include characterization of defective interfering viral genomes<sup>7</sup>, comparison of intertypic recombinant viruses<sup>103</sup> and estimation of the degree of sequence

divergence between closely related viral strains <sup>3</sup>. The comparison of RNAs from closely related viral strains <sup>22,31,45,71,92</sup> has been one of the most important uses of oligonucleotide fingerprinting.

To produce oligonucleotides for fingerprinting studies RNA molecules were digested enzymatically using ribonuclease T<sub>1</sub> (RNase T<sub>1</sub>). This enzyme, derived from the fungus Aspergillus oryzae, specifically cleaves phosphodiester bonds adjacent to guanosine (G) residues. Guanosine 3'-phosphate (Gp) and a set of oligonucleotides all terminating in Gp are produced <sup>51</sup>. The other known single base-specific RNases also cleave at G <sup>102</sup>, thus confer no advantage over RNase T<sub>1</sub>.

Prior to electrophoresis oligonucleotides were radiolabelled to enable their detection by autoradiography. Although stains such as methylene blue may be used to detect electrophoresed oligonucleotides <sup>20</sup> their sensitivity is low and they are rarely used. Radiolabelling may be carried out either in vivo or in vitro.

In vivo labelling of foot-and-mouth-disease virus (FMDV) <sup>11,92</sup> and coxsackie B3 virus <sup>31</sup> with <sup>32</sup>P has been successful, but not all RNA species incorporate ortho-(<sup>32</sup>P)-phosphate at a high enough level for fingerprint studies. Because most mRNAs and some major groups of RNA viruses fall within this category <sup>30</sup>, this study incorporated in vitro radiolabelling of oligonucleotides. In vitro labelling can be performed rapidly and requires substantially lower inputs of radioisotope than in vivo

labelling. Only small quantities (1ug or less) of chemically pure viral RNA are required <sup>51</sup>, although fingerprint quality is lower.

In vitro labelling was carried out according to the procedure developed by Frisby (1977). T<sub>4</sub> polynucleotide kinase (PNK) was used to transfer radiophosphate from ( $\gamma$ -<sup>32</sup>P)-ATP (fig.5.1.) to the free 5'-hydroxyl groups of RNase T<sub>1</sub>-generated oligonucleotides. All 3'-terminal phosphates were removed from the oligonucleotides by the action of bovine alkaline phosphatase (BAP). The combined effects of BAP and PNK catalysed the net transfer of phosphate from the 3'- to the 5'-ends of the oligonucleotides, resulting in the incorporation of <sup>32</sup>P <sup>30,51</sup>.

Once radiolabelling was complete, oligonucleotides were separated by electrophoresis in two dimensions. Such separation was first proposed in 1962 by Raymond and Aurell and has since been widely used for the fractionation of complex RNA mixtures. It is used more frequently than mapping in one dimension <sup>18,105</sup> which is generally not capable of effectively resolving the large number of "diagnostic" oligonucleotides (those longer than about 13 residues) present after digestion.

Oligonucleotide mapping was carried out using the two-dimensional technique developed by De Wachter and Fiers (1972). Electrophoresis was first carried out at a pH of 3.5, where the differences in charge of the different bases was greatest <sup>19</sup>. Electrophoretic mobilities of nucleoside monophosphates are related to net negative charge and increase in the order

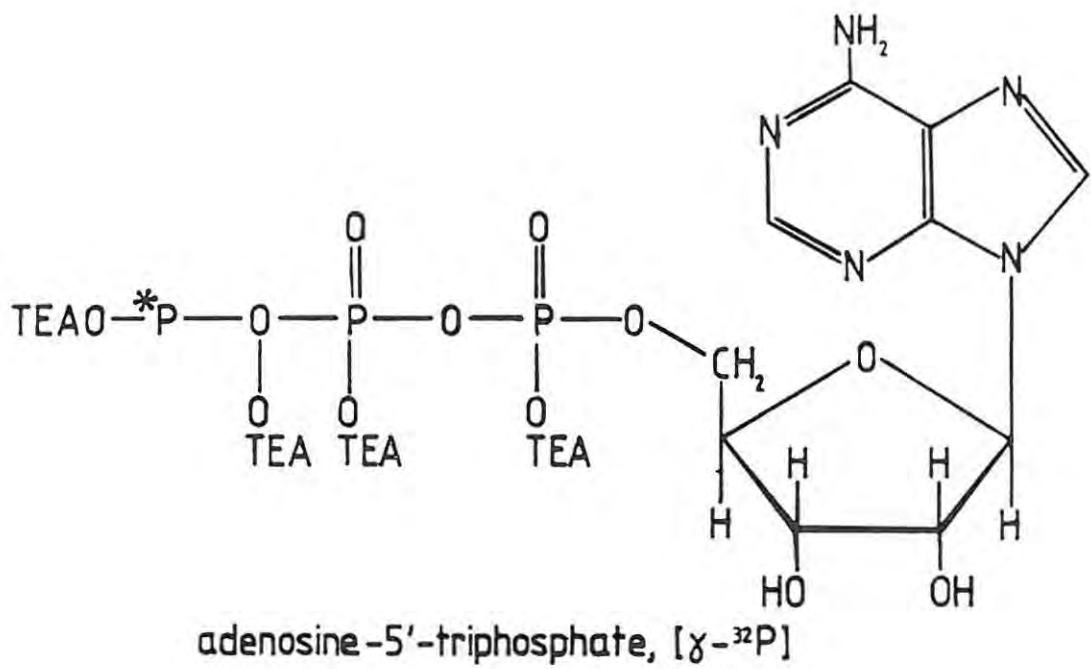


FIGURE 5.1. Structure of  $\gamma$ - $^{32}\text{P}$  - ATP.



Cp<Ap<Gp<Up. Use of a large pore gel maximized the effect of charge on mobility <sup>51</sup>.

Second-dimension electrophoresis was carried out at pH8, with migration through the gel due to the size and shape of the oligonucleotide molecule <sup>20</sup>. Figure 5.2. shows the theoretical pattern of oligonucleotide distribution after two dimensional electrophoresis. Oligonucleotides are in a graticulated pattern formed by a series of bands curving from the origin of first dimension electrophoresis. Bands form according to their uracil content with those nearest the origin containing no uracil <sup>20</sup>.

RNA oligonucleotide mapping has been used for examining isolates of FMDV <sup>3,92</sup> and the vesicular stomatitis virus (VSV) subgroup<sup>15</sup>. It has been used to study the evolution of multiple genome mutations during persistent infections of VSV <sup>45</sup>, and has been widely used for studying molecular variation in vaccine strains of poliovirus <sup>7,22,71,80</sup>. In several cases, oligonucleotide mapping has shown isolates of virus from cases of paralytic poliomyelitis to be closely related to the poliovirus vaccine strains <sup>13,67,69,114</sup>. Consequently, it was hoped that oligonucleotide mapping would be a highly sensitive technique for comparing vaccine and Gazankulu outbreak strains of poliovirus.

## 5.2. Results

Photographs of the oligonucleotide maps produced after two-dimensional electrophoresis of RNA digests from the poliovirus strains studied are shown in figures 5.3.a, 5.4.a and 5.5.a. Diagrammatic representations of the photographs are presented in

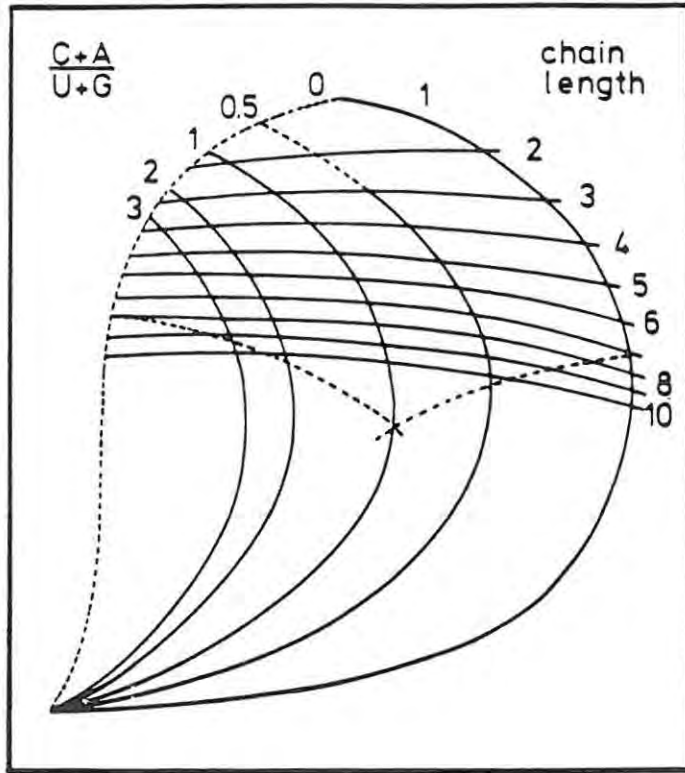


FIGURE 5.2. Theoretical pattern of oligonucleotide distribution after two-dimensional electrophoresis. Oligonucleotide position as a function of base composition and chain length. The curves marked 0, 0.5, 1, 2, 3, connect all the positions corresponding to these C+A/U+G ratios. The curves marked 2 - 10 connect the positions corresponding to these chain lengths (de Wachter and Fiers, 1982).

figures 5.3.b, 5.4.b and 5.5.b.

Only the oligonucleotide spots in the lower 1/3 to 1/2 of the maps were used for RNA comparison. These were the diagnostic spots used for identification purposes. The presence of "constellations" of spots on the oligonucleotide maps allowed comparison of the maps, and individual spots were identified by comparing corresponding constellations.

Comparison of the different poliovirus strain RNAs was carried out using the clearest and/or most highly reproducible oligonucleotides present on the maps. When photographs were not clear, the original autoradiographs were referred back to. Faint spots, with a poor reproducibility, were speculated to be artefactual. Such spots may have resulted from oligonucleotide degradation by contaminating RNases present at low levels during sample preparation.

#### 5.2.1. Comparison of RNA oligonucleotide maps of type 1 poliovirus strains

Figure 5.3.a shows photographs of the oligonucleotide maps obtained for type 1 poliovirus strains 5061, LS-c and LS-a. The photograph is represented diagrammatically in figure 5.3.b.

The oligonucleotide map obtained from type 1 Gazankulu outbreak strain 5061 differs considerably from that of vaccine strain LS-c. Of the diagnostic spots, LS-c lacks 10, while 19 new oligonucleotide spots are present. Alteration in mobility <sup>7,22</sup> has occurred in three oligonucleotides - vertical shift indicates alteration in guanine residues, lateral shift alterations in

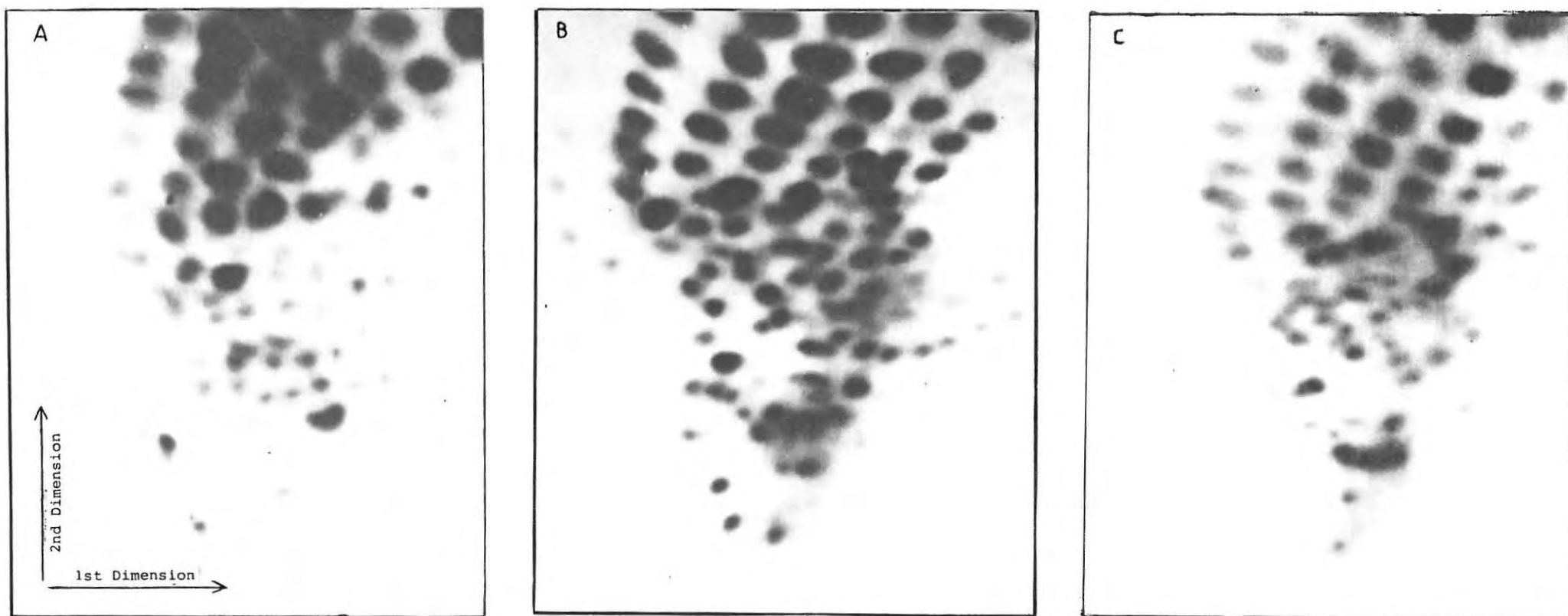


FIGURE 5.3.a. Oligonucleotide maps of RNA from poliovirus type 1 strains. A - Gazankulu outbreak strain 5061; B - Sabin vaccine strain LS-c; C - wild-type strain LS-a.

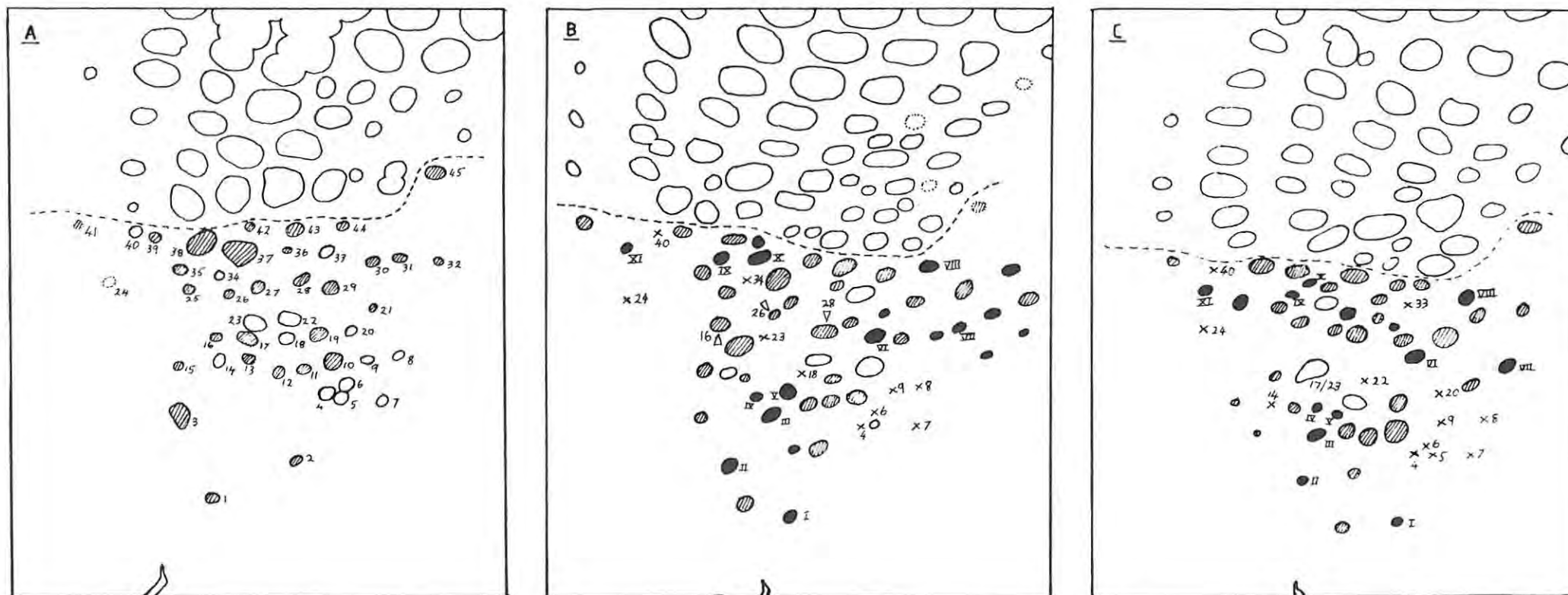


FIGURE 5.3.b. Diagrammatic representation of oligonucleotide maps of RNA from poliovirus type 1 strains. A - 5061; B - LS-c; C - LS-a. Numbering of spots on the map of 5061 is arbitrary. On maps of LS-c and LS-a only missing spots (x) are numbered. Novel spots are indicated by (●), shifted spots by (▷), with the arrow indicating direction of shift. Faint spots are indicated by a dotted outline. Roman numerals indicate spots common to vaccine and outbreak strains only. Spots common to all strains are indicated by (○). The presence of poly-A is indicated by a streak at the lower edge of the diagram. Only oligonucleotide spots below the dotted line are diagnostic and used for comparison of oligonucleotide maps. Sample origin is below the left-hand corner of the maps.

cytosine, adenine or uracil residues <sup>51</sup>.

Comparison of the maps obtained for Gazankulu outbreak strain 5061 and wild-type reference strain LS-a shows that these two strains also differ considerably. Of the diagnostic oligonucleotides, 13 are absent from the LS-a map, while 14 new ones have appeared. In contrast, a great deal of similarity exists between oligonucleotide maps of vaccine strain LS-c and wild-type strain LS-a.

Of the oligonucleotides missing from the map of vaccine strain LS-c upon comparison with that of Gazankulu outbreak strain 5061, 17 are also absent from the map of reference strain LS-a. Eleven oligonucleotide spots (indicated by Roman numerals) are shared by the vaccine and wild-type strains of poliovirus alone. In comparison, only five oligonucleotides are exclusive to the maps of type 1 Gazankulu outbreak strain 5061 and vaccine strain LS-c. This indicates that 5061 is not likely to be vaccine related.

#### 5.2.2. Comparison of RNA oligonucleotide maps of type 2 poliovirus strains

Figure 5.4.a shows photographs of the oligonucleotide maps obtained for the type 2 poliovirus strains. Diagrammatic representations of the maps are given in figure 5.4.b.

The pattern of oligonucleotide spots on the map for type 2 Gazankulu outbreak strain 5068 is very similar to that of vaccine strain P712. Comparison of the two maps shows that 7 oligonucleotides are missing from the map of P712. Ten

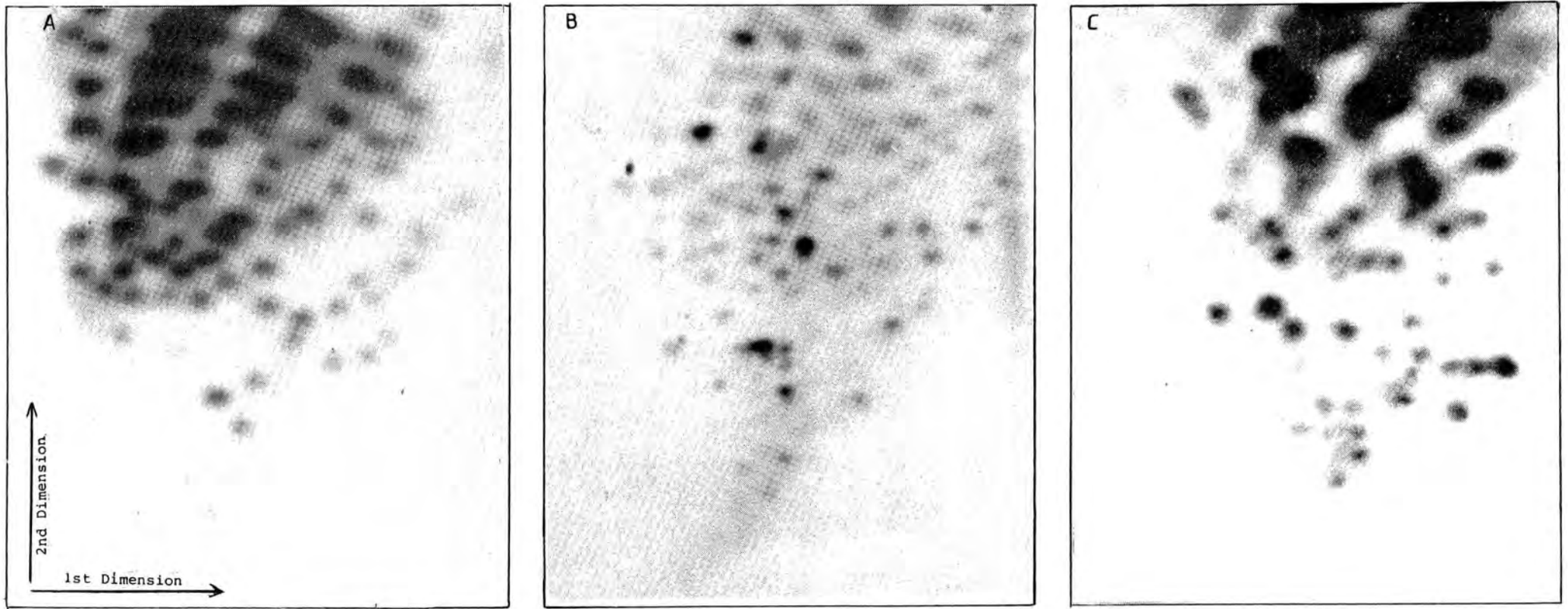


FIGURE 5.4.a. Oligonucleotide maps of RNA from poliovirus type 2 strains. A - Gazankulu outbreak strain 5068; B - Sabin vaccine strain P712; C - wild-type strain Lansing.

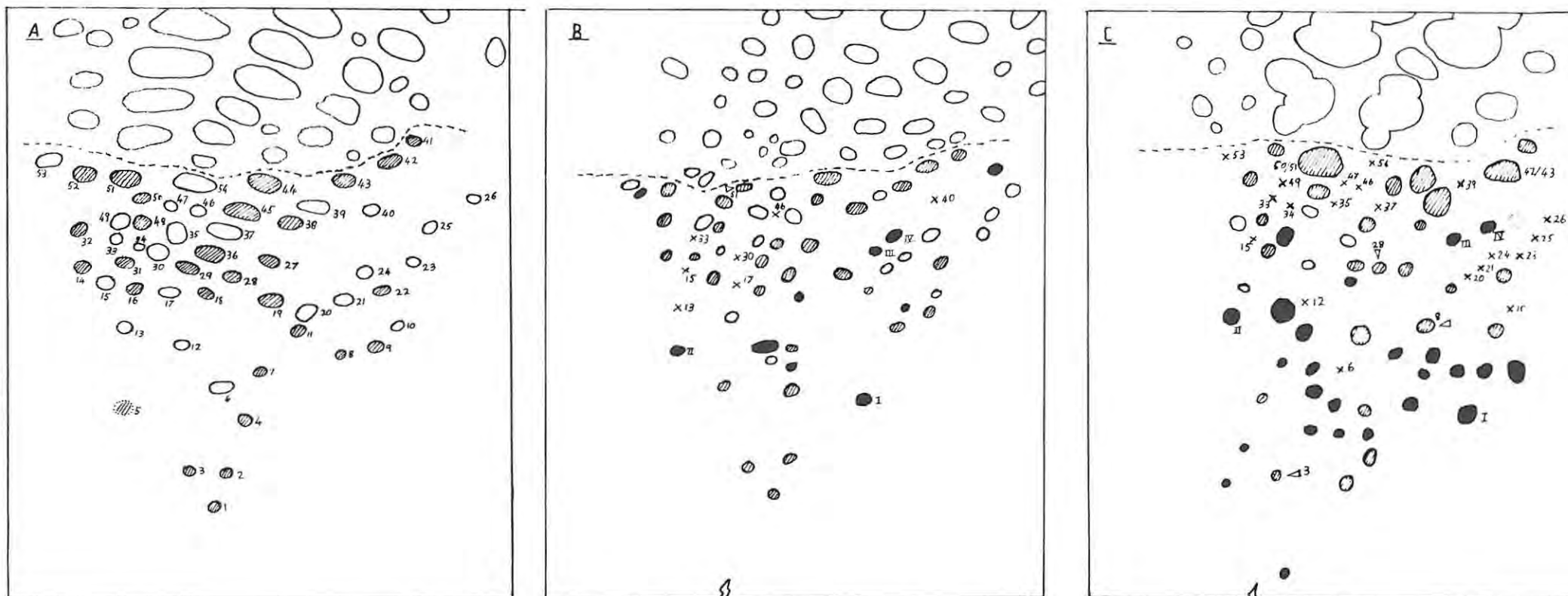


FIGURE 5.4.b. Diagrammatic representation of oligonucleotide maps of RNA from poliovirus type 2 strains. A - 5068; B - P712; C - Lansing. Numbering of spots on the map of 5068 is arbitrary. On maps of P712 and Lansing only missing spots (x) are numbered. Novel spots are indicated by (●), shifted spots by (▷), with the arrow indicating direction of shift. Faint spots are indicated by a dotted outline. Roman numerals indicate spots common to vaccine and outbreak strains only. Spots common to all strains are indicated by (⊙). The presence of poly-A is indicated by a streak at the lower edge of the diagram. Only oligonucleotide spots below the dotted line are diagnostic and used for comparison of oligonucleotide maps. Sample origin is below the left-hand corner of the maps.



additional oligonucleotides are present, while oligonucleotide 51 has shifted horizontally.

Comparison of the oligonucleotide map of Gazankulu outbreak strain 5068 with that of wild-type reference strain Lansing shows that 20 oligonucleotide spots are missing from the map of Lansing. Three oligonucleotides display an altered electrophoretic mobility and there are 25 new spots. Of these new oligonucleotides, only four are shared with the attenuated Sabin vaccine strain, P712. In contrast, a total of 16 oligonucleotides are exclusive to Gazankulu outbreak strain 5068 and vaccine strain P712.

From these results it is clear that similarity exists between the RNA of type 2 Gazankulu outbreak strain 5068 and vaccine strain P712. This similarity is considerably greater than any between Lansing, the wild-type reference strain, and either 5068 or P712. Consequently, it appears that relationship exists between the type 2 Gazankulu outbreak strain, 5068, and the Sabin vaccine strain, P712.

### 5.2.3. Comparison of RNA oligonucleotide maps of type 3 poliovirus strains

Oligonucleotide fingerprints of the two type 3 polioviruses studied are very similar. Photographs of the maps obtained are shown in figure 5.5.a, while figure 5.5.b shows diagrammatic representations of the maps.

Six of the diagnostic spots on the map of Sabin vaccine strain

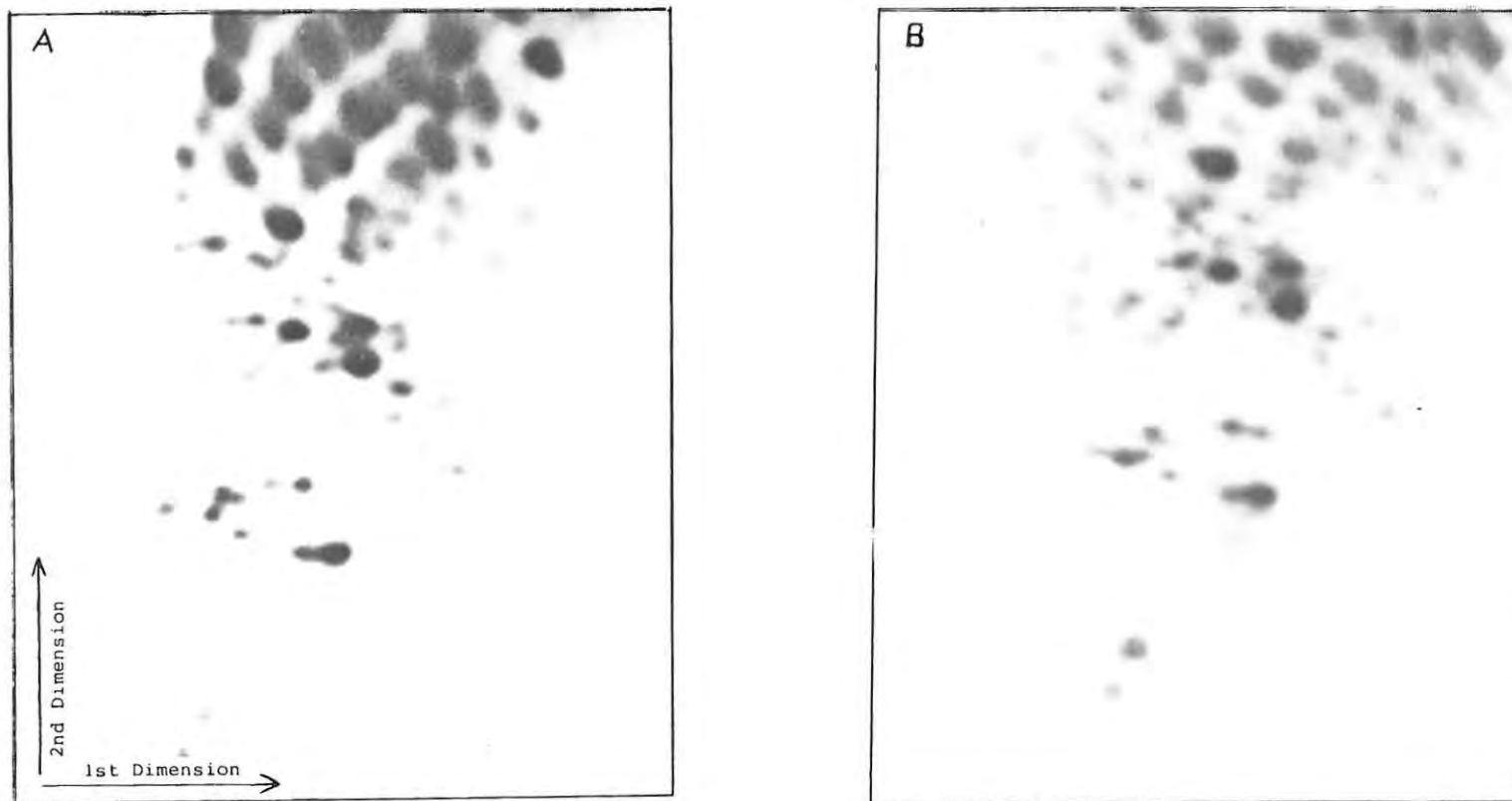


FIGURE 5.5.a. Oligonucleotide maps of RNA from poliovirus type 3 strains. A - Sabin vaccine strain Leon 3; B - wild-type strain Leon III.

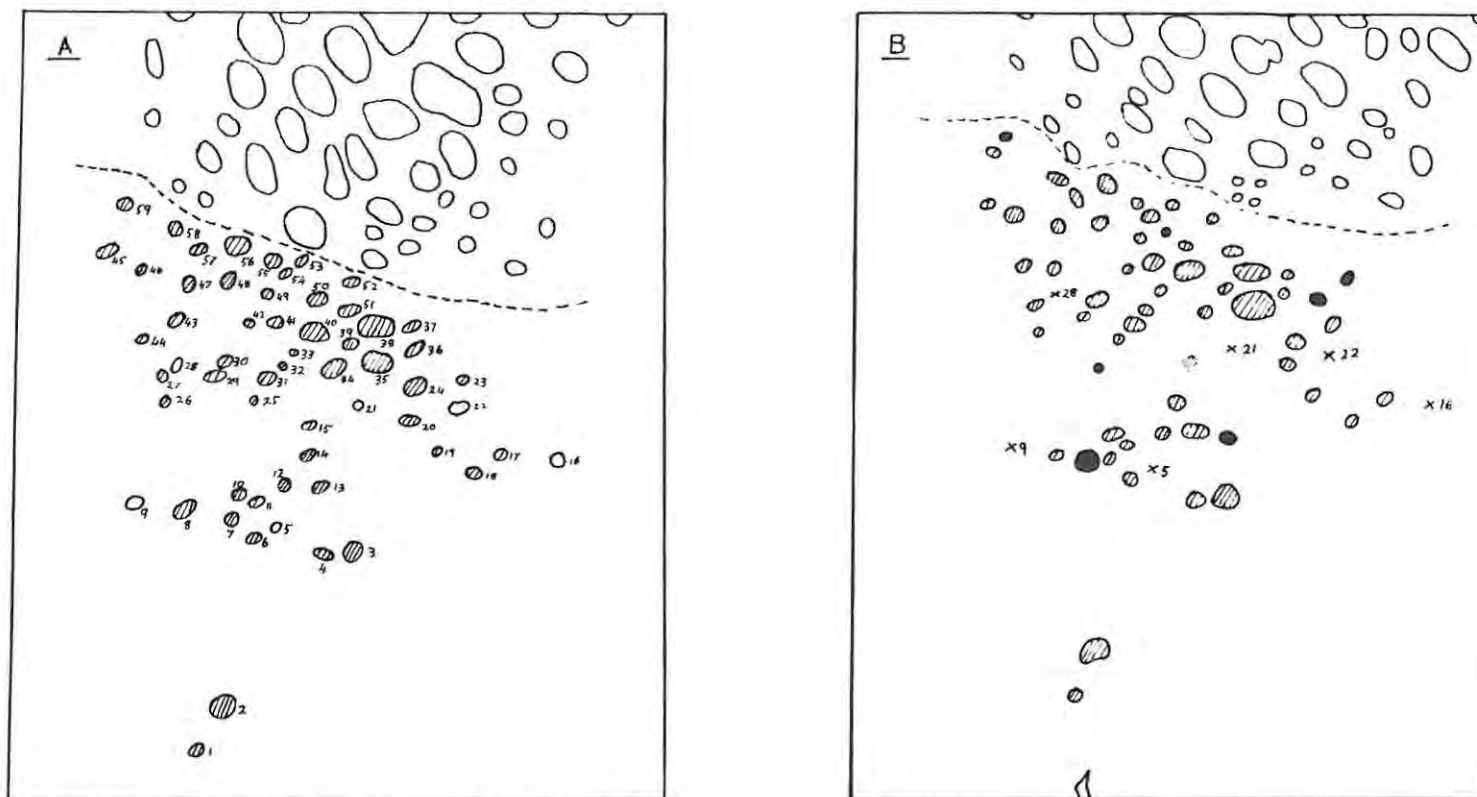


FIGURE 5.5.b. Diagrammatic representation of oligonucleotide maps of RNA from poliovirus type 3 strains. A - Leon 3; B - Leon III. Numbering of spots on the map of Leon 3 is arbitrary. On map of Leon III only missing spots (x) are numbered. Novel spots are indicated by (●). Faint spots are indicated by a dotted outline. Spots common to both strains are indicated by (⊙). The presence of poly-A is indicated by a streak at the lower edge of the diagram. Only oligonucleotide spots below the dotted line are diagnostic and used for comparison of oligonucleotide maps. Sample origin is below the left-hand corner of the maps.

Leon 3 have disappeared from the map of neurovirulent wild-type 3 strain Leon III. Seven novel spots are apparent on the oligonucleotide map of the neurovirulent wild-type reference strain. None of the oligonucleotides on the Leon III map display mobility differing from that on the map of Leon 3.

### 5.3. Discussion

Results obtained by two dimension mapping of RNase T<sub>1</sub> generated oligonucleotides of poliovirus strains are similar to those obtained using SDS-PAGE and tryptic peptide mapping. Little similarity exists between the type 1 Gazankulu outbreak poliovirus isolate, strain 5061, and type 1 vaccine strain LS-c. Similarity between oligonucleotide maps of 5061 and wild-type strain LS-a is also low. Considerable similarity exists between vaccine strain LS-c and wild-type strain LS-a, as expected from nucleotide sequences<sup>89</sup>. These results indicate that, while 5061 is probably not vaccine related, it does not appear to be closely related to wild-type reference strain LS-a either.

Comparison of the oligonucleotide map from the type 1 Gazankulu outbreak strain with those of the type 2 and 3 polioviruses shows a complete lack of similarity between them. No relationship exists between 5061 and the type 2 and 3 poliovirus strains, proving that outbreak strain 5061 has not been incorrectly serotyped.

In contrast, the oligonucleotide map of the type 2 Gazankulu outbreak isolate, strain 5068, is similar to that of type 2 vaccine strain P712. Considerably less similarity exists between

5068 and wild-type Lansing. A similar degree of difference exists between the RNA of P712 and Lansing. This is not surprising in view of the large number of differences in nucleotide sequence between the two <sup>56,104</sup>. The fact that the greatest similarity between the type 2 polioviruses studied exists between the outbreak and vaccine strains strongly indicates a relationship between 5068 and P712. The similarity is shown clearly in table 5.1.

Several differences exist between the oligonucleotide maps of type 3 attenuated Sabin vaccine strain Leon 3 and its neurovirulent parent, wild-type 3 poliovirus strain Leon III. Assuming that each nucleotide change results in alteration of one oligonucleotide, at least seven changes must have occurred in diagnostic oligonucleotides during attenuation. These oligonucleotides represent only 5% to 10% of the RNA sequence <sup>69</sup>. Consequently, a total of between 70 and 140 nucleotide changes appear to have taken place during attenuation of wild-type 3 strain Leon III.

Comparison of the nucleotide sequences of the two poliovirus type 3 strains <sup>103,104</sup> shows that 10 differences exist between attenuated vaccine strain Leon 3 and its neurovirulent parent. Only two occur in diagnostic oligo-nucleotides. The level of genome conservation between the two virus strains is thus much greater than that indicated by the experimental results. Comparison of the oligonucleotide maps with those obtained by other workers <sup>50,51,69,71</sup> indicated that differences existed primarily in the map for the vaccine strain, Leon 3.

Table 5.1. Number of oligonucleotides found to be shared between RNA of poliovirus strains within poliovirus types 1 and 2.

VIRUS TYPE	NO. OF OLIGONUCLEOTIDES SHARED BETWEEN OUTBREAK STRAIN AND:		NO. OF OLIGONUCLEOTIDES SHARED BETWEEN VACCINE STRAIN AND WILD-TYPE STRAIN.
	VACCINE STR.	WILD-TYPE STR.	
1	35	33	41
2	46	35	34

The additional spots on the vaccine strain Leon 3 map are possibly due to nuclease contamination of the polynucleotide kinase <sup>30</sup>. However, a similar level of artefactual secondary spots is not apparent on any of the other oligonucleotide maps. This indicates that the PNK was not contaminated.

The type 3 poliovirus vaccine strain is known to be highly unstable in vivo <sup>71</sup>. Possibly mutation occurred during in vitro passage of the virus, resulting in contamination of the vaccine stock by a novel virus sub-population. This would result in an increase over the expected number of oligonucleotide differences appearing between the vaccine and wild-type maps.

Although RNA viruses show a high frequency of mutation <sup>22</sup>, poliovirus is considered to be fairly stable because of its low mutation rate in cell culture <sup>22,79</sup>. During 20 years of in vitro passage of three poliovirus type 1 Mahoney strains, only one oligonucleotide alteration occurred <sup>22</sup>. It seems reasonable to expect that a much higher rate of mutation of the type 3 vaccine stock in vitro is unlikely. The fact that virus used in this study was never more than six passages away from the original stock further decreases the likelihood of in vitro mutation. Alternatively, the Sabin type 3 virus stock could have been contaminated with a sub-population of type 3 virus responsible for the anomalous oligonucleotide map <sup>69</sup>.

## CHAPTER SIX

### COMMENTS ON TECHNIQUES USED IN THIS STUDY

One aim of this study was to find a suitable technique for comparative identification of poliovirus strains. It was hoped that this technique would be rapid, inexpensive and relatively easy to perform. Of the four techniques studied, none fulfilled all of these criteria, and each had advantages and disadvantages.

The simplest and most rapid technique was discontinuous SDS-PAGE, which was used both preparatively and analytically. In a preparative context SDS-PAGE was effective in resolving the individual coat proteins of poliovirus. The capsid proteins were then used for tryptic peptide mapping. As an analytical technique SDS-PAGE was useful for rapid comparison of the coat proteins of different strains of poliovirus.

Comparison of poliovirus capsid proteins was fairly crude, and only indicated differences in electrophoretic mobility of the proteins. Electrophoretic mobility is controlled by several variables, such as amino acid composition and polypeptide size. Amino acid substitutions within a protein may alter its composition without affecting its electrophoretic mobility. Alternatively, relatively minor changes in amino acid composition may have a significant effect on the electrophoretic mobility <sup>52</sup>.

These factors were probably responsible for the difference



between the results obtained experimentally and those predicted from sequence data. SDS-PAGE indicated that between vaccine and wild-type poliovirus strains, the greatest variability in amino acid sequence occurs in VP2. Sequence data <sup>56,89,104</sup>, however, show that VP2 is highly conserved between poliovirus strains.

Because alterations in amino acid composition have a variable effect on electrophoretic mobility of polypeptides, a conclusive assessment of relatedness between vaccine and outbreak strains of poliovirus was not possible.

Despite its drawbacks, SDS-PAGE was a useful analytical tool for comparing viral proteins <sup>52,68</sup>. A problem with analysis of the capsid proteins was that results only indicated changes occurring in the portion of the genome coding for these proteins. Sensitivity of SDS-PAGE may be improved by comparing intracellular proteins produced by cells infected with poliovirus <sup>50,69</sup>. This produces more detailed results than those obtained by comparison of capsid proteins.

Of the techniques studied, SDS-PAGE of viral polypeptides was the fastest and simplest comparative technique. It was relatively inexpensive and time-effective, and results were highly reproducible. For accurate determination of viral relatedness, however, it must be used in conjunction with other more sensitive techniques.

Mapping of trypsin generated peptides of viral coat proteins using TLC and RP-HPLC gave more detailed results than SDS-PAGE. Both techniques were relatively rapid, and did not require a

great deal of technical skill.

Tryptic peptide mapping using thin layer chromatography (TLC) was a useful technique for protein comparison. Results were more detailed than those obtained using SDS-PAGE, and the technique was not too difficult or time consuming. Problems with TLC mapping of peptides included difficulty of data interpretation and determination of significant peptide spots. The maps obtained were, however, highly reproducible, increasing the ease of comparison.

Reversed-phase high-performance liquid-chromatography (RP-HPLC) was also used for mapping tryptic peptides of poliovirus capsid proteins. In virus research RP-HPLC has been primarily involved with the characterization of complete proteins<sup>43,86,107</sup>. A certain amount of work has been carried out in the analysis of peptides, both viral<sup>53</sup> and non-viral<sup>1,5</sup>.

Although potentially the RP-HPLC detection limit for peptides is in the picomole range<sup>41</sup>, in this study sensitivity was considerably lower. Two factors contributed to this decrease in sensitivity - the high trypsin concentration and the gradient elution technique.

A high trypsin concentration was necessary for efficient digestion of proteins in gel slices<sup>24</sup>, and during digestion, generation of peptides of trypsin occurred. Because of the high concentration of trypsin peptides, their absorbance trace completely masked that of the capsid protein peptides. Such masking could have been prevented by carrying out digestion at a

high protein to trypsin ratio.

Without SDS-masking, sensitivity would still have been limited due to the fact that gradient elution of peptides was carried out. At 220nm, 40% acetonitrile has a higher absorbance than 5% acetonitrile, resulting in baseline shift during a chromatographic run. At sensitivities of 0.02 AUFS (absorbance units full scale) or less, the baseline shift during a chromatographic run crossed the full absorbance scale.

Because of these factors, radiolabelling of viral proteins was necessary to detect peptides after RP-HPLC.  $^{125}\text{I}$  was chosen as the labelling isotope for both TLC and RP-HPLC, despite the fact that up to 50% of the peptides generated could not be detected (see table 4.4.).

In order for an accurate trace of radioactivity to be plotted after RP-HPLC, a large number of samples had to be collected. Sample collection and subsequent calculation of radioactivity were time consuming. One of the major advantages of RP-HPLC, which is speed, was thus lost. In addition, detection of radio-labelled peptides was not as sensitive as peptide detection using absorbance at 220nm.

A problem with RP-HPLC was the length of time that it took to develop an operational chromatography system. Additionally, equipment and chemicals were expensive. A great deal of technical expertise on the part of an operator was not, however, necessary. Overall, RP-HPLC appeared to be an accurate and fairly rapid technique for the comparison of viral capsid

proteins.

Although RP-HPLC was more costly than TLC, it has great potential sensitivity. In addition, the potential for production of maps of unlabelled peptides exists. This would allow comparison of the entire peptide complement of capsid proteins. Alternatively, methods other than  $^{125}\text{I}$  labelling using chloramine-T could be employed.

An advantage that tryptic peptide mapping of capsid proteins had over oligonucleotide mapping of RNA was that individual capsid proteins could be studied. Comparison of capsid proteins from different polio virus strains may allow determination of which capsid proteins undergo the greatest variation during attenuation and reversion.

Oligonucleotide mapping was a highly sensitive technique, allowing comparison of viral strains at a genetic level. Single nucleotide changes may result in clearly visible differences between maps of different viral strains <sup>71</sup>. Unfortunately the characteristic oligonucleotides used for comparing RNAs only comprise 5% - 10% of the genome <sup>69</sup>. Accurate comparison of different poliovirus strains was possible because they are spread through the entire genome, and are representative of the complete RNA.

Comparison of experimental and theoretical maps was carried out to determine the accuracy of oligonucleotide mapping. Charges have been assigned to each nucleotide by Minor et al (1986). Using nucleotide sequence data <sup>56,61,89,104</sup>, maps could be

produced by plotting oligonucleotide mass against charge/mass. Theoretical oligonucleotide maps were plotted for the wild-type and vaccine strains of poliovirus used in this study. The nucleotide sequence data for the Mahoney strain of poliovirus type 1 was used in place of that of LS-a, for which sequence data was not obtained.

An example of a theoretical map may be seen in figure 6.1.a. Close correlation exists between the theoretical map and the map obtained under experimental conditions (fig.6.1.b.and c.). Such correlation indicates the accuracy of oligonucleotide mapping. Good correlation also exists between the experimental results and those published by other workers <sup>50,51,69,71,79,105</sup>.

With the exception of genome sequencing, oligonucleotide fingerprint mapping is the most sensitive technique for detecting genetic differences between viral strains. Other approaches, both molecular and serological, are less sensitive but can detect more distant relationships <sup>51</sup>. Despite this, oligonucleotide mapping had several disadvantages. RNA had to be handled very carefully in order to prevent RNase contamination. The radioisotope used for labelling the oligonucleotides, <sup>32</sup>P, had a half-life of only 14 days. Finally, the ( $\gamma$ <sup>32</sup>P)-ATP required for in vitro labelling and the chemicals required for oligonucleotide mapping were expensive.

Two other techniques show promise in determining the relatedness of poliovirus strains. These are direct comparison of RNA sequences for determining homology of viral RNAs, and the use of

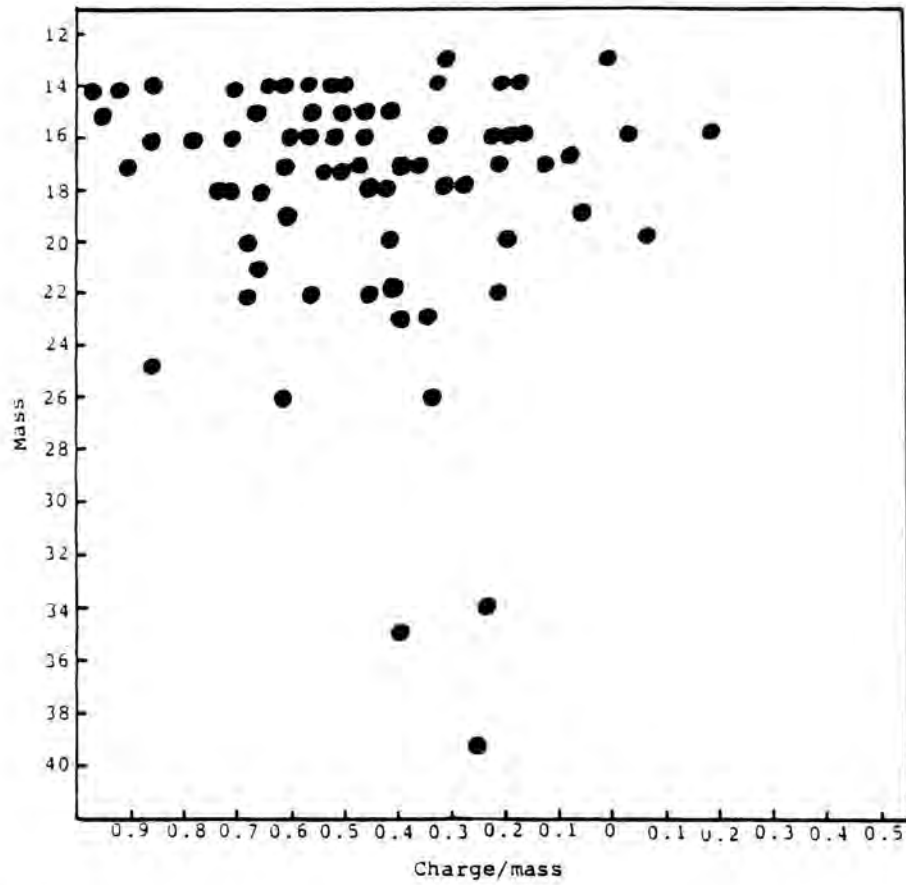


FIGURE 6.1.a. Theoretical oligonucleotide map for poliovirus type 2 strain P712, calculated from sequence data (Racaniello and Baltimore, 1981) using the system of Minor *et al* (1986).

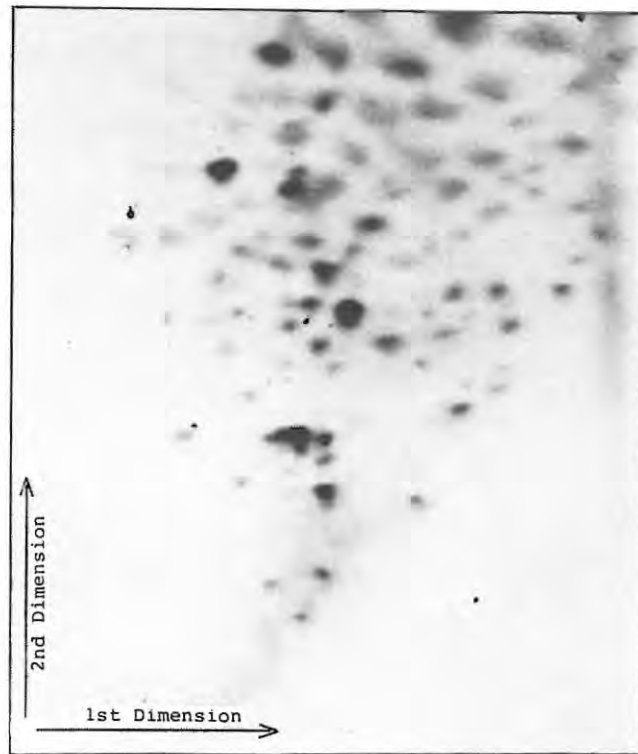


FIGURE 6.1.b. Photograph of oligonucleotide map of P712 obtained under experimental conditions.

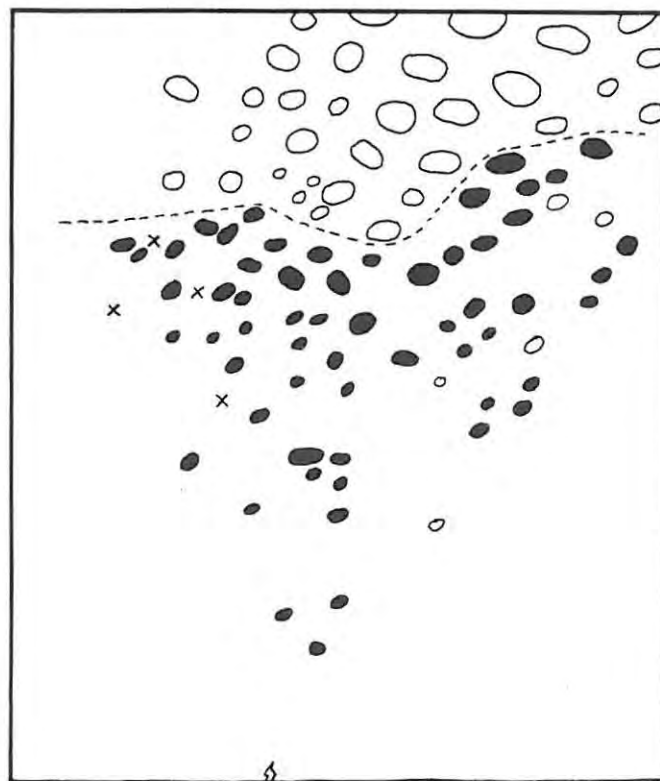


FIGURE 6.1.c. Diagrammatic representation of the experimental oligonucleotide map of P712. Spots common to those of the theoretical map are indicated by (●). Spots present on the theoretical map but absent from the experimental may be indicated by (x).

monoclonal antibodies.

Comparison of RNA sequences has been carried out using complementary DNA (cDNA) probes or by hybridization of RNAs. Competition RNA hybridization can detect homologies between virus strains sharing only 25% of their overall sequence <sup>73</sup>. Comparison of type 1,2 and 3 wild-type strains of poliovirus shows homologies of approximately 36% to 52% <sup>115,116</sup>. Calculation of homology between poliovirus RNAs is based on the resistance of double stranded RNA to RNase. Radioactive double stranded RNA is "melted" with DMSO (dimethyl sulphoxide), then mixed with an excess of non-radioactive positive poliovirus RNA. This results in re-annealing of positive and negative stranded RNAs. Subsequent treatment with RNase cleaves the annealed RNAs at any single stranded (i.e. non-homologous) regions <sup>116</sup>.

Comparison of the entire nucleotide sequence is the most accurate means of determining the relatedness of poliovirus strains. cDNA:RNA hybrids from the virus under study are cloned, and a plasmid containing a complete copy of the genome produced. This is then digested and poliovirus specific fragments isolated. The largest of these are sequenced and the nucleotide sequences compared <sup>89,100</sup>. Determination of the nucleotide sequences allows accurate comparison of viral RNAs, and the positions on the genome at which differences occur may be determined.

Although nucleotide sequence comparison is the most accurate means of determining viral relatedness, the methods are



complicated, requiring technical expertise. Consequently, nucleotide sequence determination is limited to specialized laboratories <sup>82</sup>. Because preparation of the DNA strands for sequencing is time consuming, rapid comparison of poliovirus strains is not possible. Additionally, the complexity of results necessitates computer analysis <sup>100</sup>.

Monoclonal antibodies (MoAbs) have been widely used in the study of poliovirus strains <sup>25,29,46,63,82</sup>. Mice or rats are inoculated with highly purified poliovirus and their spleens removed once sufficient antibody levels are reached. Spleen cells are fused with myeloma cells, and the resulting hybridomas produce antibodies. Cultures producing antibodies to the virus are cloned and tested for poliovirus neutralizing activity <sup>46</sup>. The antibodies produced by these murine lymphocyte hybridomas are monospecific, recognizing single epitopes on the poliovirion <sup>25</sup>.

To determine poliovirus strain relatedness, samples are reacted with a panel of monoclonal antibodies produced against a reference wild-type virus strain <sup>46</sup>. Relatedness of the viral strains may then be calculated according to the number of MoAbs they react with <sup>82</sup>.

Disadvantages of MoAbs include the technical expertise required for their production, and the time required for hybridoma production. However, once hybridomas have been produced they can be maintained, and a large panel of MoAbs obtained <sup>82</sup>. Computerised comparison of results gives accurate and sensitive

comparisons of virus strains. As a result, MoAbs may be of use as diagnostic reagents for identification of vaccine-derived strains of poliovirus <sup>29</sup>.

A combination of techniques would be best for determining the origin and relatedness of outbreak strains of poliovirus. For example, initial comparison could be carried out using SDS-PAGE. This would give a general idea of the relatedness of viral strains. Strains which appeared to be similar could then be compared by oligonucleotide mapping of their RNAs in order to determine the degree of relatedness at a genetic level.

Although only differences in the region of the RNA coding for capsid proteins can be detected using peptide mapping, Toyoda et al (1984) found that the greatest variation between poliovirus strains occurs in the regions of the RNA coding for the capsid proteins. In this study patterns of relatedness between poliovirus strains were found to be the same using peptide mapping and oligonucleotide mapping. This indicates that tryptic peptide mapping could be used as a less costly alternative to oligonucleotide mapping for virus comparison.

## CHAPTER SEVEN

### GENERAL DISCUSSION

Results obtained after comparing capsid proteins of poliovirus strains using four biochemical techniques were similar. SDS-PAGE indicated that poliovirus type 1 Gazankulu outbreak strain 5061 and vaccine strain LS-c were not related. A possible relationship existed between 5061 and wild-type reference strain LS-a. Electrophoretic mobilities of capsid proteins from poliovirus type 2 Gazankulu outbreak 5068 and vaccine strain P712 were identical, indicating a close relationship. Between 5068 and type 2 wild-type strain Lansing the relationship appeared to be minimal. Because SDS-PAGE is not highly sensitive these results were not considered to be conclusive and tryptic peptide mapping was carried out using TLC and RP-HPLC.

Tryptic peptide mapping of poliovirus capsid proteins indicated that little similarity existed between type 1 Gazankulu outbreak strain 5061 and vaccine strain LS-c. Consequently, it was probable that the outbreak strain was not vaccine related. Considerable similarity existed between type 2 Gazankulu strain 5068 and vaccine strain P712, indicating a close relationship.

Oligonucleotide mapping of the RNA was the only technique which allowed comparison of poliovirus strains at a genetic level. Results supported those obtained by peptide mapping and SDS-PAGE, which only allowed comparison of the capsid proteins.

The oligonucleotide map of RNA from type 1 Gazankulu outbreak

strain 5061 differed considerably from that of attenuated vaccine strain LS-c. Oligonucleotide maps of the type 1 vaccine and wild-type strains were clearly similar. This confirmed the conclusion drawn from the techniques comparing viral capsid proteins that 5061 was not vaccine related.

Similarity at a genetic level existed between type 2 poliovirus vaccine strain P712 and Gazankulu strain 5068. In contrast, there was a large difference between oligonucleotide maps of wild-type strain Lansing and attenuated vaccine strain P712. RNase T<sub>1</sub> oligonucleotide mapping of the poliovirus strains thus provided confirmation of the relatedness between virus strains.

Results indicated that type 1 Gazankulu outbreak strain 5061 differed from both type 1 vaccine strain LS-c and wild-type 1 strain LS-a. This implies that 5061 was a novel wild-type 1 poliovirus strain, unrelated to LS-a. This is possible, for a large number of distinct poliovirus type 1 strains exist worldwide <sup>80</sup>. Outbreaks of paralytic poliomyelitis caused by biochemically and antigenically novel poliovirus variants which suddenly appear in a population <sup>63</sup> are, however, rare. Poliovirus strains have considerable intrinsic variability, and new strains may readily arise in a single vaccinated individual <sup>71</sup>. This variability is generally responsible for the evolution of apparently novel poliovirus strains within a population. Gazankulu outbreak strain 5061 probably resulted from alterations in a poliovirus strain already present within the population.

Although poliovirus strains, particularly those of type 1 <sup>22</sup> and

type 2 <sup>113</sup> poliovirus, display a low level of in vitro mutability <sup>22,79</sup>, their in vivo mutability is high <sup>33,50,52,80</sup>. This is particularly true of strains of type 3 poliovirus <sup>13</sup>.

Minor et al (1986) have highlighted poliovirus variability by studying the evolution of virus strains after primary vaccination of an infant using the Sabin type 3 vaccine strain. Poliovirus isolates were taken at various time intervals after vaccination, and RNase T<sub>1</sub> oligonucleotide maps produced. Evolution of new strains of type 3 poliovirus occurred extremely rapidly. Within 8 hours of vaccination, maps of the virus being excreted displayed significant alterations when compared with the map of the original type 3 vaccine strain <sup>71</sup>.

While type 3 poliovirus strains are the most variable, multiple genetic changes can take place in all oral poliovaccine strains upon replication <sup>50</sup>. This gives rise to the possibility of vaccine-related cases of paralytic poliomyelitis. The vast majority of such cases are caused by poliovirus type 3 revertants <sup>13</sup>, although pathogenic reversion of the type 2 Sabin vaccine, while rare, has been recorded <sup>114</sup>. Type 1 poliovirus is least variable <sup>22</sup>, and vaccine reversion appears not to occur, though in vivo capsid protein changes have been detected <sup>52</sup>.

Cases have occurred in which all 3 poliovirus types have been isolated from a primary vaccinee suffering from paralytic poliomyelitis <sup>67</sup>. These are probably due to pathogenic reversion in a single vaccine strain, generally that of type 3 poliovirus.

Unfortunately no Gazankulu outbreak strain of poliovirus type 3

was available for study. Biochemical techniques have shown a close relationship between certain type 3 poliovirus isolates and the Sabin vaccine strain <sup>12,26,69,71</sup>, and many cases of type 3 vaccine-derived poliovirus have been reported <sup>13,29,30,67</sup>. Indeed, Evans et al (1985) showed that a single change, from uridine to cytosine at position 472 in the RNA, is sufficient to restore neurovirulence in the Sabin type 3 poliovaccine strain. These facts, coupled with the temporal association between type 3 poliovirus isolation and extensive vaccine administration in Gazankulu, indicate vaccine reversion to neurovirulence.

Despite the great intrinsic variability within poliovirus strains, reversion of Sabin vaccine strains to neurovirulence is rare. Paralysis due to pathogenic back-mutation only occurs in about 1 per 11.5 million vaccinees <sup>66</sup>. This indicates that the great majority of mutations occurring in the RNA of vaccine strains during passage through a vaccinee do not result in pathogenic reversion.

Reversion of poliovirus vaccine strains to neurovirulence in vivo occurs by mutation, in much the same way as attenuation <sup>52</sup>. The poliovirus genome mutation that occurs in vitro is probably due to genetic drift. This indicates that the genome has the potential for adaptation <sup>22</sup>. Recombination between poliovirus strains, resulting in alteration of the RNA, is also possible.

Within the RNA viruses recombination appears to be restricted to picornaviruses <sup>103</sup>, and in vivo poliovirus recombination has been detected <sup>71</sup>. Such recombination could result in excretion

of novel neurovirulent poliovirus strains by a vaccinee. Recombination of poliovirus strains <sup>2,103</sup> has been used for mapping the major determinants of neurovirulence <sup>2</sup> and may have potential in the production of safer poliovirus vaccines <sup>101,103</sup>,

Ultrasensitive techniques, such as RNase T<sub>1</sub> oligonucleotide mapping and mapping of tryptic peptides using RP-HPLC, show very clearly how great poliovirus variability is. Both have a great deal of potential in the study of poliovirus variation and recombination, but also have various drawbacks.

Of the two techniques, oligonucleotide mapping is probably the most sensitive. Single nucleotide changes within the genome may result in clearly visible differences between maps of different viral strains <sup>71</sup>. Unfortunately, only nucleotide alterations occurring in the diagnostic oligonucleotides (comprising 5% - 10% of the genome <sup>69</sup>) can be detected. Sensitivity is still high, because the diagnostic oligonucleotides are distributed throughout the entire RNA and are thus representative of it <sup>51</sup>.

The ultra-high sensitivity of oligonucleotide mapping is, in fact, one of its major drawbacks. A large number of genomic alterations, although they may be detected using this technique, do not result in changes in the RNA translation products. Comparison of sequence data of poliovirus strains <sup>56,89,100,104</sup> shows that the majority of differences between RNA of different poliovirus strains are not expressed after translation. In the case of wild-type 2 strain Lansing <sup>56</sup> and Sabin vaccine strain p712 <sup>104</sup>, only about 10% of the genomic differences between the

two strains result in altered translation products.

The high level of non-expressed genomic alterations detected using oligonucleotide mapping could be misleading. Results might indicate that two poliovirus strains shared a distant relationship, whereas comparison of their translation products could show considerable similarity. In this study, for example, oligonucleotide maps of Sabin type 2 strain P712 and Gazankulu strain 5068 displayed several differences. In contrast, their capsid proteins were very similar.

Oligonucleotide mapping is extremely useful in that it may be used to detect alterations in regions of the RNA other than those coding for the capsid proteins. These proteins only represent about 40% of the coding capacity of the RNA<sup>94</sup>, and it is likely that some biochemical determinants of neurovirulence are coded for by other regions of the genome<sup>8</sup>. This is particularly obvious in poliovirus type 3 vaccine strain Leon 3<sup>26</sup>.

Oligonucleotide mapping is very useful for plotting the evolution of poliovirus strains during an epidemic<sup>63,80</sup>, or even in individuals after vaccination<sup>50,71</sup>. Studies of this sort may provide a great deal of information on the rate at which poliovirus strains change. This would allow determination of which poliovirus strains are most prone to alteration, and would be of great use in the development of new attenuated poliovaccines. Monitoring using oligonucleotide mapping, similar to that carried out by Dreano et al (1985), could be used to ensure that in vitro alteration of vaccine strains in storage is minimal.



Because oligonucleotide mapping allows detection of minute changes at a genetic level, alteration in vaccine strains may be detected very early on. Often this may be before any difference is apparent using protein analysis techniques <sup>7,22,71,80</sup>. Comparison of neurovirulent strains, attenuated vaccine strains and pathogenic revertants may allow calculation of the minimum number of changes required in the RNA for vaccine reversion.

Possibly the greatest potential of oligonucleotide mapping is in the study of recombinant poliovirus strains and the development of safer attenuated poliovaccines. Recombination of poliovirus strains does occur <sup>2,101,103</sup>, albeit infrequently in vivo, and it is possible for recombinants to arise which are the progeny of two different poliovirus types <sup>71,103</sup>.

Recombinants of vaccine strains (especially unstable ones such as type 3 vaccine strain Leon 3, which is most prone to pathogenic reversion <sup>26,71</sup>) could be constructed using cDNA <sup>101</sup>. Although antigenically unchanged, these would be more stable than the current Sabin vaccine strains.

Oligonucleotide mapping would prove invaluable in research into recombinant vaccines. Initially, oligonucleotides involved in neurovirulence could be identified by comparing oligonucleotide maps of pathogenic and non-pathogenic strains. Nucleotide sequencing could be used to check whether these oligonucleotides contained all the sequences coding for neurovirulence. After preparation of recombinants, oligonucleotide mapping would be used to check that recombination had been successful, and that

sequences determining neurovirulence were no longer present. Although this could all be done using nucleotide sequencing <sup>56</sup>, oligonucleotide mapping is faster and less complex. It is also useful for giving a clear visual identification of the genetic constituents of a poliovirus strain <sup>71</sup>.

Mapping of tryptic peptides using reversed-phase high-performance liquid chromatography (RP-HPLC) is also extremely sensitive, potentially able to detect picomole amounts of peptide <sup>41,111</sup>. The major advantage of RP-HPLC over RNase T<sub>1</sub> oligonucleotide mapping is that protein is considerably easier to obtain and handle than RNA.

Although in this study sensitivity was decreased by the need to radiolabel peptides with <sup>125</sup>I prior to RP-HPLC, potential does exist for the mapping of unlabelled peptides <sup>5,21,38</sup>. This would greatly increase sensitivity, because all tryptic peptides present could be mapped.

Tryptic peptide mapping of poliovirus coat proteins using RP-HPLC may, like oligonucleotide mapping, be used for monitoring the evolution of new poliovirus variants during an epidemic. RP-HPLC mapping of tryptic peptides may actually be more useful than oligonucleotide mapping for such monitoring because only capsid protein alterations are detected. While the RNA is highly variable, most of the genomic differences between strains are not expressed in the translation products <sup>56,89,100,104</sup>.

Tryptic peptide mapping allows the determination of phenotypic differences between strains, and actual changes in capsid

proteins may be monitored.

Because capsid proteins are mapped individually using RP-HPLC, it is possible to determine which undergo the greatest alteration during attenuation or reversion. Although similar studies could be carried out using serological techniques such as monoclonal antibodies <sup>25,63</sup>, tryptic peptide mapping of individual capsid proteins offers greater sensitivity. This sensitivity could be increased by combining RP-HPLC tryptic peptide mapping with protein sequencing.

Combination of the two techniques would allow determination of amino acid sequences specific to coat proteins of neurovirulent strains. Once capsid proteins of a single virus strain had been sequenced in order to provide a reference, other strains could be compared with it using peptide mapping. Maps of pathogenic and non-pathogenic strains could be prepared, and the differing peptides (recovered after RP-HPLC) sequenced. Only these peptides need be sequenced, reducing complexity, time and cost.

Tryptic peptide mapping using RP-HPLC would also be useful in monitoring recombinant poliovirus vaccines. Peptide mapping would show whether recombination had been successful and the capsid proteins contained the desired peptides. Although other techniques could be used for characterising capsid proteins <sup>52</sup>, tryptic peptide mapping by RP-HPLC is very much more sensitive.

Unlike oligonucleotide mapping, which allows comparison of the entire genome, RP-HPLC of tryptic peptides as used in this study only detects changes in the capsid proteins. Despite the fact

that capsid proteins only represent 40% of the coding capacity of the RNA <sup>94</sup>, they generally reflect alterations in neurovirulence. This is because the ability of virus particles to bind to receptor sites on the surface of susceptible cells, initiating infection, is controlled by the capsid proteins<sup>88</sup>.

Tryptic peptide mapping of capsid proteins only is, nevertheless, limited. Pallansch et al (1984) detected 27 translation products of poliovirus RNA, of which only four are capsid proteins. Several of the other polypeptides control virus replication within a specific cell type and doubtless play a role in determining pathogenicity. The function played by some translation products has not yet been determined <sup>83</sup>, and these may be involved with neurovirulence.

Peptide mapping has been used to study the intracellular translation products of viruses <sup>55</sup>, and such mapping using RP-HPLC has great potential. Complete shut-off of host cell protein synthesis upon poliovirus infection occurs rapidly <sup>62</sup>. Consequently the intracellular polypeptides produced during infection are exclusively viral in origin. It is possible that after extraction and purification of these polypeptides <sup>50,69</sup>, RP-HPLC tryptic peptide mapping could be carried out.

RP-HPLC tryptic peptide mapping of intracellular poliovirus polypeptides would be considerably more sensitive than oligonucleotide mapping. These polypeptides account for 95% of the RNA coding capacity <sup>83</sup>, while the diagnostic oligonucleotides used in RNA mapping constitute 5% - 10% of the genome <sup>69</sup>.

Comparison of tryptic peptide maps of intracellular polypeptides from different poliovirus strains would allow determination of the role played in neurovirulence by individual polypeptides. It would also be an extremely sensitive way of monitoring poliovirus recombinants. Clearly this technique has a great deal of potential in the study and comparison of polioviruses at a molecular level.

Both RNase T<sub>1</sub> oligonucleotide mapping and RP-HPLC mapping of tryptic peptides are highly sensitive techniques. While neither of them (as used in this study) provide a complete overview when studying poliovirus strains, both are extremely valuable in comparative studies. Though they may also be used in diagnostic tests, other tests using phenotypic <sup>112</sup> or genotypic <sup>29,46</sup> markers are more rapid, simpler and cheaper.

Highly sensitive techniques such as oligonucleotide mapping and RP-HPLC mapping of tryptic peptides are useful for distinguishing vaccine related from wild-type poliovirus strains, and determining relatedness between poliovirus strains. This allows the relative genetic "distance" between strains to be calculated, and their relationships to one another may be plotted. This is particularly useful when monitoring evolution of poliovirus strains during an epidemic.

While both oligonucleotide mapping and peptide mapping are of use in determining the relationship between poliovirus strains and in plotting the evolution of new strains, their greatest potential lies in research into new, safer recombinant vaccines.

Both techniques could be used for extremely sensitive monitoring of recombinants at a molecular level. In this respect, RP-HPLC peptide mapping of intracellular viral polypeptides has the greatest potential. Clearly, the possibilities for future research are considerable.

## CHAPTER EIGHT

### SUMMARY

The coat proteins and RNA of two Gazankulu outbreak poliovirus isolates were compared with those of Sabin vaccine and wild-type strains of the same serotype. The results obtained indicated that the causative agent in the initial stages of the Gazankulu outbreak was a wild-type 1 poliovirus strain. This was probably the result of the inherent variability of polioviruses causing gradual evolution of an apparently novel strain.

Isolation of type 2 and type 3 poliovirus only occurred after initiation of a vaccination programme using the Sabin trivalent oral poliovaccine. Analysis of type 2 outbreak strain 5068 showed that it was closely related to the type 2 vaccine strain. This was not surprising, for isolation of vaccine strains towards the latter period of an outbreak which has been halted by vaccine administration is very common.

It is likely that type 2 Gazankulu poliovirus isolate 5068 resulted from mutations in the attenuated vaccine strain. There was no reason to believe that it was a pathogenic revertant. No type 3 poliovirus isolate from the Gazankulu outbreak was available for analysis.

Results obtained during this study confirmed that the two Gazankulu outbreak strains used had been correctly identified as type 1 and type 2 polioviruses.

Vaccine stocks recalled from the field after the Gazankulu poliomyelitis outbreak had a very low vaccine titre <sup>48</sup>, resulting from breaks in the cold chain. The low vaccine titre probably allowed completion of several poliovirus replication cycles before the virus concentration triggered an antibody response. This would increase the likelihood of variation within the virus strains, resulting in novel vaccine-related poliovirus isolates. The similarities between type 2 vaccine strain P712 and Gazankulu isolate 5068 indicate that such variation has occurred. In the case of type 3 poliovirus, which is particularly variable <sup>71</sup>, this may have resulted in evolution of pathogenic revertants <sup>26,13</sup>.

Incidents such as the Gazankulu outbreak highlight the problems inherent in the use of the live attenuated Sabin poliomyelitis vaccine. The importance of maintaining a high vaccination rate and good cold chain for vaccine storage and transport is emphasized. Clearly, research into safer alternative poliomyelitis vaccines, such as sub-particle vaccines, is indicated.



#### REFERENCES CITED

1. Abolhassani, M., Fiore, G. and Roux, K.H. (1985) Comparative tryptic peptide analysis of rabbit heavy chain allotypes by HPLC. J. Liq. Chromatog. **14**:2649-2662.
2. Agol, V.I., Grachev, V.P., Dorozdov, S.G., Kolesnikova, M.S., Koslov, V.G., Ralph, N.M., Romanova, L.I., Tolskaya, E.A., Tyufanov, A.V. and Viktorova, E.G. (1984) Construction and properties of intertypic poliovirus recombinants : First approximation mapping of the major determinants of neurovirulence. Virology **136**:41-55.
3. Anderson, E.C., Underwood, B.O., Brown, F. and Ngichabe, C.K. (1985) Variation in foot-and-mouth disease virus isolates in Kenya : An examination of field isolates by T<sub>1</sub> oligonucleotide finger printing. Vet. Microb. **10**:409-423.
4. Andrews, A.T. (1981) "Electrophoresis : Theory, Techniques and Biochemical and Clinical Applications" (A.R. Peacocke and W.F. Harrington, eds.), p.p. 25-99, Clarendon Press, Oxford.
5. Banes, A.J., Link, G.W. and Snyder, L.R. (1985) Comparison of reverse-phase columns for the separation of tryptic peptides by gradient elution. Correlation of experimental results and model prediction. J. Chromatog. **326**:419-431
6. Boffey, P.M. (1977) Polio : Salk challenges safety of Sabin's live virus vaccine. Science **196**:235-236.
7. Bellocq, C., Agut, H., van der Werf, S. and Girard, M. (1984) Biochemical characterization of poliovirus type 1 temperature-sensitive mutants. Virology **139**:403-407.
8. Bengtsson, S. (1968) Attempts to map poliovirus genome by analysis of selected recombinants. Acta. Pathol. Microbiol. Scand. **73**:592-604.
9. Bordier, C. and Crettol-Jarvinen, A. (1979) Peptide mapping of heterogeneous protein samples. J. Biol. Chem. **254**:2565-2567.
10. Bolton, A.E. (1977) "Radioiodination Techniques", Review 18, p.p. 12-13, Amersham International Ltd.
11. Brown, R. and Cartwright, B. (1963) Purification of radioactive foot and mouth disease virus. Nature **199**:1168-1170.
12. Brust, J. and Fasold, H. (1981) Microfingerprints of proteins through labelling acetylation of their proteolytic peptides. Anal. Biochem. **106**:268-272.

13. Cann, A.J., Stanway, G., Hughes, P.J., Minor, P.D., Evans, D.M.A., Schild, G.C. and Almond, J.W. (1984) Reversion to neurovirulence of the live attenuated Sabin type 3 oral poliovirus vaccine. Nucleic Acids Res. 12:7787-7792.
14. Cleveland, D.W., Fischer, S.G., Kirschner, M.W. and Laemmli, U.K. (1977) Peptide mapping by limited proteolysis in sodium dodecyl sulfate and analysis by gel electrophoresis. J. Biol. Chem. 252:1102-1106.
15. Clewley, J.P., Bishop, D.H.L., Kang, C.Y., Coffin, J., Schnitzlein, W.M., Eichmann, M.E. and Schope, R.E. (1977) Oligonucleotide fingerprints of RNA species obtained from rhabdoviruses belonging to the vesicular stomatitis virus subgroup. J. Virol. 23:152-166.
16. Chow, M. and Baltimore, D. (1982) Isolated poliovirus capsid protein VP1 induces a neutralizing response in rats. Proc. Natl. Acad. Sci. USA. 79:7518-7521.
17. Chow, M., Newman, J.F.E., Filman, D., Hogle, J.M., Rowlands, D.J. and Brown, F. (1987) Capsid protein VP4 of picornavirus particles is covalently modified at its N-terminus by Myristic acid, in press.
18. De Wachter, R. and Fiers, W. (1971) Fractionation of RNA by Electrophoresis on Polyacrylamide Gel Slabs in "Methods in Enzymology" 21, (S.P. Colowick and N.O. Kaplan, eds.), p.p. 167-178, Academic Press, New York.
19. De Wachter, R. and Fiers, W. (1972) Two-dimensional gel electrophoresis of <sup>32</sup>P-labelled RNA. Anal. Biochem. 49:184-197.
20. De Wachter, R. and Fiers, W. (1982) Two dimensional Gel Electrophoresis of Nucleic Acids in "Gel Electrophoresis of Nucleic Acids - a Practical Approach" (Rickwood, D. and Hames, B.D., eds.), p.p. 77-116, IRL Press, Oxford.
21. Diebler, G.E., Boyd, L.F., Martenson, R.E. and Kies, M.W. (1985) Isolation of tryptic peptides of myelin basic protein by reversed-phase high performance liquid chromatography. J. Chromatog. 326:433-442.
22. Dreano, M., Bellocq, C., Fichot, O., van der Werf, S. and Girard, M. (1985) Genetic variations in the Mahoney strain of poliovirus type 1. Annales de l'Institut Pasteur / de Virologie 136:101-114.
23. Eagle, M. (1959) Amino acid metabolism in mammalian cell cultures. Science 130:432-435.
24. Elder, J.H., Pickett, R.A., Hampton, J. and Lerner, R.A. (1977) Radioiodination of proteins in single polyacrylamide gel slices. J. Biol. Chem. 252:6510-6515.

25. Emini, E.A., Kao, S.-Y., Lewis, A.J., Crainic, R. and Wimmer, E. (1983) Functional basis of poliovirus neutralization determined with monospecific neutralizing antibodies. J. Virol. **46**:466-474.
26. Evans, D.M.A., Dunn, G., Minor, P.D., Schild, G.C., Cann, A.J., Stanway, G., Almond, J.W., Currey, K. and Maizel, J.V. (1985) Increased neurovirulence associated with a single nucleotide change in a noncoding region of the Sabin type 3 poliovaccine genome. Nature **314**:548-550.
27. Eve, C. (1985) Development of an accurate tryptic peptide mapping technique for determining the origin of poliovirus isolates by comparison of coat proteins. Honours Thesis, Rhodes University.
28. Feitelson, M.A., Wettstein, F.O. and Stevens J.G. (1981) Tryptic peptide mapping of picomolar quantities of protein labelled with the Bolton - Hunter reagent. Anal. Biochem. **116**:473-479.
29. Ferguson, M., Minor, P.D., Magrath, D.I., Yi-Hua, G., Spitz, M. and Schild, G.C. (1984) Neutralization epitopes on poliovirus type 3 particles : An analysis using monoclonal antibodies. J. Gen. Virol. **65**:197-201.
30. Frisby, D. (1977) Oligonucleotide mapping of non radioactive virus and messenger RNAs. Nucleic Acids Res. **4**:2975-2996.
31. Gauntt, C.J., Gomez, P.T., Duffey, P.S., Grant, J.A., Trent, D.W., Witherspoon, S.M. and Paque, R.E. (1984) Characterisation and myocarditic capabilities of coxsackievirus B3 variants in selected mouse strains. J. Virol. **52**:598-605.
32. Gentsch, J.R. and Fields, B.N. (1981) Tryptic peptide analysis of outer capsid polypeptides of mammalian reovirus serotypes 1, 2, and 3. J. Virol. **38**:208-218.
33. Ginsberg, M.S. (1980) Picornaviruses : Poliovirus in "Virology" (R. Dulbecco and M.S. Ginsberg, eds.), p.p. 1096-1109, Harper and Row Publisher, Inc., Maryland, USA.
34. Goodenham, K. (1983) High Performance Liquid Chromatography of Proteins and Nucleic Acids in "Techniques in Molecular Biology" (J.M. Walker and W. Gaastra, eds.), p.p 18-24, Croon Helm Ltd, England.
35. Greenwood, F.C., Hunter, M.W. and Glover, J.S. (1963) The preparation of <sup>125</sup>I-labelled human growth hormone of high specific radioactivity. J. Biochem. **89**:114-123.
36. Hahn, E.C. and Hahn, P.S. (1987) Properties of acrylamide gels cross-linked with low concentrations of N,N'-diallyl-tartardiamide. J. Virol. Methods **15**:41-52.

37. Hames, B.D. (1981) An introduction to Polyacrylamide Gel Electrophoresis in "Gel Electrophoresis of Proteins: A Practical Approach" (B.D. Hames and D. Rickwood, eds.), p.p 1-86, IRL Press, London.
38. Hancock, W.S., Bishop, C.A., Prestidge, R.L., Harding, D.R.K. and Hearn, M.T.W. (1978) High-performance liquid chromatography of peptides and proteins II. The use of phosphoric acid in the analysis of underivatized peptides by reversed-phase high performance liquid chromatography. J. Chromatog. **153**:391-398.
39. Hancock, W.S. (1984) Introduction to High Performance Liquid Chromatography in "Handbook of HPLC for the separation of Amino Acids, Peptides and Proteins" 1, (W.S. Hancock, ed.), p.p. 3-12, CRC Press Inc., Florida.
40. Haschemeyer, R.H. and Haschemeyer, A.E.V. (1973) Primary Structure of Proteins in "Proteins: A Guide to Study by Physical and Chemical Methods", Wiley-Interscience, New York.
41. Hearn, M.T.W. and Hancock, W.S. (1979) The Role of Ion-Pair Reversed Phase HPLC in Peptide and Protein Chemistry in "Biological/Biomedical Applications of Liquid Chromatography" 2, (G.L. Hawk, ed.), p.p. 243-271, Marcel Dekker, New York.
42. Henderson, L.E., Sowder, R., Copeland, T.D., Smythers, G. and Oroszlan, S. (1984) Quantitative separation of murine leukemia proteins by reversed-phase high performance liquid chromatography reveals newly described gag and env cleavage products. J. Virol. **52**:492-500.
43. Heukeshoven, J. and Dernick, R. (1983) Rapid analytical and preparative separation of structural polypeptides of poliovirus by reversed-phase high performance liquid chromatography. J. Virol. Methods. **6**:283-293.
44. Heukeshoven, J. and Dernick, R. (1985) Characterization of a solvent system for separation of water insoluble poliovirus proteins by reversed-phase high-performance liquid chromatography. J. Chromatog. **326**:91-101.
45. Holland, J.J., Grabau, E.A., Jones, C.L. and Semler, B.L. (1979) Evolution of genome mutations during long-term persistent infection by vesicular stomatitis virus. Cell **16**:496-504.
46. Humphrey, D.D., Kew, O.M., and Feorino, P.M. (1982) monoclonal antibodies of four different specifications for neutralization of type 1 polioviruses. Infection and Immunity **36**:841-843.
47. Ingram, V.M. (1956) A specific difference between the

globins of normal human and sickle cell anaemic haemoglobins. Nature (London) 178:792-794

48. Johnson, S., Schoub, B.D., McAnerney, J.M., Gear, J.S.S., Moodie, J.M. Garrity, S.L., Klaasen, K.I.M., Saayman, G. and Kustner, H.G.V. (1982) Poliomyelitis Outbreak in South Africa, 1982. II. Laboratory and Vaccine Aspects.
49. Jordan, E.M. and Raymond, S. (1969) Anal. Biochem. 27:205-211.
50. Kew, O.M., Nottay, B.K., Hatch, M.H., Nakano, J.H. and Obijeski, J.F. (1981) Multiple genetic changes can occur in the oral poliovaccines upon replication in humans. J. Gen. Virol. 56:337-347.
51. Kew, O.M., Nottay, B.K. and Obijeski, J.F. (1984) Applications of Oligonucleotide Fingerprinting to the Identification of Viruses in "Methods in Virology" 8, (K. Maramorosch and M. Koprowski, eds.), p.p. 41-84, Academic Press, New York.
52. Kew, O.M., Pallansch, M.A., Omilianowski, D.R. and Reuckert, R.R. (1980) Changes in three of the four coat proteins of oral polio vaccine strain derived from type 1 poliovirus, J. Virol. 33:256-263.
53. Kinney, R.M. and Trent, D.W. (1982) Conservation of tryptic peptides in the structural proteins of viruses in the Venezuelan equine encephalitis complex. Virology 121:345-362.
54. Laemmli, U.K. (1970) Cleavage of structural proteins during the assembly of the head of bacteriophage T4. Nature (London) 227:680-685.
55. Lamb, R.A. and Choppin, P.W. (1978) Determination by peptide mapping of the unique polypeptide in Sendai virions and infected cells. Virology 84:469-478.
56. La Monica, N., Merian, C. and Racaniello, V.R. (1986) Mapping sequences required for mouse neurovirulence of poliovirus type 2 Lansing. J. Virol. 57:515-525.
57. Lancet (1977) Poliomyelitis vaccines - Leading article, Lancet 2: 21-22.
58. Lancet (1982) Poliomyelitis vaccine - killed or live? - Leading article, Lancet 1:84-85.
59. Laver, W.G. (1969) Peptide mapping of viral proteins in "Fundamental Techniques in Virology", (K. Habel and N. Salzman, eds.), p.p. 371-378, Academic Press, New York.

60. Lee, Y.F. and Wimmer, E. (1976) "Fingerprinting" high molecular weight RNA by two-dimensional gel electrophoresis: Application to poliovirus RNA. Nucleic Acids Res. **3**:1647-1658.
61. Lee, Y.F., Kitamura, N., Nomoto, A. and Wimmer E. (1979) Sequence studies of poliovirus RNA. IV. Nucleotide sequence complexities of poliovirus type 1, type 2 and two type 1 defective interfering particles RNAs and fingerprint of the poliovirus type 3 genome. J. Gen. Virol. **44**:311-322.
62. Levintow, L. (1974) The Reproduction of Picornaviruses in "Comprehensive Virology", 2nd ed., (H. Fraenkel-Conrat and R.R. Wagner, eds.), p.p. 109-155, Plenum Press, New York.
63. Magrath, D.I., Evans, D.M.A., Ferguson, M., Schild, G.C., Minor, P.D., Horaud, F., Crainic, R., Stenvick, M. and Hovi, T. (1986) Antigenic and molecular properties of type 3 poliovirus responsible for an outbreak of poliomyelitis in a vaccinated population, J. Gen. Virol. **67**:899-905.
64. Martin, M.E.D. (1984) Determination of the origin of poliovirus isolates from the 1982 Gazankulu outbreak. Honours Thesis, Rhodes University.
65. Melnick, J.L. (1982) Portraits of viruses: the picornaviruses. Intervirology **20**:60-100.
66. Melnick, J.L. (1983) Enteroviruses in "Viral Infections of Humans - Epidemiology and Control", 2nd ed., (A.S. Evans, ed.), p.p. 187-251, Plenum Publishing Corp, New York.
67. Mertens, Th., Schurmann, W., Kruppenbacher, J., Rheingans, K., Kellerman, K., Maass, G. and Eggers, H.J. (1983) Problems with live virus vaccine - associated poliomyelitis. A paralytic case with isolation of all 3 poliovirus types. Med. Microb. Immunol. **172**:13-21.
68. Milstein, J.B., Walker, J.R. and Eron, L.J. (1977) Correlation of virus polypeptide structure with attenuation of poliovirus type 1. J. Virol. **23**:811-815.
69. Minor, P.D. (1982) Characterization of strains of type 3 poliovirus by oligonucleotide mapping. J. Gen. Virol. **59**:307-317.
70. Minor, P.D., Evans, D.M.A., Ferguson, M., Schild, G.C., Westrop, R.C. and Almond, J.W. (1985) Principal and subsidiary antigenic sites of VP1 involved in the neutralization of poliovirus type 3. J. Gen. Virol. **66**:1159-1165.
71. Minor, P.D., John, A., Ferguson, M., Icenogle, J.P. (1986) Antigenic and molecular evolution of the vaccine strain of type 3 poliovirus during the period of excretion by a primary vaccinee. J. Gen. Virol. **67**:673-706.

72. Minor, P.D., Schild, G.C., Bootman, J., Evans, D.M.A., Ferguson, M., Reeve, P., Spitz, M., Stanway, G., Cann, A.J., Hauptmann, R., Clarke, L.-D., Mountford, R.C. and Almond, J.W. (1983) Location and primary structure of a major antigenic site for poliovirus neutralization. Nature **301**:674-679.
73. Minson, A.C. and Darby, G. (1982) in "New Developments in Practical Virology", (C.R. Howard,ed.), p.p. 185-229, Liss, New York.
74. Molnar, I. and Horvath, Cs. (1977) separation of amino acids and peptides on non-polar stationary phases by high-performance liquid chromatography. J. Chromatog. **142**:623-640.
75. Monch, W. and Dehnen, W. (1977) High-performance liquid chromatography of polypeptides. J. Chromatog. **140**:263-265.
76. Monch, W. and Dehnen, W. (1978) high-performance liquid chromatography of polypeptides and proteins on a reversed-phase support. J. Chromatog. **147**:415-418.
77. Morrow, C.D. and Dasgupta, A. (1983) Antibody to a synthetic nonapeptide corresponding to the NH terminus of poliovirus genome-linked protein VPg reacts with native VPg and inhibits in vitro replication of poliovirus RNA. J. Virol. **48**:429-439.
78. Neville, D.M. (1971) Molecular weight determination of protein-dodecyl sulfate complexes by gel electrophoresis in a discontinuous buffer system. J. Biol. Chem. **246**:6328-6334.
79. Nomoto, A., Kitamura, N., Lee, J.J., Rothberg, P.G., Imura, n. and Wimmer, E. (1981) Identification of point mutations in the genome of the poliovirus Sabin vaccine LSc 2ab, and catalogue of RNase T<sub>1</sub>- and RNase A- resistant oligonucleotides of poliovirus type 1 (Mahoney) RNA. Virology **112**:217-227.
80. Nottay, B.K., Kew, O.M., Hatch, M.H., Heyward, J.T. and Obijeski, J.F. (1981) Molecular variation of type 1 vaccine-related and wild poliovirus during replication in humans. Virology **108**:405-423.
81. O'Farrell, P.H. (1975) High resolution two-dimensional electro-phoresis of proteins. J. Biol. Chem. **250**:4007-4021.
82. Osterhaus, A.D.M.E., van Wezel, A.L., Hazendonk, T.G., Uyt de Haag, F.G.C.M., van Asten, J.A.A.M. and van Steenis, B. (1983) Monoclonal antibodies to poliovirus. Intervirology **20**:129-136.

83. Pallansch, M.A., Kew O.M., Semler B.L., Omilianowski D.R., Anderson C.W., Wimmer E. and Ruekert R.R. (1984) Protein processing map of poliovirus, J. Virol. **49**:873-880.
84. Palmiter, R.D. (1974) Magnesium precipitation of ribonucleoprotein complexes. Expedient techniques for the isolation of undegraded polysomes and messenger ribonucleic acid. Biochemistry **13**:3606-3608.
85. Pederson, F.S. and Haseltine, W.A. (1980) A micromethod for Detailed Characterization of High Molecular Weight RNA in "Methods in Enzymology" **65**, (L. Grossman and K.Moldave, eds.), p.p 680-686, Academic Press, New York.
86. Phelan, M.A. and Cohen, K.A. (1983) gradient optimization principles in reversed-phase high-performance liquid chromatography and the separation of influenza virus components. J. Chromatog. **266**:55-66.
87. Plummer, D.T. (1978) "An Introduction to Practical Biochemistry", 2nd ed. McGraw Hill Book Co. (UK) Ltd, Maidenhead.
88. Putnak, J.R. and Phillips B.A. (1981) Picornaviral structure and Assembly. Microbiological Reviews, **45**:287-315.
89. Racaniello, V.R. and Baltimore, D. (1981) Molecular cloning of poliovirus cDNA and determination of the complete nucleotide sequence of the viral genome. Proc. Natl. Acad. Sci. USA. **78**:4887-4891.
90. Regnier, F.E. and Gooding, K.M. (1979) High-performance liquid chromatography of proteins. Anal. Biochem. **103**:1-25.
91. Rekosh, D.M.K. (1977) "The Molecular Biology of Animal Viruses" **1**, (D.P. Nayak, ed.), p.p. 64-106, Marcel Dekker, New York.
92. Robson, K.J.H., Crowther, J.R., King, A.M.Q. and Brown, F. (1979) Comparative biochemical and serological analysis of five isolates of a single serotype of foot-and-mouth disease virus. J. Gen. Virol. **45**:579-590.
93. Rueckert, R.R. (1976) On the Structure and Morphogenesis of Picornaviruses in "Comprehensive Virology" **6**, (H. Fraenkel-Conrat and R.R. Wagner, eds.), p.p. 131-215. Plenum Press, New York.
94. Rueckert, R.R., Matthews, T.J., Kew, O.M., Pallansch, M., McLean, C. and Omilianowski, D. (1979) Synthesis and Processing of Picornaviral Polyprotein in "Molecular Biology of Picornaviruses". (R. Perez-Bercoff, ed.), p.p. 113-125, Plenum Publishing Corp., New York.



95. Saayman, G., Kustner, H.G.V., Boer, P., Johnson, S., Schoub, B.D. and McAnerney, J.M. (1982) Poliomyelitis Outbreak in South Africa, 1982. I. Epidemiology.
96. Sabin, A.B. and Boulger, L.R. (1973) History of Sabin attenuated poliovirus oral live vaccine strains J. Biol. Stand. 1: 115-118.
97. Sangar, D.V. (1979) The replication of picornaviruses. J. Gen. Virol. 45:1-13.
98. Schonberger, L.B., McGowan, J.E. and Gregg, M.B. (1976) Vaccine related poliomyelitis in the United States. Amer. J. Epidemiol. 104:202-211.
99. Scraba, D.G. (1979) The Picornavirion : Structure and Assembly in "The Molecular Biology of Picornaviruses" (R. Perez - Bercoff, ed.), p.p. 1-17, Plenum Press, New York.
100. Stanway, G., Hughes, P.J., Mountford, R.C., Reeve, P., Minor, P.D., Schild, G.C. and Almond, J.W. (1984) Comparison of the complete nucleotide sequences of the genomes of the neurovirulent poliovirus P3/Leon/37 and its attenuated Sabin vaccine derivative P3/Leon/2a<sub>1</sub>b. Proc. Natl. Acad. Sci. USA 81:1539-1543.
101. Stanway, G., Hughes, P.J., Westrop, G.D., Evans, D.M.A., Dunn, G., Minor, P.D., Schild, G.C. and Almond, J.W. (1986) Construction of poliovirus intertypic recombinants by use of cDNA. J. Virol. 57:1187-1190.
102. Takahashi, K. and Moore, S. (1982) in "The Enzymes" 15, (P.D. Boyer, ed.), p.p. 435-468, Academic Press, New York.
103. Tolskaya, E.A., Romanova, L.A., Kolesnikova, M.S. and Agol, V.I. (1983) Intertypic recombination on poliovirus : Genetic and biochemical studies. Virology 124:121-132.
104. Toyoda, H., Kohara, M., Kataoka, Y., Sugunuma, T., Omata, T., Imura, N. and Nomoto, A. (1984) Complete nucleotide sequence of all three poliovirus serotype genomes. Implication for genetic relationship, gene function and antigenic determinants. J. Mol. Biol. 174:561-585.
105. Tsilimigras, C. (1985) Medical School Research Unit Report in "National Institute for Virology - Annual Report 1985", p.p.71-75.
106. Weber, K. and Osborn, M. (1975) Proteins and Sodium Dodecyl Sulfate : Molecular Weight Determination on Polyacrylamide Gels and Related Procedures in "The Proteins" 1, (H. Neurath and R.L. Hill, eds.), p.p. 179-223, Academic Press, London.
107. Welling-Wester, S., Popken-Boer, T., Wilterdink, J.B., Van Beeumen, J. and Welling, G.W. (1985) Isolation by high-

- performance liquid chromatography and partial characterization of a 57 000 dalton herpes simplex virus type 1 polypeptide. J. Virol. 54:265-270.
108. Welling, G.W., Nijmeijer, J.R.J., van der Zee, R., Groen, G., Wilterdink, J.B. and Welling-Wester, S. (1984) Isolation of detergent-extracted Sendai virus proteins by gel filtration, ion-exchange and reversed-phase high-performance liquid chromatography and the effect on immunological activity. J. Chromatog. 297:101-109.
  109. Wetz, K. and Habermehl, K.-O. (1979) Topographical studies on poliovirus capsid proteins by chemical modification and crosslinking with bifunctional reagents. J. Gen. Virol. 44:525-534.
  110. Winkler, G., Heinz, F.X., Guirakhoo, F. and Kunz, C. (1985) Separation of flavivirus membrane and capsid proteins by multistep high-performance liquid chromatography optimized by immunological monitoring. J. Chromatog. 326:113-119.
  111. Winkler, G., Wolschann, P., Briza, P., Heinz, F.X. and Kunz, C. (1985) Spectral properties of trifluoroacetic acid-acetonitrile gradient systems for separation of picomole quantities of peptides by reversed-phase high-performance liquid chromatography. J. Chromatog. 347:83-88.
  112. World Health Organization (1982) Markers of poliovirus strains isolated from cases temporally associated with the use of live poliovirus vaccine : Report on a WHO collaborative study. J. Biol. Stand. 9:163-184.
  113. Yoneyama, T., Hagiwara, A. and Hara, M. (1981) Structural proteins of poliovirus type 2 isolates. Microb. Immunol. 25:575-583.
  114. Yoneyama, T., Hagiwara, A., Hara, M. and Shimojo, H. (1982) Alteration in oligonucleotide fingerprint patterns of the viral genome in poliovirus type 2 isolated from paralytic patients. Infection and Immunity 37:46-53.
  115. Young, N.A., Hoyer, B.H. and Martin, M.A. (1968) Polynucleotide sequence homologies among polioviruses. Proc. Natl. Acad. Sci. USA 68:548-555.
  116. Young, N.A. (1973) Size of genome sequences shared by poliovirus types 1,2 and 3. Virology 56:400-403.